

UNIVERSITY OF NATAL



VARYING LEVELS OF INCIDENT SOLAR IRRADIANCE AND
MICROCLIMATIC VARIATIONS ON BANANA (*MUSA* spp)
GROWTH AND PRODUCTIVITY

by

FRED KIZITO

B.Sc. Agric (Hons) MUK

Submitted in partial fulfilment of the requirement for the degree of

MASTER OF SCIENCE IN AGRICULTURE

in the

School of Applied Environmental Sciences

Faculty of Science and Agriculture

University of Natal

Pietermaritzburg

KwaZulu-Natal

MARCH, 2001

ACKNOWLEDGEMENTS

I would like to express my most sincere gratitude to:

Professor M. J. Savage in the School of Applied Environmental Sciences (SAES), Agrometeorology, for his excellent supervision, patience, commitment and encouragement throughout my study period. He has inspired me to be a critical thinker and improved my research potential and capabilities.

Professor J. Bower of the Horticulture section of the School of Agricultural Sciences and Agribusiness, my co-supervisor, for his contribution on the horticultural side of this work.

Professor M. A. Johnston in the School of Applied Environmental Sciences (Soil Science), for his advice and contribution to this write-up as well as permission to utilise the soil physics laboratory equipment for soil analysis.

The Institute of Commercial Forestry Research (ICFR) is also credited for assistance rendered with the physical and chemical analyses that were carried out on a variety of the site soil samples.

Dr. Beverly McIntyre and Dr. John Lynam of the Rockefeller Foundation are deeply thanked for the financial support which catered for the living and study expenses. The University of Natal and the School of Applied Environmental Sciences is thanked for the logistical and financial support granted for tuition expenses as well as offers for graduate assistantships.

Ms Jothi Moodley, Mr. Peter Dovey and the entire staff of the SAES for the diversified help during field and laboratory work. Their contribution facilitated an excellent working environment.

Mr. F. S. Wallis and the farm manager, Mr. Charles Wallis of Inselele (Zulu word meaning challenge) farm are thanked and credited for permission to utilise their banana fields until the termination of the research work.

I would like to express my special thanks to my parents for their patience and support over my many years of study. My sincere gratitude goes to my friends Jackton Frederick Mwachi, Christopher Komakech and Innocent Nzeyimana among others for their encouragement, Jeffery Mthwalo for the profound help offered, Louis Mthembu who helped trace the Inselele research site, Magandaran Moodley for his advice and Gabilisile Mchunu for the moral support offered. These have been a great source of inspiration.

May the Lord's name be praised for the Wisdom he endowed upon me in this challenging research on banana growth and performance. Credit is extended to wonderful supervisors, examiners, scientists acknowledged herein and financial support from the Rockefeller foundation as well as excellent supervision offered by the University of Natal. The Lord put all this in my reach and sustained me to complete this formidable task.

ABSTRACT

A field experiment was conducted at Inselele, KwaZulu-Natal South Coast, South Africa, in 1999/2000, to assess the influence of shading as related to varying levels of incident solar irradiance as well as microclimatic variations on banana (*Musa* spp) growth, phenology trends, morphology and productivity. The trial was established in August 1999 on a ratoon plantation. The experimental site, 0.655 ha in extent, comprised of three replications with four treatments having varying levels of incident solar irradiance levels of 100 %, 70 %, 40 % and 20 % under a planting density of 1666 plants ha⁻¹. The irradiance levels were derived from black shade cloth, erected 1 m above the banana canopy level.

Banana plantations have vegetation that does not completely cover the underlying ground surface. For such a canopy, there are basically two distinct and interacting surface components, the overstorey/canopy and the understorey/soil. Independent investigations and measurements of the solar energy fluxes for each of these two components forms a vital step to comprehend the factors that control the overhead energy fluxes in the plantation. In this study, evaluation of flux components in the understorey of the canopy using plastic microlysimeters was conducted. Considering normal variations in field measurements, the agreement and consistency among the different measurements with previous findings was adequate. Microlysimeter measurements of daytime soil evaporation were generally less than 1 mm, with an average of 0.45 mm. The study did not include flux measurement at the two level approach (Bowen ratio and Eddy correlation methods) which could have been compared with the single level approach and microlysimeter results. Two methods of deriving/measurement of energy fluxes were used and the differences between them are discussed. A reassessment of the microlysimeter technique is suggested. For the understorey, the sum of sensible and latent heat fluxes derived from spreadsheet computation was equal to the available energy. Mean soil temperatures at a depth of 20 to 60 mm ranged between 13 and 16 °C. This study illustrated that energy flux measurement and interpretation in a banana plantation can be complicated especially under sparse canopy conditions. Furthermore, it is worth noting that the source area for fluxes could possibly include the adjacent blocks not

within the experimental area. Good agreement was found in the patterns of wind speed profile measurements, with the 1.5 m profile depicting a mean difference of 52 % compared to the 3 m profile between day of year (DOY) 230 and 248 inclusive. This suggested that wind speed attenuation was strongly correlated to increment in height within the plantation due to canopy roughness. Differential canopy temperatures (measured with infrared thermometry) were more sensitive to the vapour pressure deficit than to wind speed.

The most dense shade affected banana productivity indicated by a bunch weight of 22.69 and 33.65 kg under the 20 % and 100 % irradiance treatments respectively. The bunch mass reduction was 32 %. Flowering dates were delayed by 8 days, 13 days and 21 days with incident irradiances of 70 %, 40 % and 20 % of the unshaded control (100 % irradiance), respectively. The phenological responses in this study appear to be a result of a contribution or interaction of both seasonal responses and shading treatments and this is further evidenced by the high levels of correlation (98.4%) reported between these two variables. Shading resulted in diminished leaf emergence rates (LER), pseudostem circumference and pseudostem height. However, just before flowering, no significant differences were observed in the pseudostem circumferences. There was a progressive increment in pseudostem height for all the treatments, with the 20 % irradiance treatment depicting the least heights registered compared to the rest of the treatments. Evident seasonal differences were registered in the LER and emergence to harvest (EH) interval. Comparison of LER and mean air temperature trends revealed a similar curve pattern and depicted a highly positive correlation of 90.4% . The highest LER of 3.8 was recorded in the month of January at a peak mean monthly air temperature of 24.3°C while the lowest LER of 1.2 was registered in July which had the lowest mean air temperature of 14.7 °C. The EH intervals measured between September and December flowering varied from 125 days to 112 days respectively before harvest yet the April to May flowering had an EH duration of 186 to 195 days respectively. The strong seasonal influence on phenological responses is further confirmed by these EH trends. Reductions in LAI observed with time were principally due to leaf senescence.

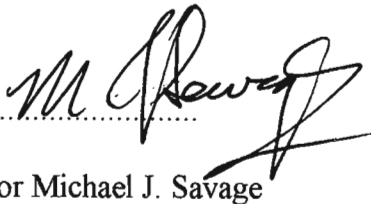
Keywords: Banana, morphology, incident solar irradiance, shade, microclimatic variations, bunch mass and flowering

DECLARATION

I FRED KIZITO hereby declare that the research reported in this thesis is the result of my own original investigations, except where acknowledged, and has not, in its entirety or in part, been previously submitted to any University or Institution for degree purposes.

Signed 

Fred Kizito

Signed 

Professor Michael J. Savage

Professor of Agrometeorology

TABLE OF CONTENTS

ACKNOWLEDGEMENTS	i
Abstract	iii
Declaration	v
Table of Contents	vi
List of Symbols	ix
List of Figures	xi
List of Tables	xiv
List of Appendices	xv
CHAPTER 1	1
1 Introduction	1
1.1 Research objectives	3
CHAPTER 2	5
2 Radiation Interception and Plant Growth Responses	5
2.1 Introduction	5
2.2 Infrared radiation dynamics	7
2.3 Leaf area indices	9
2.4 Plant morphological characteristics and phenology	10
2.4.1 Planting to harvest period	11
2.4.2 Leaf emergence rate	11
2.4.3 Seasonal root growth rates	12
2.4.4 Irradiance levels and EH intervals	12
2.4.5 Bunch development	14
2.5 Temperature effects on plant growth	15
2.6 Shade effect on banana growth, morphology and productivity	17
2.7 Effect of soil water on banana morphology and productivity	18
2.8 Crop water use	19
CHAPTER 3	21
3 Energy and Water Balance Dynamics	21
3.1 Canopy transpiration and energy dynamics	22
3.2 Crop water stress index	23
3.3 Surface temperature equation	24
3.4 Evaporation dynamics	25

CHAPTER 4	27
4 Materials and Methods	27
4.1 Site description	27
4.2 Experimental design and plot layout	28
4.3 LAI-2000 plant canopy analyser	31
4.4 Microclimatic measurements	31
4.5 Micrometeorological sensors	33
4.5.1 Net radiometer, IRT and propeller anemometer	33
4.5.1.1 Net radiometer	33
4.5.1.2 Apogee infrared thermometer	34
4.5.1.3 Three dimensional propeller anemometer	35
4.5.2 Soil heat flux plates and soil thermocouples	36
4.5.3 ThetaProbe	38
4.6 Microlysimeter measurements	39
4.7 Data handling and analysis	40
CHAPTER 5	41
5 Soil and Soil Water Characteristics	41
5.1 Introduction	41
5.2 Site soil characteristics	41
5.2.1 Particle size analysis procedure	43
5.2.2 Determination of soil bulk density	44
5.2.3 Laboratory determination of soil water content	45
5.3 Soil particle density	45
5.3.1 Procedure for soil particle density determination	45
5.4 Soil water retentivity characteristics	46
5.4.1 Retentivity determination procedure	46
5.4.2 Retentivity discussion	47
5.4.3 Soil heat flux measurements	50
CHAPTER 6	52
6 Microclimatic Variations, Solar radiation dynamics and Soil Evaporation Measurements	52
6.1 Introduction	52
6.2 Theoretical considerations of evapotranspiration	52
6.3 Penman-Monteith equation and minimum data set for modelling	56
6.4 Field data measurement, data handling procedures and computations	57
6.5 Constraints and shortcomings	59
6.6 Results and discussion	60
6.7 Light interception and Beer's law	75

CHAPTER 7	80
7 Banana growth, morphology and phenology trends in response to shading treatments	80
7.1 Introduction	80
7.2 Baseline studies on banana suckers	81
7.3 Vegetative phase	83
7.4 Flower emergence to harvest interval	85
7.5 Banana yield and production dynamics	95
CHAPTER 8	98
8 Conclusion and Recommendations for Future Research	98
8.1 Conclusion	98
8.2 Recommendations for future research	102
REFERENCES	105
APPENDICES	115

LIST OF SYMBOLS

$C_{p_{air}}$	Specific heat capacity of dry air	$J\ kg^{-1}\ K^{-1}$
C_{p_s}	Specific heat capacity of soil	$J\ kg^{-1}\ K^{-1}$
C_{p_w}	Specific heat capacity of water	$J\ kg^{-1}\ K^{-1}$
CWSI	Crop water stress index	%
EH	Emergence to harvest interval	months
FC	Field capacity	kPa
G_s	Soil heat flux density	$W\ m^{-2}$
G	Gravitational acceleration	$9.7922\ m\ s^{-2}$
H	Sensible heat energy flux density	$W\ m^{-2}$
h	Crop height	m
h	Height of the soil core	m
IRT	Surface temperature (infrared) technique	K
J	Energy stored in the crop volume	$W\ m^{-2}$
k	Extinction coefficient	m^{-1}
K_v	Exchange coefficient for latent heat transfer	$m^2\ s^{-1}$
K_h	Exchange coefficient for sensible heat transfer	$m^2\ s^{-1}$
LAI	Leaf area index	$m^2\ m^{-2}$
LER	Leaf emergence rate	Leaves emerging/month
MC	Mass of the soil core container	kg
M_w	Molar mass of water	$0.018\ kg\ mol^{-1}$
NAR	Net assimilation rate	μmols^{-1}
M_{ds}	Mass of the oven dried soil	kg
PM	Penman-Monteith technique	
RER	Root extension rate	mm/unit time
RUE	Radiation use efficiency	$g\ MJ^{-1}$ intercepted solar energy
RH	Relative humidity	%
R_a	Extraterrestrial solar irradiance	$W\ m^{-2}$
R_{net}	Net irradiance	$W\ m^{-2}$
RP	Refill point or the critical soil water content	$m^3\ m^{-3}$
R_s	Observed solar irradiance	$W\ m^{-2}$
r	Radius of the soil core	m
r_a	Aerodynamic resistance	$s\ m^{-1}$
r_{ah}	Aerodynamic resistance for heat	$s\ m^{-1}$
r_{am}	Aerodynamic resistance for momentum	$s\ m^{-1}$
r_{ap}	Aerodynamic resistance for a well watered crop	$s\ m^{-1}$
$r_{a_{stress}}$	Aerodynamic resistance for a water stressed crop	$s\ m^{-1}$
r_{av}	Aerodynamic resistance for water vapour	$s\ m^{-1}$
r_c	Canopy resistance	$s\ m^{-1}$
r_{cp}	Canopy resistance for a well watered crop	$s\ m^{-1}$
r_i	Quasi resistance	$s\ m^{-1}$
r_l	Stomatal resistance for leaves exposed to solar radiation	$s\ m^{-1}$
t	Local time	hours
T_s	Surface temperature	$^{\circ}C$

T_{air}	Air temperature	$^{\circ}\text{C}$
T_{soil}	Soil temperature	$^{\circ}\text{C}$
V	Volume of the soil core	m^3
VPD	Vapour pressure density	kg m^{-3}
Ψ_l	Leaf water potential	kPa
Δ	Slope of the saturated vapour pressure vs temperature	kPa K^{-1}
θ	Zenith angle	rad
θ_v	Volumetric soil water content	$\text{m}^3 \text{m}^{-3}$
Ψ_m	Matric potential	kPa
P	Energy flux density used in photosynthesis	W m^{-2}
ρ_{air}	Density of air	kg m^{-3}
ρ_s	Soil particle density	kg m^{-3}
ρ_b	Soil bulk density	kg m^{-3}
ρ_w	Density of water	kg m^{-3}

LIST OF FIGURES

Fig. 1.1 Radiation incident on a non-transparent object such as a banana leaf (Savage, 1998a)	9
Fig. 2.1 Basal morphological features of a banana plant (Rony and Rodomiro, 1997)	12
Fig. 2.2 Banana tree with a bunch approximately 12 to 15 weeks after emergence	14
Fig. 4.1 Left: A section of the shade netting (40 % irradiance) above the banana canopy supported by scaffolding; Right: Below shade netting (20 % irradiance) overview of the equipment for the automatic weather station	30
Fig. 4.2 Plot for research project on Inselele farm	30
Fig. 4.3 A plan view of a partial section of Inselele farm. The shaded section is the experimental site	32
Fig. 4.4 Equipment supported by scaffolding at site	33
Fig. 4.5 Soil heat flux plates and soil thermocouples for determination of the soil heat flux density	37
Fig. 4.6 Soil microlysimeter technique just before cylinder insertion	40
Fig. 5.1 Textural triangle, for percentage determination of soil fractions	44
Fig. 5.2 Retentivity curve showing measured and average θ_v (%) vs ψ_m (kPa)	49
Fig. 5.3 Mean soil heat flux density with soil temperature and soil water content for DOY 162 to 168 at Inselele	50
Fig. 5.4 Regression analysis for soil heat flux plate one buried at a depth of 70 mm versus soil heat flux plate two buried at a depth of 80 mm	51
Fig. 6.1 Resistances for the transfer of heat and water vapour (source: Thom, 1975)	54
Fig. 6.2 Typical variation of aerodynamic resistance with wind speed for DOY 145, 2000 at Inselele, assuming a crop height $h = 2.5$ m, wind speed measurement height $z = 3$ m	55
Fig. 6.3 (a) Mean variations in microlysimeter soil evaporation (mm), soil water content ($m^3 m^{-3}$) measured with ML1 ThetaProbe and wind	

- speed (m s^{-1}) with sensor placed at 3 m above ground and 0.5 m above canopy; (b) Daily total radiant density for DOY 174 to 196. Mean values were considered between 600 hours and 1800 hours determined with a pyranometer and net radiometers respectively both placed 0.5 m above the banana canopy 61
- Fig. 6.4 (a) Variation in microlysimeter soil evaporation with wind speed and soil water content measured with a ML1 ThetaProbe; b) Typical diurnal trends of R_{net} and R_n on Day 175, 2000. Soil evaporation measurements were taken between 600 hours and 1815 hours 62
- Fig. 6.5 The regression of available energy i.e. net irradiance less the soil heat flux density (W m^{-2}) as a function of solar irradiance (W m^{-2}) for Inselele banana orchard for June, 2000. Data for the time period 600 hours to 1800 hours only. Each data point is a 15 minute interval value 63
- Fig. 6.6 Hourly measurements of soil evaporation and transpiration regressed against soil evaporation for the 2.5 m banana canopy at Inselele for DOY 245, 2000 64
- Fig. 6.7 Diurnal variation in reference evaporation, soil evaporation and canopy transpiration trends with local time, on DOY 240 65
- Fig. 6.8 Components of the shortened energy balance as a function of DOY (230 to 247, inclusive for time 6 hours to 18 hours) 66
- Fig. 6.9 Diurnal variation in some of the components of the shortened energy balance as a function of local time for DOY 231 68
- Fig. 6.10 Diurnal variation in sensible heat flux density and wind speed as a function of local time for DOY 231 68
- Fig. 6.11 Variation of minimum and maximum air temperature and bunch temperature for DOY 162 to 173, 2000 69
- Fig. 6.12 Variation of minimum and maximum air temperatures and canopy temperatures as well as wind speed for DOY 162 to 173, 2000 71
- Fig. 6.13 (a) Variation in differential bunch temperature; (b) daily mean bunch temperature measured with a Hobo Temp logger and wind speed trends for DOY 160 to 190, 2000 73
- Fig. 6.14 Variation of mean air temperature, canopy temperature and differential temperatures with wind speed trends for DOY 162 to 173, 2000 74

Fig. 6.15 Regression of mean bunch temperature ($^{\circ}\text{C}$) as a function of mean air temperature ($^{\circ}\text{C}$)	74
Fig. 6.16 Variation of the surface to air temperature differential, wind speed, water vapour pressure and net irradiance for cloudless days, DOY 163 to 168.	75
Fig. 6.17 Variation of $\ln(I/I_0)$ with height (m), below a banana canopy determined using a Kipp solarimeter on DOY 201	76
Fig. 6.18 The variation in the LAI and extinction coefficient in a banana orchard over time	78
Fig. 7.1 Growth cycle of banana, <i>Musa</i> spp	82
Fig. 7.2 Mean baseline sucker pseudostem height variations with time	82
Fig. 7.3 Overall standard error trace for the mean baseline sucker height variation with time	83
Fig. 7.4 a)Variation of mean plant LAI with time measured using LAI 2000 plant canopy analyser. Progressive variation in mean pseudostem girth and mean banana height (b and c respectively)with time during the vegetative phase	84
Fig. 7.5 Banana pseudostem height and girth before flowering	86
Fig. 7.6 Variation of a)EH interval and b)LER with controlled irradiance	88
Fig. 7.7 Variation of maximum LAI of the cultivar Williams cultivar with incident solar irradiance	89
Fig. 7.8 Monthly leaf emergence rates (LER) and emergence to harvest (EH) variations of banana with month of year	90
Fig. 7.9 Comparison of monthly leaf emergence rates (LER) with monthly temperature trends ($^{\circ}\text{C}$)	91
Fig. 7.10 Variation of flowering date with different levels of irradiance	93
Fig. 7.11 Variation in heat unit accumulation for banana at Inselele	95

LIST OF TABLES

Table 2.1 Temperature thresholds for banana growth and development (Bower, 1999)	16
Table 2.2 Effect of shade on cocoa productivity (Lachenaud,1985)	18
Table 5.1 Summary of the physical and chemical soil characteristics analysed for Inselele farm	42
Table 5.2 Particle density data for the research site for the different horizons	46
Table 5.3 Volumetric water content, θ_v (%) for soils A and B	48
Table 5.4 Pore size distribution of the soil samples	49
Table 6.1 Microclimatic variations in banana orchard at Inselele farm	70
Table 6.2 Logarithmic function for variation in the ratio of incident irradiance with decrease in plant height	77
Table 6.3 Variation in banana extinction coefficient with canopy LAI	79
Table 7.1. Effect of reduced solar irradiance on LER and EH at Inselele farm	88
Table 7.2 Annual variation of monthly cumulative heat units at Inselele farm	94
Table 7.3 Influence of reduced irradiance levels on banana yield indices	96

LIST OF APPENDICES

Appendix I Datalogger program for Inselele research project	115
Appendix II Wiring map of the Campbell Scientific 21X datalogger	116
Appendix III Calculation procedure for estimating the particle size distribution (source: Gee and Bauder, 1986)	120
Appendix IV Density, surface tension and viscosity of water and viscosity of air at various temperatures (source: Johnston, 2000)	121
Appendix V Baseline sucker height measurements	122

CHAPTER 1

1 Introduction

Radiation transfers energy from the sun to the earth. The conversion of this radiant energy to stored chemical energy, in the presence of water (H₂O) and carbon dioxide (CO₂), takes place at the leaf surface. It is by this stored chemical energy that humans live (Savage, 1980). Ross and Sulev (2000) highlighted radiant energy as one of the many interchangeable forms of energy which plays an important role in various natural processes in the atmosphere, ground surface and plant canopy.

Simmonds (1962) reported that most banana species grow best in the open sun provided water is not a limiting factor. Under deep shade conditions, banana growth is restricted and ultimately the plants will not survive. Most commercial banana production is carried out in tropical areas where dense vegetation and cloud cover affect the amount of incident irradiance. While it is well known that shading does have an influence on plant productivity (Laura *et al.*, 1986; Healey and Rickert, 1998) there is limited literature documented and scanty research carried out on the influence of varying irradiance levels on banana growth and productivity.

Different canopy structures, row width and crop density are known to result in different interactions between the vegetation and its environment (Malcom and Doug, 1995; Israeli *et al.*, 1995) and these factors cause variations in the photosynthetically active radiation (PAR) intercepted by plants. The solar energy used by plants for dry matter production is confined to this limited wave band (PAR range) from 400 to 700 nm. However, the detailed aspects of PAR measurement are not covered in this study.

Commercial shade cloth materials are sometimes utilised in agricultural production as a management technique to protect plants from direct sunlight, wind effects, hail and birds.

Shading can further reduce the incidence of frost damage, decrease water consumption or delay fruit maturation. Researchers have further used shading to simulate shading by plant canopies (Samarakoon *et al.*, 1990). However, little is known about the influence of shade with specific reference to banana productivity. Most commercial banana production takes place in the tropics, where dense vegetation and cloud cover negatively affect the solar irradiance attenuation through the canopy. However, information available on the effect of solar irradiance on banana growth and production is scarce. Radiation interception by banana leaves has not received much attention, partly because of the complexity in describing the canopy regimes in the crop stands. It is worth noting that in addition to decreasing the level of incident irradiance, shading materials are likely to influence the spectral distribution of radiation in reference to the direct and diffuse components (Healey and Rickert, 1998; Savage, 1999, personal comm).

In this experiment, investigation was made on the effect of reducing incident irradiance to the primary canopy to 70 %, 40 %, 20 % solar irradiance and a control 100 % irradiance. This study also took into account the influence of soil water variations on banana productivity. The investigation was carried out on soil water status using sensors such as the ML1 ThetaProbe sensor. The influence of air temperature on the growth of banana in relation to leaf emergence rates (LER), water stress prediction as well as bunch temperature variations have been explored in this research. In an attempt to assess the influence of various microclimatic parameters on banana productivity, energy balance dynamics in a banana orchard were also investigated. These data no doubt provide a basis for interpreting growth responses observed under natural field conditions which can later be used as a yardstick to improve and optimise banana productivity.

The production of dry matter when water is not limiting directly depends on the amount of solar energy intercepted by the crop (Monteith, 1977). The fractional interception of radiation (FI), or canopy cover, is used in crop models to predict the accumulation of dry matter (Campbell and Stockle, 1993) and to partition total evaporation into evaporation from the soil surface and transpiration (Ritchie, 1972). Crop growth can be considered as the product of radiation intercepted by the crop and the efficiency with which that radiation is used to produce biomass, i.e. radiation use efficiency (RUE). The RUE is generally considered constant for a given crop

species (Monteith, 1977; Muchow and Sinclair, 1994). The amount of radiant energy absorbed depends on the canopy size (leaf area index) and the radiation extinction coefficient (k).

Shading results in photo-inhibition and this is particularly important if a tropical crop like banana is grown under subtropical conditions. Dry matter and PAR are linearly related when soil water and nutrients are not limiting (Gallagher and Biscoe, 1978). The slope of this relationship is referred to as the radiation use efficiency (RUE) (Stockle and Kiniry, 1990). Shading results in alteration of the crop radiation environment. Changing of the radiation environment consequently affects the partitioning of assimilates and hence calls for the need to ascertain tolerable irradiance levels for dense commercial productivity or in areas where naturally reduced solar irradiance levels are prevalent.

1.1 Research objectives

The major aim was to simulate the effect of naturally reduced solar irradiance caused by long periods of cloudiness. The effect of shading on plant morphology, growth and potential production was investigated in this study. The principal objectives of this study were to:

1. Evaluate the influence of varying incident solar irradiance levels in a banana plantation on plant vegetative growth, flowering date, yield, rate of leaf emergence, leaf area, plant height as well as pseudostem circumference with reference to a ratoon crop production cycle¹. The aim was to simulate the effect of naturally reduced solar irradiance levels that can be caused by long periods of cloudiness, increased plantation densities or inter-cropping and agro-forestry where mutual shading is of major concern.
2. Assess the relative contribution of canopy attributes such as LAI and canopy extinction coefficient (k), on the growth and development of banana in a relatively non-stressed environment. There is limited information on canopy development, canopy geometry and RUE in banana under non-limiting conditions coupled with good plantation management;

¹Plant growth changes were investigated using a ratoon crop and not a plant crop

3. Investigate the influence of mean canopy and air temperature differentials on banana growth and productivity in a subtropical environment;
4. Evaluate the reliability of the plant canopy analyser (PCA) in estimating the radiation extinction coefficient (k) of a banana canopy;
5. Estimate banana water requirements, water use patterns, soil water content variations by
 - i) Evaluating results derived with the ML1 ThetaProbe frequency domain reflectometer for surface soil water content measurement
 - ii) Assessing evaporation dynamics in a banana plantation.

CHAPTER 2

2 Radiation Interception and Plant Growth Dynamics

2.1 Introduction

Solar irradiance and water play major roles in governing food production. The daily water balance is largely determined by solar irradiance since this is the largest energy source and is able to change large quantities of liquid water into water vapour (FAO, 2000). Crop yields are consequently highly sensitive to solar energy variations. Knowledge of the vertical distribution of solar irradiance levels in a given crop canopy is therefore indispensable in irrigation management. This knowledge is particularly important in areas such as Uganda where the seasonal rainfall is erratic. The vital importance of photosynthetically active radiation (PAR) intercepted by a crop has been reported by Mariscal *et al.* (2000) as the main factor that determines dry matter production. This implies that the supply of radiation sets a limit to potential production.

Potential productivity is determined by the incident irradiance as well as the optical and architectural properties of a given crop stand (Mariscal *et al.*, 2000). Within a heterogeneous stand, the attenuation of radiation resulting from absorption and scattering by leaves creates a vertical gradient of mean irradiance. Further horizontal variation of the transmitted radiation results from the highly directional distribution of the incoming direct solar radiation creating sunflecks and shaded areas (Baldocchi *et al.*, 1986).

A banana orchard is a heterogeneous stand, since the canopy is classified as both primary (for the older plants) and secondary (for the developing suckers). The canopy distribution will also depend on the planting pattern as well as row orientation. Therefore for these types of canopy, interactions between the stand structure and radiation components are complicated issues to deal with in field trials. An analogous situation in olive orchards was reported by Mariscal *et al.* (2000).

The radiation use efficiency (RUE) represents a crop canopy's ability to convert intercepted solar irradiance to dry matter. The RUE is frequently used in simulation models and can vary with a given crop and environment (Malcom and Doug, 1995). The total amount of above ground dry matter produced by a crop in a non-stressed environment is directly related to the amount of intercepted photosynthetically active radiation (IPAR) (Kiniry *et al.*, 1989). This concept relates to one of the principal objectives of this study in assessing the effects of varying intercepted photosynthetically active radiation (IPAR) in banana (*Musa* spp) in relation to plant morphology and productivity. Gallagher and Biscoe (1978) further demonstrated that the relationship between IPAR and the amount of dry matter a cereal crop produced is linear. The slope of this relationship reflects the efficiency of solar energy conversion to dry matter or a crop's canopy RUE. Gallo *et al.* (1993), working on corn, further determined that indirect measurement of IPAR, derived from measured leaf area indices (LAI) excludes interception of radiation by non-green leaves and provides best seasonal estimates of IPAR and RUE. In some instances, intercropped species may compete with bananas for nutrients and water as well as solar irradiance, thus reducing banana yield. Murray and Nichols (1965) reported an analogous situation in cocoa. However, the removal or reduction of shade has been reported to increase yields in fertile soil conditions (Bonaparte, 1967).

Matching of the canopy size with irradiance patterns through agronomic practices can lead to an improvement in crop performance. The spatial distribution of a given canopy is an important factor in canopy-atmosphere exchange processes, and the knowledge of the vertical profile of leaf area serves as a critical input in models of these processes (Ross and Ross, 2000). The amount of foliage in a vegetative canopy can be assessed with measurements of solar irradiance (400 to 700 nm) through the crop canopy. By measuring this attenuation at several angles from the zenith, foliage orientation information can also be obtained. The LAI-2000, marketed by Li-Cor Inc., Lincoln, USA, can conveniently measure diffuse sky irradiance at five zenith angles simultaneously (LI-COR, 1991).

The amount of radiation intercepted by the leaf canopy can be determined from the radiation it receives and transmits. This can be assessed by using tube solarimeters or suitable plant canopy

analysers placed beneath the crop canopy at varying profile distances depending on the type of crop and then compare these measurements to those of the incident radiation above the canopy. Uniform stands are essential to get reliable cost effective measures of radiation interception using tube solarimeters. However, even in a fairly well managed non-uniform crop such as sugarcane, reliable estimates of intercepted radiation are known to require four solarimeters per plot measuring approximately 75 m² (Muchow *et al.*, 1994).

Spot measurements, around solar noon, can be taken below the canopy using a line sensor and compared to incident solar irradiance above the canopy (Gallo and Daughtry, 1986). Spot measurements are usually confined to sunny days to avoid measurement difficulties associated with transient clouds. However, restricting measurements to sunny days with high fractions of direct radiation results in biased fractional interception (FI) estimates that are low. Interpolation between spot measurements also contribute to errors inversely proportional to the frequency of the measurement (Sinclair and Muchow, 1999). Monteith (1994) highlighted the temporal error associated with spot measurements when done at one time of the day, usually midday, because FI is a function of time of day. Therefore RUE estimates based on spot measurements should be examined very cautiously. Various methods have been used to estimate the components of RUE with many associated errors. Regularly calibrated and well-sited sensors are required to measure daily incident solar irradiance. A more appropriate measure is to fit a linear relationship between cumulative biomass accumulation and cumulative radiation interception, with the RUE calculated as the slope of the linear relationship (Sinclair and Muchow, 1999).

2.2 Infrared radiation dynamics

One of the techniques employed in this study involves the utilisation of environmental remote sensing using infrared thermometry to measure canopy and air temperature differentials which are critical in water stress prediction. There are several physical laws that explain the properties of infrared radiation. The first and probably most important of these laws states that there is a positive relationship between radiant efficiency and the temperature of an infrared source.

The proportion of energy transmitted from a heat source by each of the three heat source methods is dependent on the physical and ambient characteristics surrounding the heat source, and in the source's temperature. The Stefan-Boltzmann law of radiation states that as the temperature of a heat source is increased, the emittance increases to the fourth power of its temperature. The Stefan-Boltzmann law for a perfect radiator is expressed by:

$$E = \sigma T^4 \quad 2.1$$

where E , the emittance, is the radiant energy emitted by the surface per unit time per unit area (W m^{-2}) at temperature T (K) and σ is the Stefan-Boltzmann constant ($5.673 \times 10^{-8} \text{ W m}^{-2} \text{ K}^{-4}$). This law can be written in a more generalised form:

$$E_\lambda = \epsilon_\lambda \sigma T^4 \quad 2.2$$

where E_λ indicates wavelength dependence. The quantity ϵ_λ is termed as emissivity, is a function of wavelength and is less than or equal to 1. The emissivity, ϵ_λ , is defined as the ratio of the emittance of a given surface (at a specified wavelength and temperature) to the emittance of a perfect radiator at the same wavelength and temperature (Savage, 1998a). The conduction and convection components increase only in direct proportion with the temperature changes. In other words, as the temperature of a heat source is increased, a much greater percentage of the total energy output is converted into radiant energy (<http://www.industryzone.com>, Internet 2000).

The radiation incident on a leaf is in part reflected, in part absorbed and in part transmitted (Fig. 1.1). This conversion of radiant energy is expressed by the equation: $i = a + r + t$ where i is the amount of radiant energy incident on a given surface and a , r and t the amounts absorbed at the surface, reflected by the surface and transmitted through, respectively (Savage, 1998a). This concept is important and has to be put into consideration if the influence of incident irradiance and how it is transmitted through a given canopy is to be well comprehended.

A critical function of the wavelength of infrared radiation is its ability to penetrate an object. The shorter the wavelength, the greater its penetrating power. Colour sensitivity is yet another characteristic of infrared radiation that is related to source temperature and wavelength. Response time is a characteristic of infrared radiation that is not dependent upon temperature or wavelength. Sources with heavier mass take longer to heat to the desired temperature.

The rate of response however becomes a more important consideration especially when applying infrared radiation to delicate and flammable materials (Industryzone.com, Internet, 2000). The infrared technique is used in detecting leaf surface temperatures and assessing the crop water stress index (CWSI) (Hamlyn, 1999; Savage *et al.*, 1997).

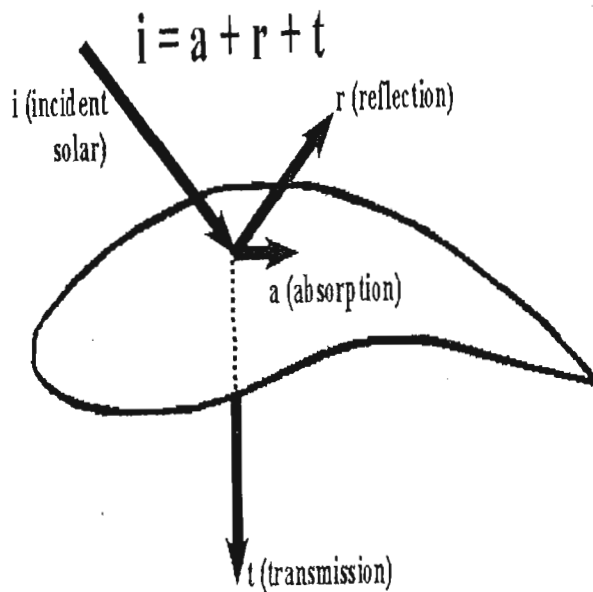


Fig. 1.1 Radiation incident on a non-transparent object such as a banana leaf (Savage, 1998a)

2.3 Leaf area indices

Canopy structure has great importance in studies of the interaction between plants and their environment. In practice, descriptions of the canopy structure are based on a few parameters. The foliage surface per ground area (Leaf Area Index, LAI) is the parameter most often used, since it has been shown to be associated with key ecosystem processes (Francisco *et al.*, 2000). In ratoon crops, the LAI varies from two to more than six depending on the variety (Stover *et al.*, 1987), season (Turner, 1972) and plantation density (Robinson and Nel, 1986). It should be noted that plantation vigour is one of the most important determinants of LAI. Stover (1984) proposed the leaf area index as a useful management guide in Central America for controlling the canopy by

desuckering², a value of 4 to 4.5 was associated with maximum use of PAR. Canopy characteristics such as LAI and transmission of PAR can be correlated to yield levels to determine the optimum density for a given level of plantation vigor (Stover, 1984).

2.4 Plant morphological characteristics and phenology

Banana morphology and phenology helps to predict the production potential of the crop under given climatic, soil and management conditions. Phenology entails the study of plant developmental responses in relation to climate, with particular reference to air temperature (Kuhne *et al.*, 1973; Robinson, 1993). For the majority of citrus, deciduous and tropical fruit tree species, phenological studies are facilitated by specific flowering and harvest times which are determined seasonally. With the banana crop, however, floral initiation seems to be independent of the external factors. Thus flowering and harvest can occur at any time of the year. This unpredictability makes the reproductive phenological studies with banana more complicated, especially in subtropical zones like southern Africa. The tremendous variation in air temperature under subtropical conditions, is a cause of concern for close monitoring of these patterns if optimum productivity is to be achieved. By contrast, Stover and Simmonds (1987) stated that the effect of season in the humid lowland tropics is negligible and that flower distribution throughout the year reaches almost uniform proportions within a few years of planting although some variation could be caused by temporary air temperature decreases. Robinson (1996) reiterated that very few phenological studies have been conducted in the tropics over the past ten years due to lack of relevance. Numerous detailed studies have however been conducted in the subtropics and in Mediterranean countries, where the knowledge of banana phenological cycles is a common tool for focused plantation management decision making. The critical phenological parameters of importance include the planting to harvest period, leaf emergence rates and primary root growth as outlined below.

² Desuckering is an agronomic practice whereby extra suckers are removed from the parent crop to reduce competition for resources such as radiation, water and nutrients. This ensures a vigorous and less stressed crop.

2.4.1 Planting to harvest period

A knowledge of this period is useful for planning when to plant in relation to a desired harvest period. One needs to link this period to the LER each month of the year and ascertain the effects of air temperature on flower initiation and bunch development. The LER has an influence on the flowering pattern. During emergence of the last leaf, floral induction takes place.

2.4.2 Leaf emergence rate

This is a useful index of the vegetative development rate. It is calculated as the number of leaves emerging per month and correlates closely to air temperature. Usually air temperature is used as the measure of temperature because of the difficulties of measuring temperature at the growth point of the plant (Gevers, 1987). In plant crops, LER can vary in subtropics from 0 to 7. Ratoon crops are known to have a lower LER due to competition, especially resulting from reduction in levels of incident irradiance (Stover, 1984). The LER is useful parameter in the subtropics as it indicates when management practices must be applied (Robinson, 1995). Aspects of management include fertiliser application, pest control, propping, mulching, irrigation, desuckering and weed control.

Optimal management should be in the spring months of September and October through the summer months of November, December, January, February, March and possibly April depending on the location and season. It is during this period when the LER is highest as opposed to the winter period when growth inhibition and consequently LER is high. It is therefore important to ensure that all the variables that can be controlled must be optimized during this time (Bower, 1999). It is advisable to manipulate the plant crop and plant accordingly based on leaf growth rates. In winter, air temperature is the major constraint and therefore other management practices such as fertiliser application makes little difference. One could withhold water but this would lead to water stress and yet over-application of irrigation after fertiliser application would lead to leaching (Bower, 1999). In the tropics, management must always be optimal and overgrowth avoided to reduce undesirable plant competition.

2.4.3 Seasonal root growth rates

Primary root extension rate (RER) is yet another index of vegetative growth in bananas. Root development is closely correlated to soil temperature just as LER is positively correlated to air temperature. A soil temperature of below 11 °C causes root growth to stop under subtropical conditions. The maximum root growth rate coincides with an optimum soil temperature of 15 °C (Robinson, 1996). Efficiency of water and mineral absorption depends on new root growth that emerges from the cortex region (Fig. 2.1). Due to the cessation of root development during the winter months there is no need to fertilise during this period and irrigation can be reduced considerably.

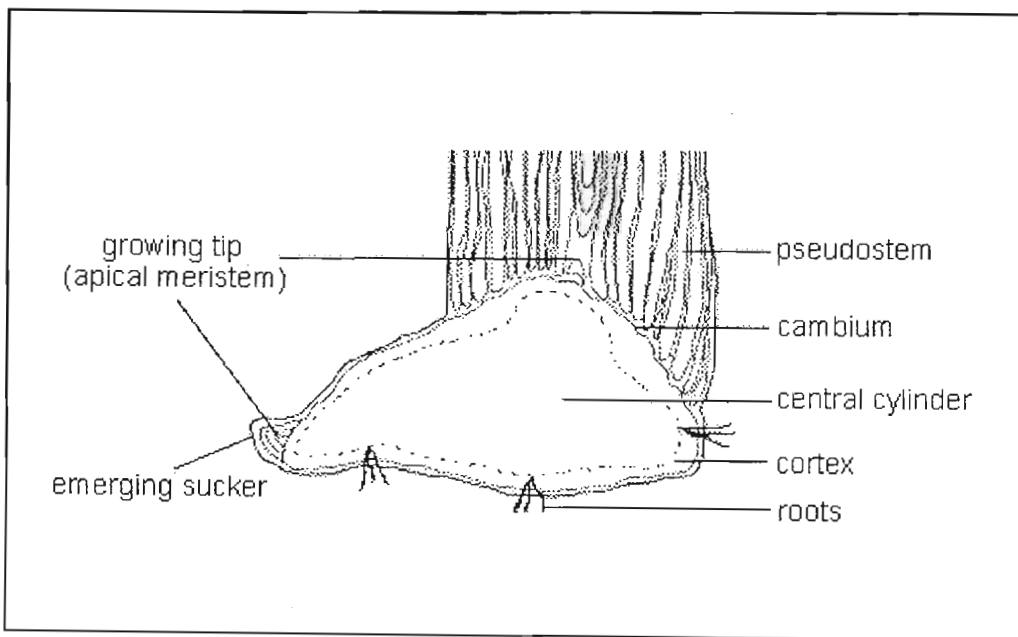


Fig 2.1 Basal morphological features of a banana plant (Rony and Rodomiro, 1997)

2.4.4 Irradiance levels and EH intervals

The strong relationship between increased canopy cover or shade and an extended production cycle time was studied by Robinson (1983). Robinson and Nel (1985) reported that more leaves per plant were produced till flowering under increasing competition for light and on the other hand, leaves were produced more slowly under lower growth temperature conditions.

The banana is a tropical lowland plant requiring uniformly warm and humid conditions for optimum growth and production. In a subtropical climate, the banana growth cycle is prolonged considerably due to cold winter temperatures reducing the LER (Turner, 1972). Phenological responses to climate in the tropical and subtropical zones are best illustrated by comparing LER and EH^3 intervals.

Within the subtropical regions, the banana cultivar 'Dwarf Cavendish' has historically been regarded as most adapted to extremes of climate. The main drawback of the short cultivar is "choke throat" which occurs when normal leaf emergence is restricted hence leading to constriction of the bunches emerging during the winter months (Robinson and Nel, 1985). However, in 1974, the tall 'Williams' which is also a member of the Cavendish subgroup, was released to the South African banana industry, primarily to eliminate choke throat and possibly enhance yield potential.

Phenological studies conducted on 'Williams' banana from 1974 to 1980 at Burgershall in Mpumalanga showed that there was a complete absence of choke throat in 'Williams', thus enhancing yield and quality, but this cultivar suffered from 'November dump'. 'November dump' occurs when flower initiation inside the pseudostem coincides with very low night temperatures during mid-winter. Bunches initiated at this time emerge from the plant from mid-October to mid-November and are usually small and malformed (Robinson, 1996). It is recommended that plantation establishment takes place with use of tissue cultured plants, which are essentially disease-free vigorous suckers.

³EH: Bunch emergence to harvest period

2.4.5 Bunch development

Bunch development is a critical reproductive index in the subtropics. The days from emergence to harvest vary according to the climatic conditions. In Mpumalanga province, northern region of South Africa, it takes 110 days for the November summer flowering to 204 days for the April winter flowering.

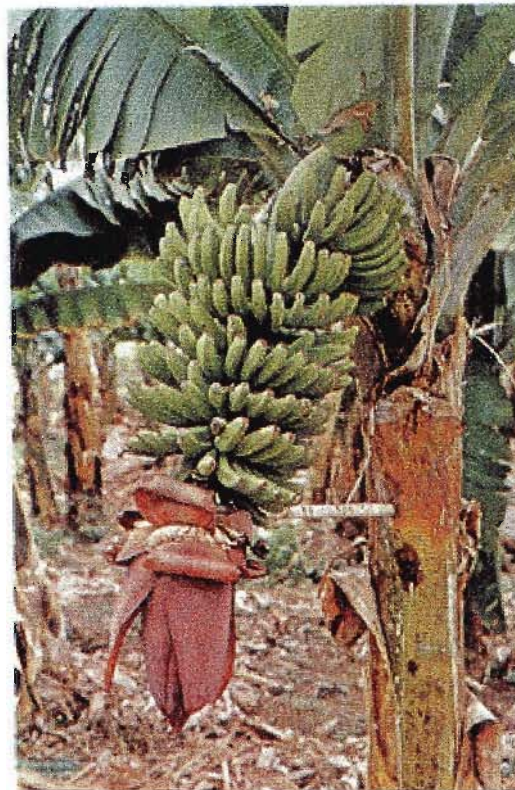


Fig. 2.2 Banana tree with a bunch approximately 12 to 15 weeks after emergence

However the EH interval is almost constant at slightly more than 100 days in the tropics. Heat units can also be calculated to determine the effect of temperature. When the flowering period is known, an expected mean harvest date can be calculated and this calculation can be based on heat units. These calculations can then be modified to suit different geographical areas.

2.5 Temperature effects on plant growth

The banana (*Musa* spp) is a plant of tropical origin but commercially, it is grown from the equator to latitudes of 30° or more. Temperature in the subtropical regions is marginal in winter for banana production, causing reduced growth and slower development. High air temperatures in summer may prevail resulting in short, pale plants and even sun-scorch (Stover *et al.*, 1987).

In a banana plantation, plants of many stages of development are present at one time. An overall assessment is that the rate of development is influenced by air temperature but growth is likely to be more of a function of water supply (Israeli *et al.*, 1995). In the tropics large variations in air temperature do not occur. Thus seasonal variation in growth is perhaps more related to variation in solar irradiance and water supply (Stover *et al.*, 1987).

Field studies investigating the relationship between air temperature and the rate of banana leaf emergence have been made in the tropics and subtropics (Turner, 1972). These indicate an optimum temperature of about 28 °C to 30 °C (mean diurnal air temperature). Turner and Lahav (1983) established a relationship between the temperature of the pseudostem and bunch size and found a lower optimum of 22 °C to 24 °C. They reported an optimum air temperature for crop growth to be about 25 °C to 27 °C. Turner (1972) explored the effects of air temperature on growth of the banana in a range of controlled environments, measured dry matter production, growth rates and partitioning of dry matter as well as leaf development, plant water status and leaf geometry. These data help provide a base for interpreting growth responses observed in the field.

Although bananas are a fairly adaptable crop (Stover and Simmonds, 1987; Robinson, 1996), it is important to have some insight into their production limitations under subtropical conditions. When water is not limiting, the rate of banana growth and development is determined by temperature (Turner and Lahav, 1983; Robinson, 1996). Plant growth slows below 16 °C and it ceases at 10 °C (Table 2.1).

Table 2.1 Temperature thresholds for banana growth and development (after Robinson, 1996; Bower, 1999)

Temperature (°C)	Category	Crop response
0	Actual ⁴	Frost damage, leaf death. Avoid planting bananas
6	Actual	Leaf chlorophyll destruction
14	Mean ⁵	Minimum mean temperature for growth and dry matter assimilation
16	Mean	Minimum mean temperature for development. Leaf area and LER increase
22	Mean	Optimum mean temperature for net assimilation rate (NAR) but LER is reduced. Optimum for flower initiation
27	Mean	Overall optimum for productivity, i.e. optimum balance between NAR and LER
31	Mean	Optimum temperature for LER but NAR is reduced
34	Actual	Physiological heat stress is possible in the afternoon
38	Actual	Growth cessation and heat stress sets in. Stomata close and plants wilt. Leaf temperature can rise to 45 °C if leaves are not cooled using overhead sprinklers
40	Actual	Leaf temperature could approach thermal danger point
47.5	Actual	Thermal danger point for leaf temperatures. Leaves dry out in patches and burns

Symptoms of chilling injury (temperatures below 16 °C but above 0 °C) include failure of the flowering stalk or fruit bunch to emerge from the pseudostem leading to choke throat, development of a dull yellow or greenish-gray colour to ripening fruit, distorted fruit shape, and an increase in fruit rotting. Temperatures below 0 °C result in die back. However, new growth usually sprouts from the underground rhizome with the inception of warm weather (Jonathan and Carlos, 2000)

⁴Actual = the specific temperature at which either heat or cold damage is induced

⁵Mean = mean monthly temperatures related to various growth and development processes $\{(\text{mean maximum} + \text{mean minimum}) \div 2\}$.

2.6 Shade effect on banana growth, morphology and production

Most banana species grow best with full solar irradiance (100%), as long as water is not a limiting factor. Under deep shade, growth is restricted and ultimately the plants die. Stover (1984) observed that when the density of a commercial banana plantation is high and solar irradiance transmitted to the under-story is reduced to 10 % of that above the canopy, growth and production of the plants is severely affected. In a tropical environment, the rate of flowering declines significantly some six months after a period of low solar irradiance (Stover and Simmonds, 1987). Robinson and Nel (1988) observed a prolonged cycle time and a decrease in bunch mass under increased plantation density in the cultivar 'Williams' grown in a subtropical climate. They proposed that the reduction in incident solar irradiance to the secondary canopy contributes to these effects.

In an effort to assess the influence of shade effects on plant productivity, research has been undertaken by conducting studies through comparison of the productivity of cocoa trees grown with and without shade (New Africa, 2000). Results emanating from this research revealed that flowering and the weight of the beans in each pod tended to be lower in the trees grown under shade (Table 2.2). The shade reduced the amount of incident solar irradiance and hence photosynthetic activity which then led to reduced productivity.

Table 2.2 Productivity factors influenced by the presence of shade in cocoa (New Africa, 2000)

Treatments	Shade	Sunlight and fertiliser	Sunlight without fertiliser
Average intensity of flowering/month	504.8a	1346.1c	1103.1b
Number of pods/tree	25.09a	69.6bc	62.21b
Fresh bean weight/pod	87.97a	116.21bc	112.55b

Numbers in a row followed by different letters indicate significant differences at $P=0.05$

2.7 Effect of soil water on banana morphology and productivity

Bower (1999) highlighted that after air temperature, soil water is the most critical variable for banana productivity. Bananas have a high water demand throughout the year and are an important international fruit crop that needs considerable amounts of water for high production (Turner and Thomas, 1998). They are very sensitive to soil water deficits and require water replenishment at frequent intervals. Soil water should not be allowed to fall below 20 to 30 % of the total available water (TAW) if optimum growth and potential are to be maintained (Robinson and Bower, 1987). The relationship between the water status of plant organs and their physiological functions are empirical. However, measurements of the thermodynamic status of water in the tissues of lactiferous plants such as bananas are quite difficult because the lactifers have a positive hydraulic pressure and exude fluids when cut (Turner and Thomas, 1998).

Bananas are grown in South Africa under sub-tropical summer rainfall regions with little or no rainfall during May to September/October. In Port Shepstone, Natal South coast, the average rainfall is below 100 mm/month for approximately seven months of the year (January and April to September). Four of these months are during winter when the crop water requirement is lower. Uniform distribution of rainfall cannot be guaranteed even during the months of sufficient total rainfall (Gevers, 1987). Occasional prolonged droughts also present a problem where there are no facilities for supplementary irrigation.

Recommended rates of irrigation water application in the tropics are 1.2 to 1.4 of the class A pan evaporation (Stover and Simmonds, 1987). It is important to understand the physiological responses of this plant if the desired optimum production potential is to be achieved. Early studies that assess the leaf water status in bananas principally used volumetric and morphological techniques such as relative leaf water content, Φ , or relative leaf folding (Turner and Lahav, 1983). Other workers have examined the effects of soil water deficits on a single process, such as leaf transpiration, E_t (Robinson and Bower, 1987) or seasonal leaf gas exchange (Eckstein and Robinson, 1996).

A cloud of uncertainty remains regarding the best way to measure the water status of plants and some debate over what these measurements mean (Kramer, 1988; Schulze *et al.*, 1988). Despite the shrouded mystery, each of the thermodynamic, volumetric or morphological techniques has its strengths and weakness and can indicate different aspects of the water status of leaf tissues. The widespread use of thermodynamic methods (e.g., leaf water potential, ψ_1) was challenged by Sinclair and Ludlow (1985). These workers pointed out that many of the plant responses to drought occurred at a common leaf relative water content, Φ , and not a common ψ_1 . However, Turner and Thomas (1998) reported that these two descriptors are not mutually exclusive because of 'osmotic adjustment' in droughted plants.

2.8 Crop water use

Water is becoming increasingly scarce. Comparison of water use among cropping systems requires techniques that are robust and capable of being used in a variety of locations. A banana plant requires large quantities of water for maximum productivity. Stover and Simmonds (1987) reported that a tropical banana plantation can consume 900 to 1800 mm water in the ten months from planting to harvest. This amounts to a consumptive use of 3 to 6 mm day⁻¹ depending on the leaf area index, air temperature, humidity, solar irradiance, wind speed and management. Evaluation of water use provides a better understanding of the impact of different cropping practices in both semi arid and humid climates on water use efficiency. However, evaluating differences in water use requires techniques for monitoring daily evapotranspiration. With the increase in demand of water supplies and concerns over groundwater contamination which results from over irrigation, it is becoming increasingly important to know how much water crops need. This information would be most useful if it is supplied in real-time using modern dataloggers as the water loss occurs (Campbell, undated).

Agronomists are faced with the dilemma of reconciling two vital but opposing requirements for crop growth. The need to maximize the absorption of solar radiation conflicts with the need to minimise latent heat exchange. Bower *et al.* (1978) reported an analogous situation in avocado *Persea americana* (Mill) where it was indicated that incoming solar irradiance and internal water

status are crucial stress factors. Monteith (1994) pointed out that, the word *efficiency* is inappropriate to the concept of water use efficiency in that a maximum established by theory or observation does not exist for reference. As a result, the older term *transpiration ratio* is preferable, and it is symbolised by R_T . When the crop water loss includes evaporation from the surface of the soil and crop canopy then the term evapotranspiration R_{ET} is used.

In tropical countries such as Uganda, the water requirements of banana are met by effective rainfall that is fairly well distributed throughout the year. In subtropical regions like South Africa, the water requirements of banana are derived increasingly from supplementary irrigation to avoid water deficits in the dry months. Precautions should be taken to provide for efficient drainage systems to remove excess water that accumulates in the root zone (Robinson, 1996). Banana plants are not flood tolerant. In general, plants may survive 24 to 48 hours of flooding caused by moving water. Stagnant water kills the plants quickly. As a management technique, bananas should not be planted in flood-prone areas. Symptoms of continuously wet but not flooded soil conditions include plant stunting, leaf yellowing and reduced yields (Jonathan and Carlos, 2000).

CHAPTER 3

3 Energy and Water Balance Dynamics

The lack of water is frequently the major factor limiting crop production. The most sensitive plant responses to soil water deficit, and hence those with the greatest potential value for irrigation scheduling, tend to be actual growth rate and stomatal closure. These responses are generally much more sensitive to soil water status than the leaf water potential (Ψ_l) (Davies and Zhang, 1991). An important consequence of stomatal closure that occurs when plants are subject to water stress is that energy dissipation is decreased so leaf temperature tends to increase. The concept of using leaf or canopy temperature as an indicator of plant water stress can help derive a 'crop water stress index' (CWSI) (Hamlyn, 1999; Savage *et al.*, 1997). This index can be based on the difference between canopy temperature, as measured using infrared thermometry (IRT), and that of a 'non-water stressed baseline' representing the typical canopy temperature of a well watered crop.

The available energy at a given surface like a leaf surface for instance, ($R_{\text{net}} - G$) is equated to the consumption of the energy ($\lambda E + H + \mu P + A + J$) (Stone *et al.*, 1974). This energy balance is expressed as:

$$R_{\text{net}} - G = \lambda E + H + \mu P + A + J \quad 3.1$$

where R_{net} is the net irradiance (W m^{-2}), G is the soil heat energy flux density (W m^{-2}), λE is the latent heat energy flux density (W m^{-2}), λ is the latent heat of vaporization (J kg^{-1}), E is the water vapour flux density ($\text{kg s}^{-1} \text{m}^{-2}$), H is the sensible heat energy flux density (W m^{-2}), μP is the energy used in photosynthesis (W m^{-2}), μ is the quantum yield (J kg^{-1}), P is the carbon dioxide density ($\text{kg s}^{-1} \text{m}^{-2}$), A is the advection energy flux density (W m^{-2}) and J is the energy stored in the crop volume (W m^{-2}).

The energy flux density stored in the crop volume (J) or in the crop tissue and in the air inside the canopy is usually neglected. Thus neglecting these components and advection, the energy balance becomes:

$$R_{\text{net}} - G = \lambda E + H \quad 3.2$$

The sign convention is such that the energy flux density towards the crop is positive and away from the crop canopy is negative (Savage, 1998a). Blad and Rosenberg (1974) stressed that strong advection increased latent heat to a point of using more than the available energy flux density which is $(R_{\text{net}} - G)$.

3.1 Canopy transpiration and energy dynamics

The canopy surface temperature is measured indirectly using an infrared thermometer. The net energy exchange at the surface in the banana plantation is important. This energy is used to evaporate water, heat the soil and atmosphere, and some is used as light energy for photosynthesis. Following the treatment of Savage *et al.* (1997), one can determine the sensible heat flux density from the measured canopy and air temperature differential and wind speed u (m s^{-1}). The momentum flux density τ (Pa) is defined by the friction velocity u_* (m s^{-1}) and in addition defines the flux density of momentum. Hence:

$$\tau = \rho u_*^2 = \rho u / r_a \text{ where } \rho \text{ is the air density (kg m}^{-3}\text{) and } r_a \text{ (s m}^{-1}\text{) is the aerodynamic resistance.}$$

Rearranging, we get $r_a = u / u_*^2$

Using the wind profile equation for neutral conditions, we have:

$$u = u_* / k \cdot \ln((z-d)/z_0) \text{ where } k \text{ is the von Karman's constant } (\approx 0.41), z \text{ the height above the surface (m), } d \text{ the zero displacement height } (\approx 2/3 \text{ of the canopy height) and } z_0 \text{ the roughness length } (\approx 1/10 \text{ of the canopy height}).$$

Substituting for u_* in $u = u_* / k \cdot \ln((z-d)/z_0)$ into

$$r_a = u / u_*^2, \text{ we get}$$

$$r_a = [\ln((z-d)/z_0)]^2 / (k^2 u)$$

Since, assuming similarity, the sensible heat flux density $H = \rho_{\text{air}} C_p (T_{\text{canopy}} - T_{\text{air}}) / r_a$

where $r_a = r_{\text{am}}$ (for momentum) = r_{ah} (for sensible heat) and T_{canopy} and T_{air} are the canopy and air temperatures respectively, we get :

$$H = \rho_{\text{air}} C_p (T_{\text{canopy}} - T_{\text{air}}) \cdot k^2 u / [\ln((z-d) / z_o)]^2 \quad 3.3$$

In South Africa, Robinson and Bower (1988), confirmed the extreme sensitivity of bananas to soil water stress, by recording a 35 % reduction in stomatal conductance (Cs) at 25 % depletion of total available water (TAW), equivalent to a soil matric potential of -28 kPa. The stomatal behaviour at a particular level of soil water stress was found to vary greatly according to the vapour pressure deficit (vpd). With the soil water content at field capacity, these workers discovered that summer transpiration rate of 'Williams' bananas in South Africa, peaked between 1300 and 1500 hours, and that no environmental stress was recorded at a peak vpd of 3.5 kPa (ambient temperature = 31 °C; relative humidity = 22 %).

3.2 Crop water stress index

The CWSI is defined in terms of the actual and potential evaporation which can be calculated using the Penman-Monteith method and the surface temperature technique (Idso *et al.*, 1981; Campbell and Norman, 1990):

$$\text{CWSI} = 1 - \lambda E_a / \lambda E_p \quad 3.4$$

where λE_a is the actual and λE_p is the potential latent heat flux density (i.e. potential evaporation). Potential evaporation can be determined using measurements or estimates of the potential vpd, canopy and aerodynamic resistances, and surface to air temperature differentials. The actual to potential evaporation ratio is estimated using the Penman-Monteith method (Campbell and Norman, 1990) as

$$\lambda E_a / \lambda E_p = \{ [\Delta (R_{\text{net}} - G) + \rho_{\text{air}} C_{p,\text{air}} \delta e / r_a] / [\Delta + \gamma (1 + r_c / r_a)] \} / \{ [\Delta (R_{\text{net}} - G) + \rho_{\text{air}} C_{p,\text{air}} \delta e / r_a] / [\Delta + \gamma (1 + r_{cp} / r_a)] \} = [\Delta + \gamma (1 + r_{cp} / r_a)] / [\Delta + \gamma (1 + r_c / r_a)] \quad 3.5$$

where Δ represents the slope of the saturation water vapour pressure vs temperature relationship (kPa K⁻¹) and γ represents the psychrometric constant.

This ratio was used to estimate the CWSI as follows:

$$\text{CWSI} = 1 - \lambda E_a / \lambda E_p = [\gamma (1 + r_c / r_a) - \gamma (1 + r_{cp} / r_a)] / [\Delta + \gamma (1 + r_c / r_a)] \quad 3.6$$

This expression relates a stress index to the fractional change in canopy resistance. Derivation of the above equation assumes that the net irradiance, soil heat flux and vpd will be the same under water stress conditions and under non-water stressed conditions. Soil heat flux is dependent on the soil water content and therefore its magnitude tends to be larger under well-watered soil conditions than under drier conditions. The net irradiance depends on the longwave emitted from the surface and subsequently on the absorptivity, emissivity and reflectivity characteristic of the surface, solar irradiance (I_s) and reflected solar irradiance (rI_s) which also depends on the water content at the surface. In the above equation, the ratio $\lambda E_a / \lambda E_p$ varies from 1 for a well watered crop (where $r_c = r_{cp}$) to 0 for a water stressed crop (r_c) with CWSI varying from 0 to 1.

Alternatively, the CWSI can further be estimated using the actual, potential and non-transpiring (or upper limit) surface to air temperature differential (Hatfield, 1983; Campbell and Norman, 1990):

$$CWSI = [(T_{can} - T_{air})_a - (T_{can} - T_{air})_p / (T_{can} - T_{air})_u - (T_{can} - T_{air})_p] \quad 3.7$$

where $(T_{can} - T_{air})_a$ is the actual measured or estimated surface to air temperature differential ($^{\circ}C$), $(T_{can} - T_{air})_p$ is the non-water-stressed baseline or the lower limit of the surface to air temperature differential under potential conditions ($^{\circ}C$) and $(T_{can} - T_{air})_u$ is the non-transpiring surface to air temperature differential or the upper limit of the surface to air temperature difference when vpd = 0 kPa. The subscripts a , p and u refer to actual, potential and stress conditions, respectively.

3.3 Surface temperature equation

Surface temperatures may be used to estimate latent heat flux density using the energy balance equation with the sensible heat flux estimated from Ohm's law. The sensible heat from the leaf surface to the atmosphere would encounter an aerodynamic resistance for heat (r_{ah}) defined as:

$$r_{ah} = \rho_{air} C_{p_{air}} (T_{can} - T_{air}) / H \quad 3.8$$

where r_{ah} is the aerodynamic resistance for heat ($s\ m^{-1}$), ρ_{air} is the density of air ($kg\ m^{-3}$), $C_{p_{air}}$ is the specific heat capacity of dry air at constant pressure ($J\ kg^{-1}\ K$), T_{can} is the temperature of intercellular spaces ($^{\circ}C$) and T_{air} the air temperature ($^{\circ}C$).

$$\lambda E_{(IR)} = (R_{net} - G) - \rho_{air} C_{p_{air}} (T_{can} - T_{air}) / r_{ah} \quad 3.9$$

where the index (IR) indicates the surface temperature (infrared) technique. This equation depends on the net irradiance, soil heat flux density, surface and air temperature and wind speed. For a larger field of view (FOV), the measured surface temperature may reflect the extent of soil temperature, especially in crops like banana with a mixture of soil and vegetation cover (Luvall and Holbo, 1986). It is worth noting that Hatfield (1984), working on maize and sugarcane, reported systematic over-estimations of evaporation using this technique.

3.4 Evaporation dynamics

In many tropical regions, banana is grown either in wet and dry climates characterized by erratic rainfall patterns and prolonged dry periods of over three months with mean rainfall of less than 500 mm, or in fertile but semiarid lands under irrigation (Ghavani, 1974; Hill *et al.*, 1992). Knowledge of crop water use is important in planning and comparing cropping systems and for proper allocation of scarce water resources during the dry seasons.

Loss of water from the soil surface through evaporation is often a major component in the soil water balance of agricultural systems (Jackson and Wallace, 1999). This is particularly the case for sparse canopies such as banana orchards where full ground cover is not achieved (Allen, 1990). However, micro-meteorological techniques are not suitable for regions characterised by partial, sparse or heterogeneous canopies such as the case in banana plantations or agroforestry systems (Ashktorab *et al.*, 1989). This is because the relative contribution of evapotranspiration from the soil and plant canopy results in small-scale spatial variations. It is a major bottleneck when it is necessary to separate the processes of canopy evaporation from soil evaporation (Jackson and Wallace, 1999). Allen (1990) reported that under such circumstances, soil evaporation can be determined gravimetrically by use of soil microlysimeters.

Microlysimeters were used in this study to determine the daily soil evaporation (E_s) with a minimum alteration of the field. Their use has been extensively described by Boast and Robertson

(1982) as well as by Ham *et al.* (1991). Precaution must be taken regarding the maximum number of days of use of the same sample, minimum length of the microlysimeter and the thermal differences between the sample and the adjacent soil as affected by wall and end cap materials (Savage *et al.*, 1997).

Depending on the prevailing climatic conditions and method of measurement, it is crucial to estimate annual evapotranspiration (ET) of banana in order to evaluate its water use patterns and recharge the profile if found necessary. Estimates of annual evapotranspiration (ET) of banana plantations range from 1200 to 2690 mm (Robinson and Alberts, 1989). The high evaporative demand in semiarid environments combined with a large transpiring surface area and sometimes a fairly shallow rooting system make the crop susceptible to water deficits and lodging. Consequently, banana plants may require irrigation during the dry periods to prevent reductions in yield and plant quality (Norman *et al.*, 1984). This aspect however is not applicable to some equatorial countries like Uganda. Evaporation is a major component of the soil water balance, and can be determined from measurements made on soil, crop and the microclimate. Methods of obtaining estimates of ET range from direct measurement techniques using microlysimeters to energy balance measurements based on the Bowen ratio, flux profile and eddy correlation techniques. Eddy correlation and the surface temperature techniques can provide estimates of evaporation using the energy balance equation and the estimated sensible heat for crops such as grass (Savage *et al.*, 1997).

Evaporation measurements provide valuable information about temporal changes in water use by a given cropping system. However, lysimeter methods can only measure one cropping system at a given location. The use of micrometeorological techniques is preferred because of easy automation and sound theoretical basis. Micrometeorological techniques provide a way of comparing ET rates among different cropping systems and can be more easily located in multiple fields to estimate evapotranspiration from a number of different cropping systems than lysimeters can. However, Jackson and Wallace (1999) reported a new microlysimeter method for estimating evapotranspiration which can overcome this shortcoming, details of which are reported later.

CHAPTER 4

4 Materials and methods

4.1 Site description

The research was conducted on Inselele farm, located at latitude 30° 19'S; longitude 29° 28'E, Mtwalume, in KwaZulu-Natal, South Africa. The site has an approximate slope of 1.5 % and is at an elevation of about 95 m above sea level. The KwaZulu-Natal south coast is characterised by steeply undulating terrain. The valleys are subject to large diurnal and seasonal air temperature fluctuations (Gevers, 1987). The minimum and maximum air temperatures cited for the coldest month, July, were 7.44 °C and 28.5 °C respectively and a mean monthly temperature of 15.64 °C. The hottest month was January with minimum and maximum temperatures of 19.63 °C and 31.24 °C respectively and a mean temperature of 24.32 °C (Table 6.1). The main rainy season is February to April, with little or no rainfall during May to September/October. Bananas require an optimum growth temperature of 27 °C preferably in humid lowland tropical regions where the annual rainfall varies between 1000 mm to 2500 mm (Gevers, 1987). In Mtwalume, with specific reference to Inselele, average rainfall is below 100 mm/month for approximately six months of the year which include January and May to September (Gevers, 1987). However, four of these months are during winter when water requirement is lower (South Africa Sugar Association, 1999). It is therefore evident that the rainfall in the region is relatively low. However, it has a fairly high level of relative humidity, which alleviates the effects of high temperature by reducing the evaporative demand since the vapour pressure deficit would be minimal. This region is also prone to regular off-shore winds (Gevers, 1987).

The plantation was irrigated with a 4-5 day cycle with the drag line method during the dry season. This resulted in a fairly low soil water tension, and ensured that water stress was not a limiting factor. The experimental field (Fig. 4.3) was bordered on the east side by sugarcane, south by sugarcane and shrubs, while the north and west sides were occupied by banana.

The baseline data for the individual banana variates such as height (m), pseudostem circumference (m), number of leaves and leaf emergency rates (LER) were measured at regular intervals of 30 days between day of year (DOY) 215 and DOY 365, 1999, resulting in six baseline data sets. The plants sampled were ratoon suckers in order to determine the impact of three shade levels and a control (solar irradiance with no artificial shade) on morphology, growth and productivity of bananas during their production cycle. The radiation screens (Fig. 4.1), Knitex type were black and had mesh sizes of 30 % knitting, 60 % knitting and 80 % knitting yielding 70 %, 40 % and 20 % irradiances respectively. These were erected on DOY 28, 2000 and sampling continued till DOY 304, 2000. This helped compare plant morphological features before and after the treatments were imposed.

4.2 Experimental design and plot layout

Each treatment plot had 16 banana trees (4 rows by 4 trees in each row) that were sampled from it. Hence there were 48 data plants sampled from each of the three blocks. The banana spacing was at three meters between the tree rows and two meters within the tree rows creating a planting density of 1666 plants ha⁻¹. The plot sizes were 12.5 m by 6 m (75 m²) occupying a portion equivalent to 0.09 hectares of the total area of 0.655 hectares designated to bananas depicted by the shaded section in Fig. 4.3.

During plant data sampling, the key growth stages were closely monitored, namely, the mid vegetative stage, pre-flowering stage, flowering emergence and harvest marked by the beginning of ripening (physiological maturity). Muchow *et al.* (1994) proposed removing of dead leaves at weekly intervals from areas where tube solarimeters and the LAI-2000 are used. The LAI was determined from both the pre-flowering and flowering stages. At least 50 % green leaf material was the yardstick for measurement with a leaf area meter (Sinclair and Muchow, 1999).

Measured growth parameters included plant height, pseudostem circumference (girth), number of leaves and leaf emergence rates. The pseudostem height was measured from the exposed mid corm level to the neck of the bunch stalk at flowering and stem circumference was measured 1000

mm above the exposed mid corm level which was very close to the soil level, about 100 mm shy of the soil surface. The leaf emergence rate (LER) was calculated monthly on the sampled plants with the aid of coloured marker paints. The flowering emergence dates (E) and harvest dates (H) in each plot were closely monitored in order to accurately compute the EH interval. Banana bunch temperature variation was monitored with a HOBO® Temp thermistor datalogger placed in the center of a bunch at 2.4 m height, for the months of June and July 2000, DOY 160 to 190. The Hobo was sealed in two ziplock bags, with much of the air expressed first to ensure a non-condensing environment. Yield parameters took into account the bunch mass which was inclusive of the fruit stalk, hands per bunch as well as the finger length, number and mass from the third hand. Experimental data on pseudostem girth and vegetative phenology was recorded according to the methods described by Robinson and Nel (1988). The canopy extinction coefficient (k) was determined based on attenuation of radiation through the canopy profile and this was then periodically compared to the LAI variations with time (Table 6.2). Soil sampling for analysis was carried out in the top 0 to 300 mm and 300 to 600 mm depths, for particle size distribution and soil water retentivity characteristics. Surface soil profile water content was measured using horizontally inserted time-domain reflectometry (TDR) Thetaprobos at 100 mm. Good contact (lack of air voids) between the wave guides and the soil was emphasized (Topp *et al.*, 1980).

Banana (*Musa acuminata* AAA) cultivar 'Williams' growth was monitored under four varying levels of solar irradiance. Black shade cloth, supported by wooden frames, was used to modify the radiation environment in the plots. The four treatments were replicated three times and were laid out as a randomised complete block design (Fig. 4.2). The four radiation treatments were: an uncovered control equaling 100% of the incident irradiance, covering with black radiation screens of different densities, as explained earlier, were installed above the canopy level (Fig. 4.1) providing 70 %, 40 % and 20 % of the incident irradiance.

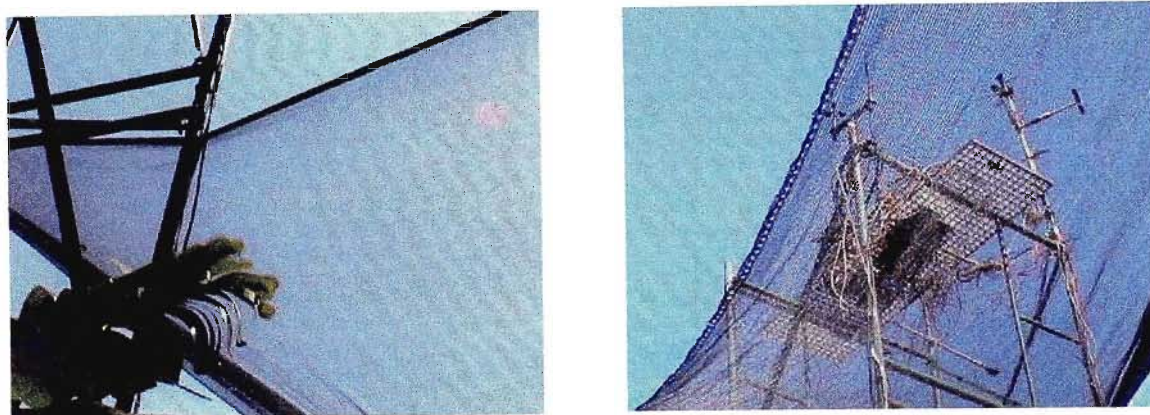


Fig. 4.1 Left: A section of the shade netting (40 % irradiance) above the banana canopy supported by scaffolding; Right: Below the shade netting (20 % irradiance) overview of the equipment for the automatic weather station supported by scaffolding

BLOCK I

1	2	3	4
---	---	---	---

BLOCK II

3	1	4	2
---	---	---	---

BLOCK III

4	3	2	1
---	---	---	---

Fig. 4.2 Plot lay out for research project on Inselele farm

The figures in the plots correspond to the treatments shown below:

1: 100 % irradiance; 2: 70 % irradiance; 3: 40% irradiance; 4: 20% irradiance

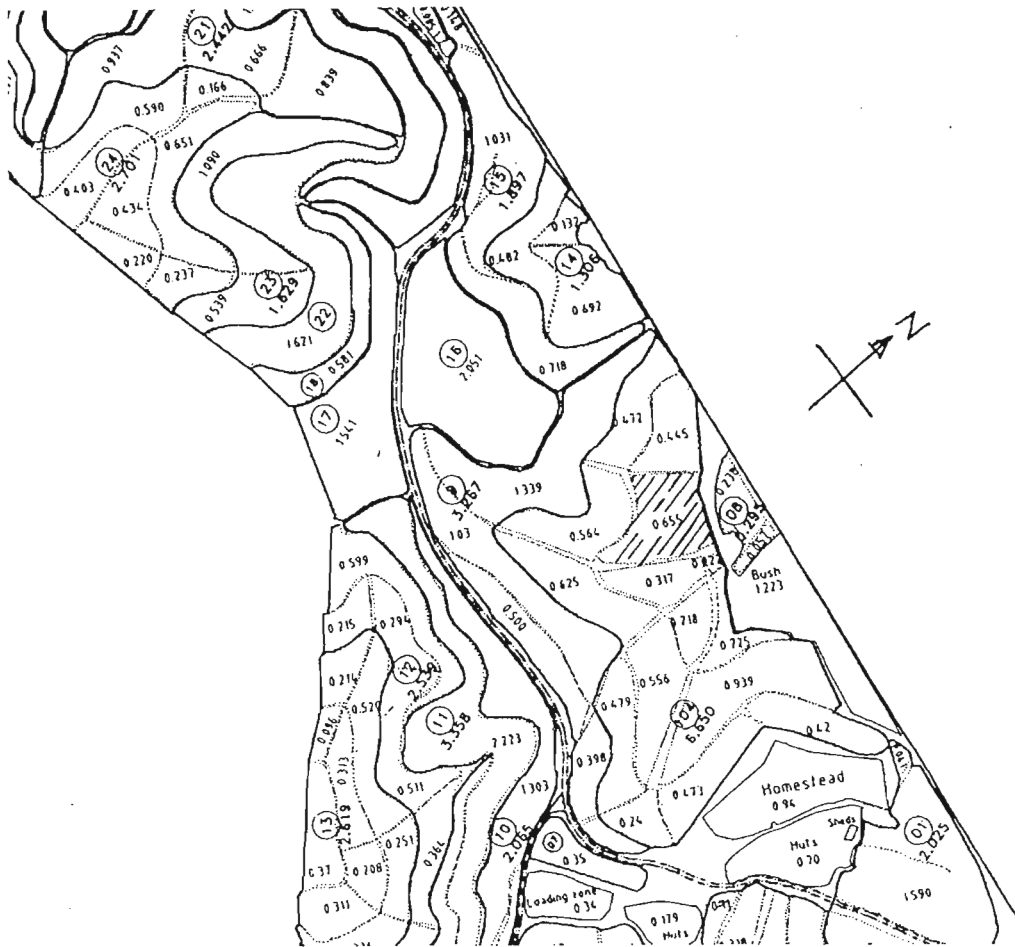
4.3 LAI-2000 plant canopy analyser

Leaf area indices of the banana canopy were measured with a LAI-2000 plant canopy analyser. Measurements were performed at sunset and a single measurement with the LAI-2000 consisted of a minimum of ten numbers, five of which were signals from the five detectors when the optical sensor was above the canopy, and the remaining five were measurements made with the sensor below the canopy. From the transmittances at all the five zenith angles, the LAI-2000 then calculated foliage area (leaf area index, LAI) and foliage orientation (mean foliage tilt angle, MTA). The LAI-2000 collects all necessary angular responses simultaneously. The control unit can also be programmed in remote mode for automatic recording of fractional interception of radiation (FI) and leaf area index (LAI). Gap fractions at five zenith angles were measured by taking an above canopy (A) measurement done in a sufficiently large clearing (radius greater than 3 times the canopy height), followed by the below canopy (B) measurements, and finally another above canopy measurement in the clearing. Multiple below-canopy measurements were made to improve the spatial average readings for the site.

4.4 Microclimatic measurements

An automatic weather station was installed on scaffolding in one of the control plots in the field to perform microclimatic measurements. A Campbell Scientific 21X datalogger was used to execute single ended measurements on all the attached sensors (Appendix III). Air temperature and relative humidity were measured using a Vaisala CS500 relative humidity and air temperature sensor inserted in a six plate Gill radiation shield. The three components of wind velocity were monitored by a three dimensional propeller anemometer (Model-08234, WeatherTronic, West Sacramento, CA, USA). Wind direction was calculated using: $\theta = \arctan (v/u)$. Pulse measurements of rainfall amount were performed by a tipping bucket rain gauge which had a resolution of 0.5 mm. Soil temperature was monitored at the 20 mm and the 60 mm depths with copper constantan averaging thermocouples. Soil heat flux (F_s) was measured at 80 mm depth with two soil heat flux plates. Signals from these sensors were monitored every 30

seconds and averaged, sampled or totaled at an execution interval of 15 minutes using the Campbell Scientific 21X datalogger.



Scale: 1 mm² represents 45.965 x 10⁻⁴ hectares (45.965 m²)

Fig. 4.3 A plan view of a partial section of Inselele farm. The shaded section is the experimental site



Fig. 4.4 Equipment supported by scaffolding , the red oxide metal box housed the datalogger and batteries, on the right background is the 3D propeller anemometer and the right foreground is the RM young anemometer

4.5 Micrometeorological sensors⁸

4.5.1 Net radiometer, IRT and Propeller anemometer

4.5.1.1 Net radiometer

The net radiometer used (Fritschen-type, model Q7.1, REBS, Seattle, WA, USA) has a spectral response between 250 and 60000 nm and a time constant of 30 s. The sensor has a high output 60 junction thermopile with a nominal resistance of 4 ohms which generates a millivolt signal proportional to net irradiance. The thermopile is mounted in glass-reinforced plastic with a built-in level. It has black paint which absorbs the internally reflected radiation.

8

Disclaimer: The use of trade names in this publication is solely for the purpose of providing specific vital academic information. The University of Natal or the author does not guarantee or warranty the products named, and any references to them in this publication does not signify our approval to the exclusion of other products of suitable composition.

When using the net radiometer, getting too close to the canopy causes a shadow problem. It is also possible for the net radiometer to be in a zone where there is a large temperature difference between the surface and the overlying air. This therefore calls for proper placement height for this sensor. Suppose that a net radiometer is placed a distance d from the banana canopy and "sees" an area A . The view factor F for this area A for a distance d between the soil surface and the net radiometer is given by:

$$F = A / (A + \pi * d * d) \quad 4.1$$

where π is approximately 22/7 (Savage *et al.*, 1997).

In order to avoid shading, the sensor was installed with its head facing north and the support arm facing south. It was horizontally mounted using a spirit level with the down dome facing downwards and the upper dome facing upward. The instrument was mounted at 1.5 m height above the canopy surface and approximately 3.5 m from the soil surface. This distance gives a view factor of 0.8 (Eq. 4.1). It allows the sensor to sense the emitted long wave and the reflected solar irradiance from the crop surface. This distance is relatively sufficient to avoid the negative effect of its own shadow. The net radiometer domes are cleaned every 21 to 30 days using distilled water and camel hair brush and they are replaced when need arises. The silica gel is replaced when its colour changes from blue to pink. If the radiometer domes have a "milky white" appearance, they should be replaced and, ideally, the net radiometer recalibrated at the same time. The sensor should be recalibrated at least twice a year (Savage *et al.*, 1997). Net irradiance measurements, R_{net} , are fundamental in the Penman-Monteith equation calculation as will be illustrated in later chapters.

4.5.1.2 Apogee infrared thermometer

Two self-powered high precision Apogee infrared, type K thermocouple sensors were used to monitor leaf surface temperatures. The IRTs have dimensions of 60 mm long by 23 mm diameter with an accuracy of $\pm 1^\circ\text{C}$ when the sensor body and target are at the same temperature. The relative energy received by the IRT detector depends on the sensor field of view (FOV). The FOV is 50° for a full angle with 90 % of the target. The sensors were placed at 1.5 m above the

canopy and this is referred to as a 1.5:1 FOV (Placed at 1.5 meters from the sensor the FOV is 1 m diameter circle) (Internet: <http://www.apogee-inst>, 2000).

A wide FOV integrates a larger target area than a narrow FOV. The distance between the IRT and the object dramatically affects the size of the area viewed. The radiation incident on a typical radiation sensor is determined by the cosine of the angle viewed, which therefore means that the incoming signal is primarily from the region directly in front of the sensor, but there is significant peripheral vision. The error in temperature measurement caused by the peripheral vision depends on the relative radiation emitted by the target and by the surroundings.

There are significant disadvantages to a narrow FOV. They see less of the target and more of their own temperature, which implies that they have increased sensitivity to sensor body temperature. They also have a reduced signal to noise ratio and are more expensive than wider FOV sensors. The best approach therefore is to use the sensor with the widest FOV possible and place it fairly close to the target (Internet: <http://www.apogee-inst>, 2000).

4.5.1.3 Three dimensional propeller anemometer

A three dimensional propeller anemometer (Model-08234, WeatherTronic, West Sacramento, CA, USA) was used to measure wind speed and wind direction. The propeller anemometer is a sensitive precision component wind speed instrument fitted with a structural foam polystyrene propeller moulded in the form of a true helicoid. The propellers have a very linear response for winds above 1 meter per second. Increased slippage occurs down to the threshold speed of 0.2 meters per second. The propeller drives a miniature direct current tachometer which produces an analogue output voltage proportional to wind speed. All voltages were measured every 30 s using a Campbell Scientific 21 X datalogger. The instrument measures both forward and reverse wind flow and the tachometer produces corresponding positive and negative currents. The propeller responds to only the component of wind in the axis of the instrument. The response follows closely to the cosine law. When the wind is at 90° to the axis, the propeller will stop all together.

Caution should however be exercised when handling and working around the instrument as the propellers are fragile and can break with impact (Savage, 1999a).

All propellers are made from a single cavity mould to ensure uniformity and repeatable accuracy. The smaller diameters are made from 230 mm mouldings by cutting with a hot wire. All propellers are then sprayed and balanced using a special acrylic paint. The effective pitch of the propeller is slightly different for each diameter. The 190 mm diameter propeller has a pitch of 300 mm and is considered the nominal and the 150 mm propeller 2 % less than normal. It should be noted that for all full scale calibrations to 6 m s^{-1} or below, maximum accuracy is achieved by using a 0.13 m s^{-1} zero offset and the 300 rev min^{-1} (or 250 rev min^{-1}) calibration point in reference to low speed calibration. For higher ranges use $1800 \text{ rev min}^{-1}$ (or $1500 \text{ rev min}^{-1}$) calibration point without zero offset (Savage, 1999a).

4.5.2 Soil heat flux plates and soil thermocouples

Two soil heat flux plates (Middleton Instruments, Model CN3, Australia) were buried at a depth of 80 mm. Soil heat flux plates, if placed too close to the surface, disrupt energy and mass flow soil, hence burying them at that depth is recommended (Savage *et al.*, 1997). Four thermocouples connected in parallel were used to measure the average temperature in the soil layer above the plates.

The soil heat flux density G was calculated using a spreadsheet (Savage, 1999b) as the sum of the measured soil heat flux using a heat flux plate (G_p) and that stored in the layer above the soil heat flux plate (G_{stored}) calculated from the thermocouples as:

$$G = G_p + G_{\text{stored}} \quad 4.2$$

The stored heat varies with changes in soil temperature (dT_{soil}) during a time interval, the soil bulk density (ρ_{bsoil}), the depth of the layer (Δz), the specific heat capacity of the soil (C_{p_s}) and water (C_{p_w}), and the soil ($\rho_{\text{bsoil}}/\rho_{\text{soil}}$) and water (θ_{va}) fraction in the soil system (ρ_{soil} refers to the soil particle density). All the parameters were related by Hillel (1982) as follows:

$$G_{\text{stored}} = \rho_{\text{bsoil}} \Delta z dT_{\text{soil}} [(\rho_{\text{bsoil}}/\rho_{\text{soil}}) C_{p_s} + \theta_v C_{p_w}] \quad 4.3$$

The soil bulk density was determined as described (Section 5.2.2), the particle density (ρ_{soil}) of 2650 kg m^{-3} was assumed as constant for mineral soil (Hillel, 1982). Two thermocouples were buried horizontally at 20 mm while the other two at 60 mm depths for soil temperature measurement. This measurement is above the soil heat flux plate in order to calculate the stored soil heat energy above the plate. The probes were wired to average these two measurements (Fig. 4.5), but occupied only one datalogger channel (Appendix III). A hoe and spade were used to cut the soil in the vertical and horizontal positions. The soil was then replaced carefully in the formed hole in order to restore the pre-existing conditions and make good contact with the sensors and soil. A diagrammatic illustration of the installation of the soil heat flux plates and soil thermocouples for determination of the soil heat flux density is shown in Fig. 4.5.

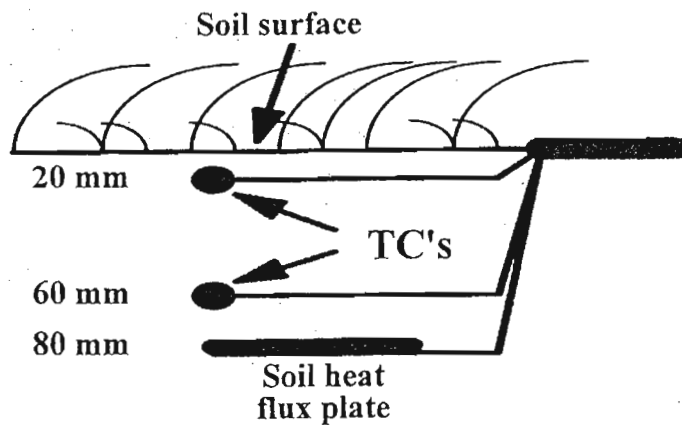


Fig. 4.5 Diagrammatic representation of the placement of a soil heat flux plate and thermocouples for the measurement of $F_{\text{soil}} = G + F_{\text{stored}}$ and the change in soil temperature dT_{soil} over the time interval between consecutive datalogger outputs (typically 15 min) (source: Savage *et al.*, 1997)

4.5.3 ThetaProbe

An ML1 ThetaProbe was used to monitor surface soil water content variations. The sensor rod dimensions were 26.5 mm diameter; 60 mm long, 3 mm rod diameter, four rods, one central. The physical dimensions were: 125 mm long plastic rod at rear of metal rods; additional smaller diameter plastic rod at the rear of this (30 mm long). So the total length of the probe is approximately 215 mm with a 40 mm outside diameter. The sensor wiring is such that the sensor leads - yellow to 1 high, green to 1 low and white to earth. The power leads - red to +12V and blue to earth. The stabilization time is 10 s from the time the power is switched on.

The ThetaProbe (Delta-T Devices, 1995) is essentially a frequency domain reflectometry (FDR) sensor that depends on the frequency shift or ratio between the oscillator (for 100 MHz signal) voltage and that reflected by rods installed in soil. The ratio of the two voltages is dependent essentially on the apparent dielectric constant, of the soil, which is determined by the soil water content. A fifth order polynomial of the sensor analog output voltage V (in volts), can be used to estimate the square root of the dielectric constant of the soil as (Delta-T Devices, 1995):

$$\sqrt{\epsilon} = 1 + 6.19V - 9.72V^2 + 24.35V^3 - 30.84V^4 + 14.73V^5 \quad 4.4$$

The soil water content θ_v ($\text{m}^3 \text{m}^{-3}$) is calculated from the square root of the apparent dielectric constant by using soil calibration constants a_o and a_l :

$$\theta_v = (\sqrt{\epsilon} - a_o) / a_l \quad 4.5$$

where $a_o = \sqrt{\epsilon_o}$ is the square root of the apparent dielectric constant (Eq. 4.5) obtained using the ThetaProbe voltage measured in an air-dry soil. The term $a_l = 1$, is the difference between the square root of the dielectric constant of saturated soil (Eq. 4.5 for the corresponding voltage) and dry soil divided by the soil water content at saturation:

$$a_l = (\sqrt{\epsilon} - \sqrt{\epsilon_o}) / \theta_{vs} \quad 4.6$$

Factory values for a_l and a_o of 8.4 and 1.6 for mineral and 7.8 and 1.3 for organic soil are used respectively. The ML1 ThetaProbe is a fast, precise, automated, non-destructive and an *in situ* measurement technique. However, dielectric-based techniques (TDR and FDR) are influenced by factors that affect the dielectric constant of soil components other than water. For example,

the effect of clay, organic matter, bulk density and soil temperature has been reported by (Topp *et al.*, 1980). High clay content leads to a higher specific surface which restricts the rotational freedom of water molecules, so that its dielectric constant is lower than that of free water because of the strong retention in the soil matrix (Jacobsen and Schjonning, 1993 a, b). Roots, earthworms channels, cracks and stones can also cause small variations in water content estimated using the TDR technique (Jacobsen and Schjonning, 1993b).

4.6 Microlysimeter measurements

Soil evaporation measurements can conveniently be obtained using a microlysimetric method (Savage *et al.*, 1997). Microlysimeter (ML) plastic cylinders (Fig. 4.6) about 125 mm long and 73 mm internal diameter and a wall thickness of approximately 3 mm were used to measure evaporation from the soil. The walls were tapered at the bottom to facilitate insertion into the soil. The practical considerations taken into account for using cylinders quite small in diameter include ease of insertion into the soil and the ability to determine the mass of the microlysimeter on precision balances. After the microlysimeter is weighed, it was then be put in a zip lock plastic bag in order to protect the outside of the cylinder by the surrounding soil.

Steel MLs conduct heat more readily and their surfaces are significantly cooler during the day and warmer at night than either plastic MLs or the adjacent field soil. The walls of the microlysimeter should be constructed of material with low thermal conductivity and the end caps should be designed to maximise thermal transfer between the soil inside and below the ML. A length of at least 300 mm is recommended if measurements are needed at the same location for several days. The one edge should be sharpened and sprayed with teflon (Savage *et al.*, 1997).

Boast and Robertson (1982) reported that the microlysimeter can be repeatedly weighed and replaced in the formed hole as long as it is not kept an appreciable time in the weighing environment, where evaporation may not occur at the same rate as in the field. The soil in the microlysimeter must be discarded when the no flow boundary condition causes evaporation to deviate too much from the reality (Jackson and Wallace, 1999).



Fig. 4.6 Two plastic soil microlysimeters of low thermal conductivity, before insertion into the soil. Aluminium foil with high thermal conductivity is covered at the bottom of the cylinders. In the background is a zip lock bag where the microlysimeters are inserted and then folded in order not to protrude above the soil surface

The microlysimeter method while labour intensive, requires very limited equipment. Evaporation can also be determined under circumstances where traditional methods are impracticable. They can be used at a large number of locations for just a few days where the cost of larger lysimeters would be prohibitive. Evaporation can further be measured as a function of distance from a crop row, under conditions of partial cover and partial shading, or in other situations for which the spatial resolution of traditional lysimeters is too large.

4.7 Data handling and analysis

The experimental data from the datalogger were imported as PRN files into a QPro spreadsheet which was used to manually compute the required numeric variables. Data from the data logger was specifically output at 15 minute intervals and after importation into a QPro spreadsheet for inspection, it was later analysed with both Genstat Release 5 and PlotIT for Windows Version 3.2. Statistical analysis included analysis of variance and Duncan's multiple range test to compare and rank means of the replicated treatments (PlotIT V3.2, 1999; Genstat, 1983).

CHAPTER 5

5 Soil and Soil Water Characteristics

5.1 Introduction

Soil is a complex system, made up of three phases: heterogeneous mixture of solid, liquid, and gaseous material. This complex system is hardly in a state of equilibrium and it alters with changing environmental conditions. It is therefore important to carry out analyses in order to characterise a given soil since different soils have differing attributes which can affect crop productivity. These analyses could include aspects such as particle size distribution, bulk density, aggregate stability, water retention and pore size distribution among others.

5.2 Site soil characteristics

The soil samples used in this study were from a gently undulating area with a slope of approximately 1.5 % that was under banana cultivation, representing a sandy loam soil (Table 5.1). Soil from the 0 to 300 mm horizon had a grey to dark grey colour and was fairly loosely held presenting a crumb like structure. It was humic, friable and had numerous soil fauna such as crickets and earthworms. The soil had a gravimetric water content of 9.2 %. Soil from the 300 to 450 mm horizon showed a gradual shift in colour from black to dark brown, though under very close observation, the colour of the B horizon did not seem to differ from the A horizon. Horizon B had a gravimetric water content of 8.7 %. The soil was sandy and had a low organic carbon content (Table 5.1). It had an Orthic A horizon characterised by waterlogging and anaerobic conditions, weakly structured and was subject to wetness. Soil characteristics indicated that the soil can be classified as a Katspruit form.

The most important cations in soil that are demanded by banana plants are phosphorus (P), potassium (K), calcium (Ca) and magnesium (Mg) (Robinson, 1996). The banana crop is very demanding on K and large quantities are removed from the soil. The ratio of K to Mg (meq/100g)

is approximately 0.25 in sandy soils and a higher ratio of 0.5 would be desirable on heavier soils.

Results (Table 5.1) indicate that the ratio of K to Mg was approximately 0.5, which depicts a relatively high ratio. In the case of high K/Mg ratio, Mg should be applied as dolomitic lime to effect a favourable balance between these cations (Robinson, 1996).

The soil pH ranged from 5.48 to 5.58 in the B horizon while the A horizon registered a higher pH ranging from 5.87 to 5.96. The soil is fairly acidic. The optimum pH requirements of banana have been reported to be in the range between 5.8 and 6.5 (Robinson, 1996). This presents a fairly conducive range within the recommended class for optimum productivity. However, a note of caution is raised to prevent subsoil acidity due to a lower pH range observed in the B horizon. Farina *et al.* (2000), working on South African soils, reported subsoil acidity as an important yield limiting factor and amelioration could be achieved through mechanical procedures of deep lime incorporation and surface applications of gypsum.

Table 5.1 Summary of the physical and chemical soil characteristics analysed for Inselele⁹

Soil horizon	Silt	Clay	Sand	Texture	pH (KCl)	Ca	Mg	K	Na	CEC	O.C ¹⁰
mm	%	%	%			meq/100g	meq/100g	meq/100g	meq/100g		%
A1 ¹¹ 0-300	22	17	61	SL ¹²	5.87	12.3	2.31	1.38	0.11	16.1	3.46
B1 ¹³ 300-600	19	16	65	SL	5.58	6.96	2.45	1.2	0.12	10.7	2.81
A2 0-300	21	17	62	SL	5.96	11.3	2.3	1.09	0.11	14.8	3.4
B2 300-600	18	16	66	SL	5.56	6.91	2.48	1.13	0.11	10.6	2.75
A3 0-300	20	16	64	SL	5.96	10.1	2.34	1.32	0.11	13.8	3.45
B3 300-600	19	16	65	SL	5.48	6.79	2.37	1.05	0.1	10.3	2.68

⁹Six composite soil samples from three depth ranges (Two replications/depth range)

¹⁰O.C: Represents Organic carbon on a wet basis

¹¹Top soil (Horizon A) extends from 0 to 300 mm. Depth range includes A2 and A3

¹²Sandy loam soil textural classification

¹³Sub soil (Horizon B) extends from 300 to 600 mm. Depth range includes B2 and B3

5.2.1 Particle size analysis procedure

Particle size analysis is a measurement of the size distribution of individual particles in a soil sample. This measurement consists of dispersing a sample of soil in an aqueous suspension or determining the settling velocity of the agitated soil particles. This analysis was aimed at determining the particle size distribution in the A and B horizons in the banana field (Table 5.1). A 20 g soil sample was dispersed chemically and mechanically by treating it with calgon solution and ultrasound respectively. The suspension was then made up to 1 liter in a measuring cylinder. The clay and silt fractions were measured with a double pipette by the sedimentation procedure. The samples were then oven dried at 105 °C for 24 hours. Sand fractions were measured by dry sieving through a nest of sieves consisting of 0.500 mm for coarse (coSa), 0.250 mm for medium (meSa), 0.106 mm for fine (fiSa) and 0.053 mm for very fine (vfiSa) in order to determine the sand grade. The suspension of clay and silt was made up to 1 liter by adding distilled water. A 20 ml sample was then taken from the cylinder at zero time after proper agitation to determine the coarse silt (coSi), fine silt (fiSi) and clay. At 4 minutes and 22 seconds another sample was taken at a depth of 100 mm to determine the silt and clay. Further samples were taken after 5 hours and 43 minutes at a depth of 75 mm to determine the clay content. Time and depths were determined using Stoke's law for a room temperature of 23 °C. Samples were taken using a pipette and dried in the oven for 24 hours at 105 °C.

Gee and Bauder (1986) considered the textural classification as a rather arbitrary method. A possibly better method of characterising soil texture is to show the continued distribution of particle sizes. From the data obtained (Table 5.1) and according to the textural class determination (Fig. 5.1), horizon A is classified as a sandy-clay. The soil is predominantly composed of sandy particles and can be considered as a relatively light soil. This condition of soil texture is likely to have low matric water potential and a moderately low capacity to store water. It is not surprising therefore that it has a lower water content than soil B. Table 5.1 depicts horizon B with a higher sand fraction in comparison to horizon A. This is possibly attributed to the slow degradation and weathering of the parent rock with time presenting a slightly higher percentage of finer soil fractions in the A horizon and a higher coarse fraction in the B horizon.

The textural class of this soil is a sandy loam soil (Fig. 5.1).

5.2.2 Determination of soil bulk density

Soil bulk density was determined using a core method (Blake and Hartge, 1986). Undisturbed soil cores, with diameter of 74.45 mm and thickness of 48.80 mm, were taken from the midpoint of depth ranges 0 to 150 mm and 150 to 300 mm. Two samples were taken for each depth to have more representative results owing to soil variability. The samples were dried at 105 °C in the oven for 24 hours and the mass of dry soil in kg (M_{ds}) was determined. The bulk density ($kg\ m^{-3}$) was calculated as follows:

$$\rho_{bsoil} = M_{ds} / V = M_{ds} / (\pi r^2 h) \tag{5.1}$$

where V is the volume of the container (m^3) full of soil, r is the radius and h is the height of the container (m).

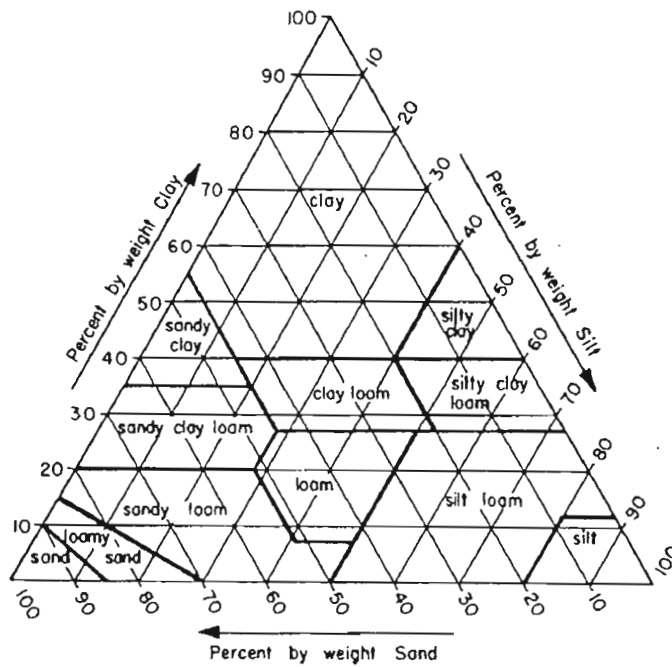


Fig. 5.1 Textural triangle, showing the percentages of clay (less than 0.002 mm), silt (0.002 to 0.05 mm), and sand (0.05 to 2.0 mm) in the basic textural classes (source: Hillel, 1998)

5.2.3 Laboratory determination of soil water content

The volumetric soil water content (θ_v) was determined gravimetrically using the following equation (Hillel, 1982) $\theta_v = \theta_m \rho_{\text{bsoil}} / \rho_w = [(M_{\text{ws}} - M_{\text{ds}}) / M_{\text{ds}}] \rho_{\text{bsoil}} / \rho_w$ 5.2

where θ_m is the mass soil water content ($\text{m}^3 \text{m}^{-3}$), $\rho_w = 998 \text{ kg m}^{-3}$ is the density of water, ρ_{bsoil} is the soil bulk density (kg m^{-3}), M_{ws} is the mass of the wet soil, and M_{ds} is the mass of the oven dry soil. All the masses are expressed in kg.

5.3 Soil particle density

The particle density of soil ρ_s (kg m^{-3}) refers to the density of the solid particles collectively. It is expressed as the ratio of the total mass of the solid particles to their total volume, excluding pore spaces between particles. Units used are usually g cm^{-3} .

5.3.1 Procedure for particle density determination

The particle density of a 25 g soil sample was calculated from two measured quantities, namely mass of the sample and its volume. The mass was determined by weighing, and the volume by calculation from the mass and density of water displaced by the sample. The density dependence of water on temperature was corrected for. The density of soil A was 2311 kg m^{-3} and soil B was 2353 kg m^{-3} . In most mineral soils the mean density of the particles is about 2600 to 2700 kg m^{-3} . The presence of organic matter lowers the value of ρ_s . Since the site is humic, it could probably be the reason why the soils have lower ρ_s of 2311 and 2353 kg m^{-3} (Table 5.2), notwithstanding discrepancies due to experimental errors. The relationship between particle density and bulk density will be discussed further later.

Table 5.2 Particle density data for the different horizons on research site

Top soil	Ms-Ma (g)	Msw-Mw (g)	(Ms-Ma)-(Msw-Mw) (g)	Density(ρ_s) (kg m ⁻³)	Mean(ρ_s) (kg m ⁻³)
A1	25.030	13.94	11.09	2250.4	2311
A2	25.151	14.59	10.56	2374.0	
Sub soil					2353
B1	24.862	14.20	10.66	2325.9	
B2	25.678	14.92	10.75	2380.2	

The particle density (ρ_s) is calculated (Johnston, 2000) as follows:

$$\rho_s = \rho_w (Ms-Ma) / (Ms-Ma) - (Msw-Mw)$$

where:

ρ_w = density of water at temperature observed (used 997.08 kg m⁻³; see Appendix IV)

Ms = mass of volumetric flask plus soil sample corrected to oven-dry condition (kg)

Ma = mass of empty volumetric flask (kg)

Msw = mass of flask filled with soil and water (kg)

Mw = mass of volumetric flask filled with water at temperature observed (kg)

5.4 Soil water retentivity characteristics

The soil water characteristic represents the relationship between soil water content (θ_m or θ_v) and matric potential, ψ_m . It characterises the ψ_m at different water contents for a particular soil. This represents vital information for the description of soil water relations. The characteristics of the curve are influenced by texture, structure and degree of compaction since these factors affect pore size distribution and surface area of the soil. The aim was to derive the pore size distribution, description of the degree of compactness or looseness of the soil and bulk density derivation.

5.4.1 Retentivity determination procedure

Undisturbed cores were subjected to various low (1, 2, 3, 5 and 10 kPa) and high (33 and 100 kPa) suction (Table 5.3). A hanging water column was used for the low suction while a pressure chamber was used for the high suction. The pressure was changed after the attainment of

equilibrium. Each time the cores were weighed before subjecting them to a different suction. Finally the cores were oven dried at 105 °C and re-weighed to determine the water content on a dry mass basis. Bulk density was also determined in order to convert θ_m to θ_v . $\theta_v = (\theta_m \times \rho_b / \rho_w)$. The calculated porosity at saturation was compared to the graphical value (55 %) using the formula, $P = 1 - (\rho_b / \rho_s)$ 5.3

Hence $1 - 1.4055/2.311 = 0.5223 = 52.23 \%$. This value was slightly higher than the measured value. The bulk density (ρ_b) was calculated by determining the mass of the oven dry soil. The height and internal diameter of the soil core was measured with a vernier caliper scale in order to get the bulk volume ($V = \pi r^2 H$) which was expressed as a fraction to the mass of the oven dry soil. The mean value of ρ_b for cores 1 and 2 was found to be 1400 kg m^{-3} . The dry bulk density ρ_b was smaller than the particle density ρ_s . Hillel (1998) reported that for a soil in which the pores constitute half the volume, ρ_b is half of ρ_s . In comparison to the experimental findings, a bulk density of 1400 kg m^{-3} is close to half the determined particle density 2311 kg m^{-3} . In sandy soils, ρ_b can be as high as 1600 kg m^{-3} , whereas in aggregated loams and in clay soils it can be as low as 1100 kg m^{-3} (Hillel, 1998). Since the soil (A) was classified as a sandy soil, these findings are in agreement with the experimental results. The ρ_b is affected by the structure of the soil (its looseness or degree of compaction), as well as its swelling and shrinkage characteristics, which are dependent upon the wetness. Since the ρ_b is low (less than the ρ_s) and with a porosity of 52 % the soil can be considered as fairly loose with minimal compaction and poorly graded.

5.4.2 Retentivity discussion

The retentivity curve (Fig. 5.2) reveals that the soil has an average water content of approximately 50% at saturation with a gradual decrease in the order of approximately 25 % at field capacity. This shows that the soil has a fairly high water holding capacity at saturation and can be regarded as a sandy loam or medium textured soil. The results derived for the field capacity and plant available water content data indicated that the soil has a fairly high volumetric water content (Fig. 5.2) and this could be attributed to the presence of a high water table underlying the subsoil. High water retention could not be attributed to a high organic matter content which was less than 1.8 %, Farina *et al.* (2000), (Table 5.1) neither a dominant clay presence since the clay mineral

fraction is not high enough. A porosity of approximately 48 to 50 % poses no threat to water logging conditions and reflects a soil that is fairly loosely held, friable and easily workable. This is further reflected by an air filled porosity (AFP) of 10 % which is regarded as the yard stick for good AFP (Gee and Bauder, 1986; Hillel, 1998). Good air porosity in soil can influence the extent of root penetrability in search for water which is a desirable attribute in agriculture especially for banana plants since they are shallow rooters (Robinson, 1996; Bower, 1999).

Table 5.3 Depicting volumetric water contents, θ_v (%) for horizons A and B

ψ_m (kPa)	MC1 (g)	MW1 (g)	NW1 (g)	θ_{v1}			θ_{v2}		θ_V average (%)
				Horizon A (%)	MC2 (g)	MW2 (g)	NW2 (g)	Horizon B (%)	
0.1	614.1	416.72	118.1	52.63	605.4	411.42	105.52	47.83	50.23
1	609.6	412.22	119.68	47.64	599.7	405.72	99.82	42.4	45.02
2	604.9	407.52	114.98	44.18	595.1	401.12	95.22	31.35	37.77
3	601.4	404.52	111.48	42.83	592.1	398.12	92.22	27.21	35.02
5	599	401.62	109.08	36.87	589.9	395.92	90.02	21.64	29.26
10	592.6	395.22	102.68	31.24	584.3	390.32	84.42	20.21	25.73
33	591.7	394.32	101.78	26.42	582.6	388.62	82.72	18.84	22.63
1000	-	-	-	17.48	-	-	-	13.53	15.51
1500	-	-	-	16.21	-	-	-	12.51	14.36
M_{ds} (g)	298.64	305.9			307.46	315.8			

where

ψ_m : Matric Potential

MC1: Mass of soil sample + core 1

MW1: Mass of wet soil sample 1- core 1

NW1: Net Mass of water for Sample 1

MC2: Mass of soil sample + core 2

MW2: Mass of wet soil sample 2- core 2

NW2: Net Mass of water for Sample 2

M_{ds} : Oven dry soil (g)

The soil has a high macroporosity which could be attributed to the sandy loam structure and the numerous soil fauna (earthworms) present. These play a role in adjusting the structure of the soil

Table 5.4. Depicting the pore size distribution of the soil sample, horizon A

ψ_m (kPa)	Pore size (μm)	Pore diameter (μm)	Cumulative diameter (μm)	Pore radius limits (μm)	Water content %	% Pore space occupied by that size range
0	-	-	-	-	50.23	
1	146	292	838.99	>146	45.02	5.21
2	73	146.0	546.99	146 to 73	37.77	7.25
3	48	96.0	400.99	73 to 48	35.02	2.75
5	29.2	58.4	231.99	48 to 29.2	29.26	5.76
10	14.6	29.2	46.63	18.25 to 14.6	25.73	3.53
33	4.42	8.84	17.43	14.6 to 4.42	22.63	3.1
1000	0.146	0.292	0.486	4.42 to 1.5	15.51	7.12
1500	0.097	0.194	0.194	<1.5	14.36	-

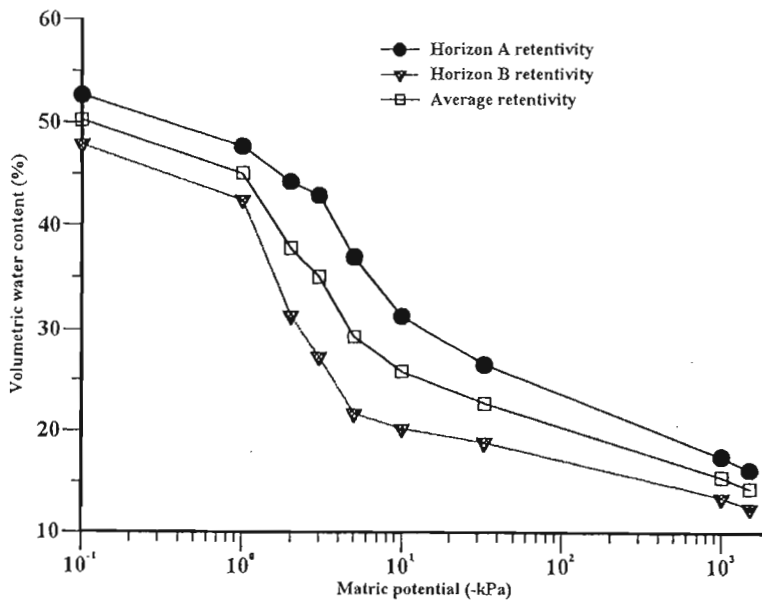


Fig. 5.2. Measured and average¹⁴ volumetric water content θ_w (%) vs matric potential ψ_m (-kPa)

¹⁴average θ_v was determined by getting the mean of the volumetric water content for soils A and B. It has been unconventionally referred to as transitional retentivity

through constant boring of tunnels which in turn results in improved porosity and hence good air and water permeability.

Application of irrigation water would help to recharge the soil water profile since it depicted fairly low θ_v values at -1000 and -1500 kPa. However, it is worth noting that the soil water content did not decrease below 10% even at -1500 kPa. The percentage pore space (Table 5.4) between 146 to 73 μm was obtained from the difference in interpolated water content: $(50.23 - 45.02) \% = 5.21\%$. The rest of the values were also consistently calculated in a similar way.

5.4.3 Soil heat flux measurements

The soil heat flux density is usually small compared to the net irradiance, particularly when the surface is covered by vegetation. There was a very close pattern (Fig. 5.3) observed in the curves for F_{plate} and F_{soil} . The mean soil temperature principally varied between 14 °C and 15 °C for DOY 162 to 168 and it varied between 14 °C and 16 °C for the greater duration of the study (Table 6.1).

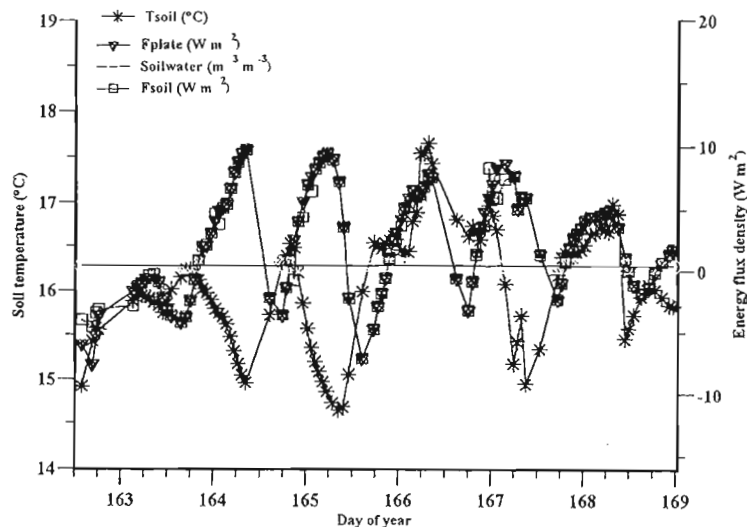


Fig. 5.3 Variation in mean soil heat flux density with soil temperature measured with averaging thermocouples and soil water content measured with a ML1 ThetaProbe for DOY 162 to 168

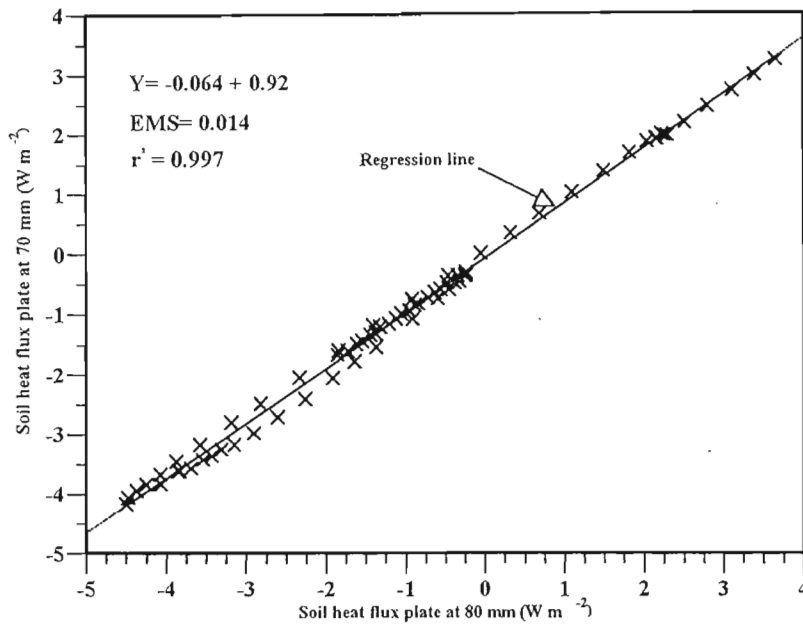


Fig. 5.4 Regression analysis for soil heat flux plate one buried at a typical depth of 70 mm versus soil heat flux plate two buried at a depth of 80 mm. Thermocouples were used to estimate the heat energy flux density stored above both plates

It is evident that there was a fairly constant soil water content recorded during these 7 days. As result, no trends can be depicted between soil water content variation in relation to either G_{plate} or G_{soil} .

A plot of the regression analysis (Fig. 5.4) depicts a close linear relationship between the two heat flux plates that were used for the study. The r^2 relationship is very close to 1 and hence there is a possibility of predicting values of heat flux plate one using the fitted equation (Fig. 5.4).

CHAPTER SIX

6 Microclimatic Variations, Solar Radiation Dynamics and Soil Evaporation Measurements

6.1 Introduction

Orchards and many other land surface types have vegetation that do not completely cover the underlying ground surface (Daamen *et al.*, 1999). For these land surfaces there are at least two distinct and interacting surface components, the overstorey/canopy and the understorey. Soil is a major component of the understorey region. The soil evaporation (E_s) process is determined by the amount of energy available to vaporise water. Solar radiation is the largest energy source and is able to change large quantities of liquid water into water vapour. The loss of water from the soil surface through evaporation (E_s) is often a major component in the soil water balance of agricultural systems in both tropical and sub-tropical regions (Jackson and Wallace, 1999). The potential amount of radiation that can reach the evaporating surface is determined by its location and time of the year.

Due to differences in the position of the sun, the potential radiation differs at various latitudes and in different seasons. The actual solar radiation reaching the evaporating surface depends on the turbidity of the atmosphere and the presence of clouds which reflect and absorb major parts of the radiation (FAO, 2000). When assessing the effect of solar radiation on evaporation, one should also bear in mind that not all available energy is used to vaporise water. Part of the solar energy is used to heat up the atmosphere and the soil profile (FAO, 2000; Daamen *et al.*, 1999).

6.2. Theoretical considerations of evapotranspiration

Evaporation of water requires relatively large amounts of energy, either in the form of sensible heat or radiant energy. Hence, evapotranspiration (ET) is governed by energy exchange at the

vegetation surface and is limited by the amount of energy available and as a result of this limitation, it is possible to predict the rate of ET given a net balance of energy fluxes (Allen *et al.*, 1994). Among the meteorological methods for partitioning the energy balance into its various components include profile (aerodynamic) and combination methods which require various measurements of air temperature, resistance to water vapour flow and the surface roughness as well as other height parameters such as canopy height. The primary energy components which replenish or diminish energy at a vegetation surface are net radiation (R_{net}) from the atmosphere, sensible heat from the equilibrium boundary layer (H), and sensible heat from the soil (G). For an extensive and flat surface, the net irradiance is regarded as the sum of the incoming short (I_s) and long (L_d) wave irradiances, less the short wave reflected (rI_s) and long wave (L_u) emitted by the surface:

$$R_{net} = I_s - rI_s + L_d - L_u \quad 6.1$$

This is commonly referred to as the radiation energy balance equation (Eq. 6.1). The available energy flux density in $J s^{-1} m^{-2}$ or in $W m^{-2}$ is the difference between the net irradiance (R_{net}) and the amount G stored by and entering (or leaving) the soil surface as depicted in Eq. 6.2.

$$\text{Available energy} = R_{net} - G = \lambda E + H + mP + A + J \quad 6.2$$

All these energy terms have previously been defined in the preceding chapters. In reference to Eq. 6.2, the other fluxes or sinks which are present such as P, A and J are relatively small to R_{net} , H and G. The sum of R_{net} , H and G will equal to the flux density of energy that is converted into latent heat energy, λE , during the ET process. Hence the energy balance can be expressed in terms of these four components as

$$\lambda E = R_{net} - G - H \quad 6.3$$

where λE is the latent heat flux density, taken as positive upward from the surface; R_{net} is the net radiation flux density, positive downward toward the surface; H is the sensible heat flux density, positive upward from the surface; and G is the soil heat flux density; positive downward from the surface under day time conditions while the reverse is true during the night (Savage, 1998a).

In Eq. 6.3, the energy terms on the right side of the energy balance can be computed from measured or estimated climatic and crop parameters. The climatic parameters include the short wave and long wave radiant fluxes from and into the atmosphere, effects of horizontal air

movement (wind speed), air and surface temperatures on H , and soil heat fluxes (G). The crop parameters include the resistance to diffusion of vapour from within the plant leaves and stems and the resistance to diffusion of vapour from near the vegetation surface upward into the atmosphere. For both modelling and prediction purposes, the complex structures within and above vegetation canopies and the effects of partitioning of net irradiance and energy within the canopies can be described in terms of simple resistances, namely canopy and aerodynamic resistances. These two resistances, (Fig. 6.1), operate in series between leaf interiors and some reference height above

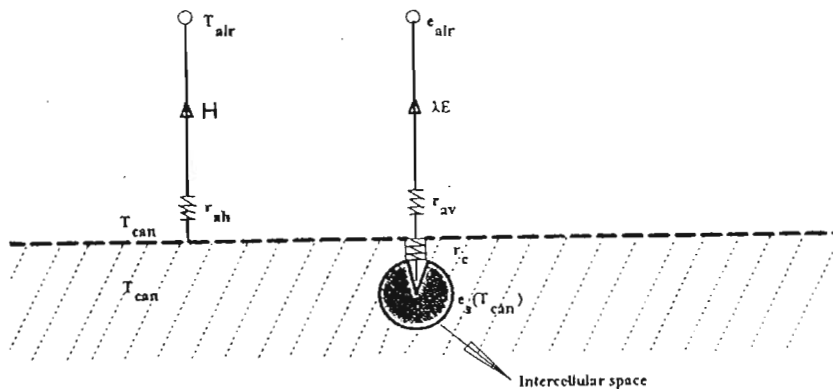


Fig. 6.1 Resistances for the transfer of heat and water vapour (source: Thom, 1975)

the vegetation. Canopy resistance (r_s) can be computed from the resistance of vapour flow through the individual stomata openings and the total leaf area of the vegetation. The aerodynamic resistance (r_a) describes the resistance to the random, turbulent transfer of vapour from the vegetation upward to the reference (weather measurement) height and the corresponding vertical transfer of sensible heat away from or toward the vegetation (Allen *et al.*, 1994). The aerodynamic resistance includes the effects of diffusive resistance through thin molecular layers along leaf surfaces, momentum transfer through pressure forces within the plant canopy, and turbulent transfer among canopy leaves and above the canopy.

Savage, (1998b), reported that it is the aerodynamic resistance that determines the resistance for sensible and latent heat energy transfer from the vegetated surface to the atmosphere. This transfer is accentuated by high wind speeds and reduced if the wind speed is low. Hence, under windy

conditions, r_a is small and large if the atmosphere is calm. Typical trends of these two variables are depicted in Fig. 6.2. The lowest value of wind speed, 1 m s^{-1} registered the highest r_a value of 16.67 s m^{-1} while the highest wind speed of 2.9 m s^{-1} registered the lowest r_a value of 5.75 s m^{-1} . It is not surprising therefore that there is a consistent decline in the point curve, Fig. 6.2, which is in agreement with Savage, (1998b). In summary, r_s is relatively small if the crop is well supplied with water and larger if the crop is stressed, r_i is relatively small if the atmosphere is saturated or nearly saturated with water and large if the atmosphere is relatively dry while under windy conditions, r_a is small whereas under calm conditions, r_a is large (Savage, 1998b).

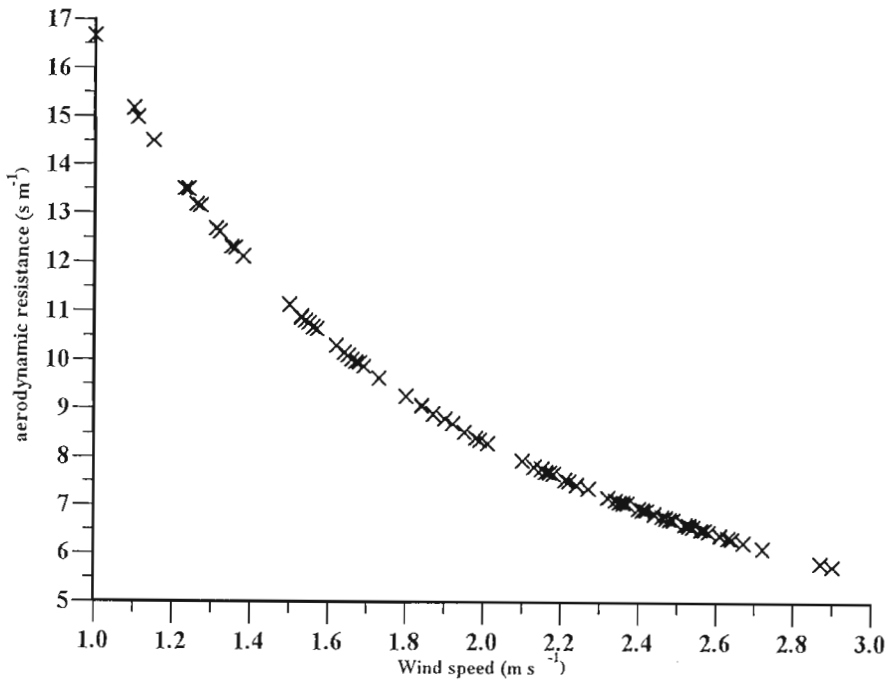


Fig. 6.2 Typical variation of aerodynamic resistance with wind speed for DOY 145, 2000 at Inselele, assuming a crop height $h = 2.5 \text{ m}$, a wind speed measurement height $z = 3 \text{ m}$

The relationship depicted assumes that the neutral wind profile relationship:

$$U = (U_* / k) \ln \{(z-d) / z_0\}$$

may be applied where U is the wind speed (m s^{-1}) at height z (m), U_* the friction velocity (m s^{-1}),

k the von Karman constant (≈ 0.41), d the displacement height (m) where $d \approx 2/3 h$, and z_0 the roughness length (m) where $z_0 \approx 1/10 h$. By combining the neutral wind profile relationship with the momentum flux density written in two forms:

$$\tau = \rho U / r_{am}$$

$$\text{and } \tau = \rho U_*^2$$

where r_{am} is the aerodynamic resistance for momentum ($s\ m^{-1}$) and ρ is the density of air, we get:

$$\begin{aligned} r_a &= \rho U / (\rho U_*^2) = \rho U / [\rho U^2 k^2 / \{\ln\{(z-d) / z_0\}\}^2] \\ &= \{\ln\{(z-d) / z_0\}\}^2 / (U k^2) \end{aligned}$$

$$\text{or } r_a = c / U$$

$$\text{where } c = \{\ln(z-d) / z_0\}^2 / k^2 = 16.669, \text{ for } z = 3\text{m and canopy height } h = 2.5\text{ m} \quad 6.4$$

The value of 16.669, Eq. 6.4, defines the hyperbolic function depicted in Fig. 6.2.

6.3 The Penman-Monteith equation and minimum data set for modelling

This study attempted to discuss the source, measurement and computation of the data required for the calculation of the reference evapotranspiration in a banana orchard by means of the FAO Penman-Monteith method. Rearrangement of the energy balance Eq. 6.3 in terms of parameters R_{net} and G and parameters within the H and λE components using the assumptions for extrapolating temperature and vapour pressure from the weather measurement height to the evaporating surface results in a combination equation of Penman (1948). The meteorological factors determining evapotranspiration are weather parameters which provide energy for vapourisation and removal of water vapour from the evaporating surface.

The Penman-Monteith equation depicts that as far as the determination of surface evaporation is concerned, there are some climatic variables needed to quantify the environment of the plant in micrometeorological terms. The principal climatic/weather parameters used as the minimum data set for modelling that were measured with the automated weather station included solar radiation, air temperature, relative humidity and wind speed. In the discussions that follow, a number of conversions, calculations (Savage, 1999b), and assumptions were utilised to convert these parameters to fit the parameters of the PM equation. The Penman-Monteith (PM) equation

can be written as:

$$ET_o = \{\Delta(R_{net}-G) / \lambda(\Delta+\gamma^*)\} + \{\gamma^*M_w(e_a-e_d) / R\theta r_v(\Delta+\gamma^*)\} \quad 6.5$$

where ET_o is the potential evaporation ($\text{kg m}^{-2} \text{s}^{-1}$ or mm s^{-1}), R_{net} the net radiation (W m^{-2}), G the soil heat flux density (W m^{-2}), M_w the molecular mass of water ($0.018 \text{ kg mol}^{-1}$), R the gas constant ($8.3143 \times 10^{-3} \text{ kJ mol}^{-1} \text{ K}^{-1}$), θ the Kelvin temperature, e_a-e_d the vapour pressure deficit of the air (kPa), λ latent heat of vapourisation of water (2450 kJ kg^{-1}), r_v the canopy plus boundary layer resistance for vapour (s m^{-1}), Δ the slope of the saturation vapour pressure function ($\text{Pa } ^\circ\text{C}^{-1}$), γ^* the apparent psychrometer constant ($\text{Pa } ^\circ\text{C}^{-1}$) (Campbell, undated).

Under reference evaporation conditions, above a crop surface not short of water, the PM equation is applied with a fixed canopy resistance, r_c of 70 s m^{-1} (Campbell, undated) and the other variables (solar radiation, wind speed, vapour pressure deficit and air temperature) would be measured at 2 m above the soil surface. A canopy resistance (r_c), empirically derived using the PM equation (Eq. 6.5) and actual evaporation measurements, do provide a generalised r_c estimate. Furthermore, it is appropriate to have a site specific reflection coefficient for use in the simulation of the net radiation and solar irradiance, air temperature and wind speed measured at 2 m above the canopy all of which are utilised in the computation of actual evaporation.

The PM equation has been successfully employed in numerous crop surfaces such as agricultural crops and pastures (Russell, 1980) and forest canopies (Campbell, undated). For closed canopies, the Penman-Monteith model provides a useful quantitative interpretation of total evaporation measurements. However, doubt arises about the credibility and accuracy of this model under sheltered orchard conditions (Daamen *et al.*, 1999) or when the canopy is completely or partially wet (Rose and Sharma, 1984).

6.4 Field data measurement, data handling procedures and computations

Microclimatic measurements of incident solar irradiance, air temperature, vapour pressure deficit and wind speed were made in an attempt to derive the energy balance terms prevailing in a

banana orchard at Inselele between DOY 230 to DOY 245, 2000. The data were measured directly with sensors attached to a Campbell Scientific 21X datalogger. Excluding stored canopy and biochemical energy and advection, the principle energy terms considered comprised of net irradiance (R_{net}), soil heat flux density (G) and the energy flux density (λE) stored in the soil. However, the exclusion of advected energy from the energy balance with reference to boundary layer measurements has been known to lead to underestimations in the calculation of λE of up to 45 % (Savage *et al.*, 1997).

There were some problems encountered with both the net irradiance and soil heat flux data. The measured net irradiance and soil heat flux data were generally used, and in cases of suspect data, the net irradiance was calculated with the soil heat flux (G) assumed to be 0.1 of the net irradiance (measured or calculated). An altitude of 100 m was assumed appropriate for the site location and this lies within the range of the site altitude (95 m). The daily total reference evaporation values were computed in a QPro spreadsheet (Savage, 1999b) and these were compared to the other measurements such as soil water, crop growth and LAI. The energy balance for the reference evaporation conditions, using the measured net irradiance and soil heat were also empirically derived in a QPro spreadsheet (Savage, 1999b). These reference evaporation values needed a crop factor to convert to actual evaporation. Single (time-averaged) crop coefficients, K_c , and mean maximum plant heights for a non-stressed, well-managed crop in subhumid climates (minimum relative humidity $\sim 45\%$, $U_2 \sim 2 \text{ m s}^{-1}$) for use with the FAO Penman-Monteith ET_o in particular reference to banana were used. A crop coefficient of 1.1 representing the mid crop growth stage was used for this study (Texaset, 2000).

The energy balance calculations were done using the canopy to air temperature differentials and the wind speed to calculate H . This was not possible in cases where the wind speed was zero since it would imply having zero in the denominator. Hence, the equation was modified so that if wind speed was zero then 0.02 m s^{-1} was added to the wind speed. Checking these H values using eddy correlation measurements was beyond the scope of this study. The λE was calculated as $R_{net} - H - G$ unless it was negative. If it was, then it was forced to be zero. The λE data from around DOY 180 onwards were much improved with λE seldom negative during the day.

The reference evaporation was calculated as elucidated in Chapter 2 of this study. It goes without saying that one of the assumptions included an assertion that the banana orchard was a well watered crop and was not short of water. However, under conditions of a normal dragline irrigation system, the water content fluctuated at certain periods.

6.5 Constraints and shortcomings

The interpretation of flux measurements may be complicated by surrounding shelter from neighbouring tree canopy. Hence the source area of an overhead flux may include that from the adjacent orchard block canopy. Standard methods for estimating the effective source area or 'footprint' contributing to flux measurements above a surface (Schmid, 1994) are not suited to measurements at these obstacle shelter heights above an orchard canopy because the shelters affect both wind speed and turbulence above the orchard (McNaughton, 1988; Judd *et al.*, 1996; Daamen *et al.*, 1999). Published work on sparsely covered canopy orchards is quite scanty. However, in a sheltered kiwi fruit orchard, McAneney *et al.* (1992) found the sum of the sensible and latent heat fluxes measured at shelter height was equal to the available energy within the orchard block. However, their kiwi block was surrounded by other similar kiwi fruit blocks and therefore, the analysis revealed little about the source area contributing to the fluxes (Daamen *et al.*, 1999). Singh and Szeic (1980) reported that the major practical problem of the combination method lies in the estimation of the canopy resistance (Aston, 1984).

The FAO-Penman equation in particular has been known to overestimate ET by about 20 % (Batchelor, 1984). It therefore appears that, based on the tendency to overestimate ET and the additional complexity of having crop factors, a different approach to estimating ET with the combination equation is warranted.

It is further worth noting that the definition of ET_0 includes the requirement for an actively growing crop completely shading the ground and not short of water. Validation, therefore, would require a densely planted and maintained crop stand with adequate levels of soil water availability and drainage, all of which demands rigorous management. The aspect of full canopy cover is

however not easily applicable in sparse canopies like banana.

6.6 Results and discussion

The evaporation curve, Fig. 6.3a, showed a similar trend to the wind speed pattern despite an almost constant soil water content. There was a sharp and drastic increment in the soil water content on DOY 179. The rise in evaporation between DOY 178 and 182 is justified by an increase in soil water content after an irrigation, hence there was more water available at the soil surface for evaporation. Furthermore, trends in the energy fluxes, Fig. 6.3a, indicate a rise of these components on these aforementioned days which are prerequisites for evaporation. Curves for the energy fluxes R_{net} and I_s , depicted a similar pattern though, surprisingly, the solar irradiance curve had higher energy flux densities compared to the net irradiance. The minimum values of both R_{net} and I_s , 1.3 MJ m^{-2} and 2.4 MJ m^{-2} respectively, were on DOY 175 no doubt registering one of the lowest evaporation values. Results of DOY 178 also had relatively low values. Typical diurnal trends in both soil evaporation (E_s) and soil water content $\text{m}^3 \text{ m}^{-3}$, Fig. 6.4 a, agree very closely with the general trends observed over time in Fig. 6.3 a and b. Peak values of E_s were observed between 1000 hours and 1200 hours, during this period, wind speed registered high values and both R_{net} and I_s registered the greatest values i.e. 231.4 W m^{-2} and 463 W m^{-2} respectively. The effect on E_s of increasing wind speeds is illustrated by the slope of the curve in Fig. 6.3 a, the more windy the atmosphere, the larger was the effect on E_s and the greater the slope of the evaporation curve. These findings are in agreement with Chay *et al.* (1998) and Monteith and Unsworth (1990). These workers found that the evaporation from a wetted vegetated surface is governed by a combination of incident radiant energy supply and atmospheric turbulence conditions of which no doubt wind speed is the major component of the latter.

In an effort to investigate evaporation trends, one can relate lysimeter evaporation to the available energy. However, this relationship is applicable under high rainfall and humid conditions, usually during the summer months when evaporation is greatest (Savage *et al.*, 1997). It is possible to calculate equilibrium evaporation from air temperature and $R_{\text{net}} - F_s$. Often though, $R_{\text{net}} - F_s$ data are unavailable, there is a correlation with solar irradiance from an automatic weather station

(Savage *et al.*, 1997).

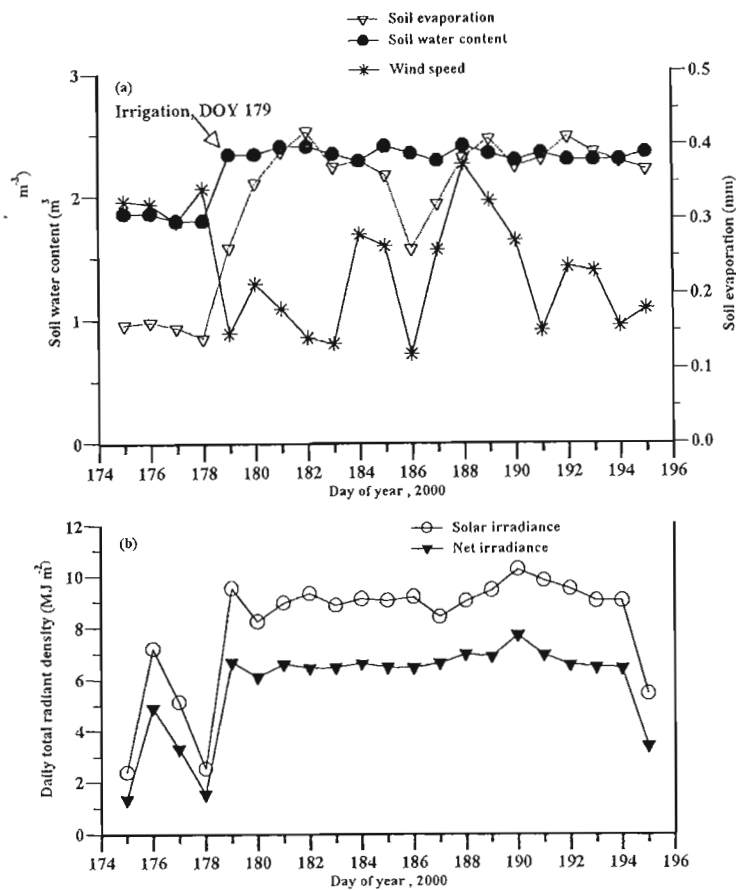


Fig. 6.3 (a) Mean variations in microlysimeter soil evaporation (mm), soil water content ($\text{m}^3 \text{m}^{-3}$) was measured with ML1ThetaProbe at 0.3 m depth and average wind speed (m s^{-1}) for each day with sensor placed at 3 m above the ground and 0.5 m above canopy; b) Daily total radiant density for DOY 174 to 196 inclusive. Mean values were considered between 600 hours and 1800 hours determined with a pyranometer and net radiometers respectively both placed 0.5 m above the banana canopy;

The fraction of available energy partitioned into evaporation is denoted by:

$$\lambda E_{\text{equilibrium}} = \left\{ \frac{\Delta}{\Delta + \gamma} \right\} \cdot (R_{\text{net}} - G) \quad 6.6$$

The constants Δ and the psychrometric constant γ , Eq. 6.6, are usually on the psychrometric charts, the former by the slope of the saturation water vapour pressure at a specific temperature and the latter by the negative slope of the wet-bulb temperature lines.

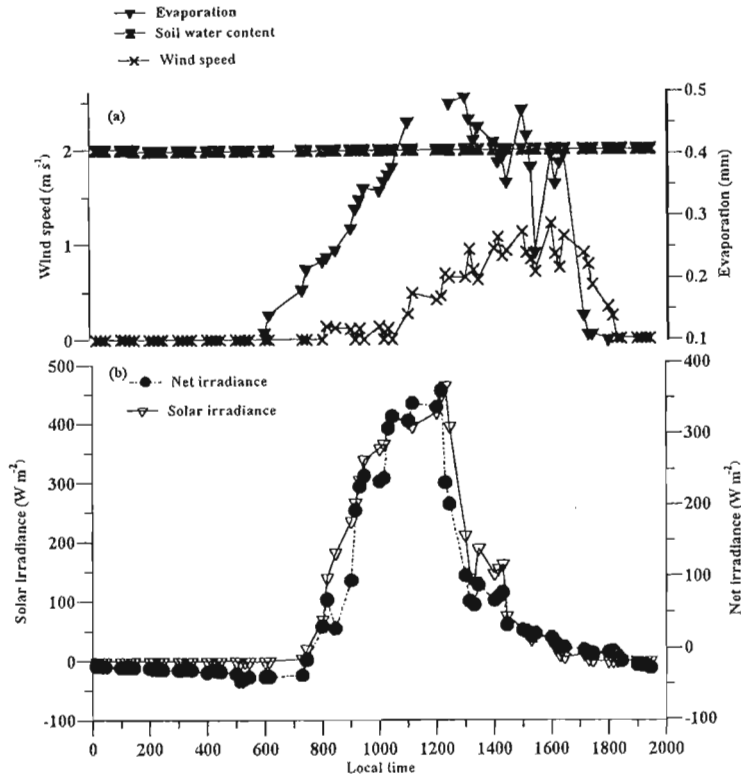


Fig. 6.4 (a) Variation in soil microlysimeter evaporation with wind speed and soil water content measured with a ML1 ThetaProbe; (b) Typical diurnal trends of R_{net} and I_s on DOY 175, 2000. Soil evaporation measurements were taken between 600 hours and 1815 hours

These constants are fundamental to the transfer of water from vegetative surfaces to the atmosphere and are probably as significant as other constants such as the solar constant, gravity and the Universal gas constant (Savage, 1998b). It is unfortunate that this method is only applicable under 'equilibrium conditions' i.e. during calm and wet periods (humid atmosphere and wet canopy) of any year, and not during the more crucial and dry periods which are difficult to measure and this would not be of much importance outside of the rainy season in southern Africa (Savage *et al.*, 1997). The solar radiation absorbed by the atmosphere and the heat emitted by the earth increases air temperature. The sensible heat of the surrounding air transfers energy to the crop and exerts as such a controlling influence on the canopy temperature and the rate of evapotranspiration as well. In sunny and warm weather, the loss of water by evapotranspiration

is deemed to be greater than in cloudy and cool weather (FAO, 2000).

The regression plot for July had a slope of about 0.75, r^2 of 0.49 and an intercept of 11.2 W m^{-2} (Fig. 6.5). This regression suggests that $R_{\text{net}}-G$ could be calculated from measured solar irradiance R_n . The scatter (Fig. 6.5) could have been due to the low values in the soil heat flux data, otherwise most of the plotted values appeared to be close to the 1:1 regression fit line.

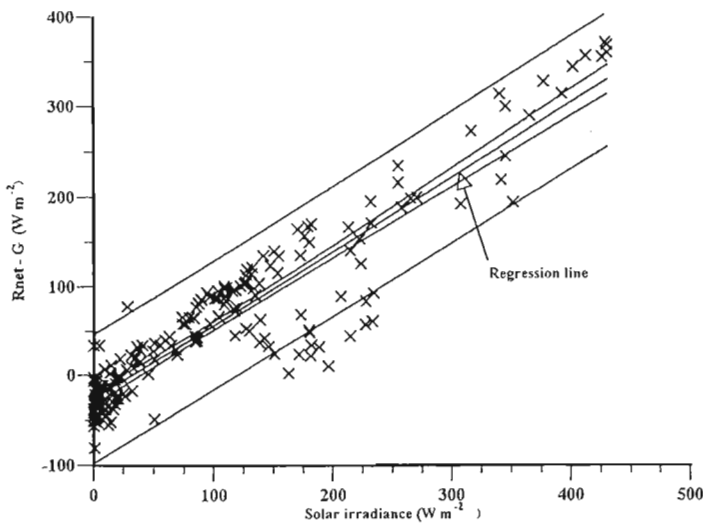


Fig. 6.5 Available energy i.e. net irradiance less the soil heat flux density (W m^{-2}) as a function of solar irradiance (W m^{-2}) for Inselele banana orchard for June, 2000. Data is for the time period 0600 hours to 1800 hours only. Each data point is a 15 minute interval value. The wide limits are the 95 % confidence limits for an estimated single y value and the narrower limits are the 95 % confidence limits for the population mean. Also shown is the regression line

Soil microlysimeter measurements and calculated ET both expressed as mm hr^{-1} (Fig. 6.6) yielded good correlation ($r^2 = 0.978$). Results of the evaporation from the soil microlysimeter depicted a mean difference of approximately 18 % compared to both the soil evaporation and transpiration values.

This is in agreement with the fact that reference evaporation should always be greater than soil evaporation (Fig. 6.7). The soil evaporation is subtracted from the reference evaporation to calculate canopy transpiration (Savage, 2001, personal comm). The diurnal patterns (Fig. 6.7) undeniably conform to these trends. The three curves yielded bell shaped trends with both soil evaporation and canopy transpiration lower than the reference evaporation. Peak trends were principally observed between 1100 hours and 1400 hours. This was primarily due to the energy flux density trends, with Figs 6.9 and 6.10 used as a true analogy though these energy flux density results were recorded on a different DOY. During this time of the day, there is more energy available for evaporation of water. Hence an increment in the energy flux density trends would result in higher soil evaporation and canopy transpiration. Furthermore, on DOY 245, there was a mean bias of approximately 40 % overestimation of the calculated ET compared to the soil microlysimeter measurements. This is in agreement with the findings of Allen *et al.* (1994), Jensen *et al.* (1990) and Batchelor (1984) who reported an overestimation of 35 % of ET by the Penman method, working under humid locations during peak months.

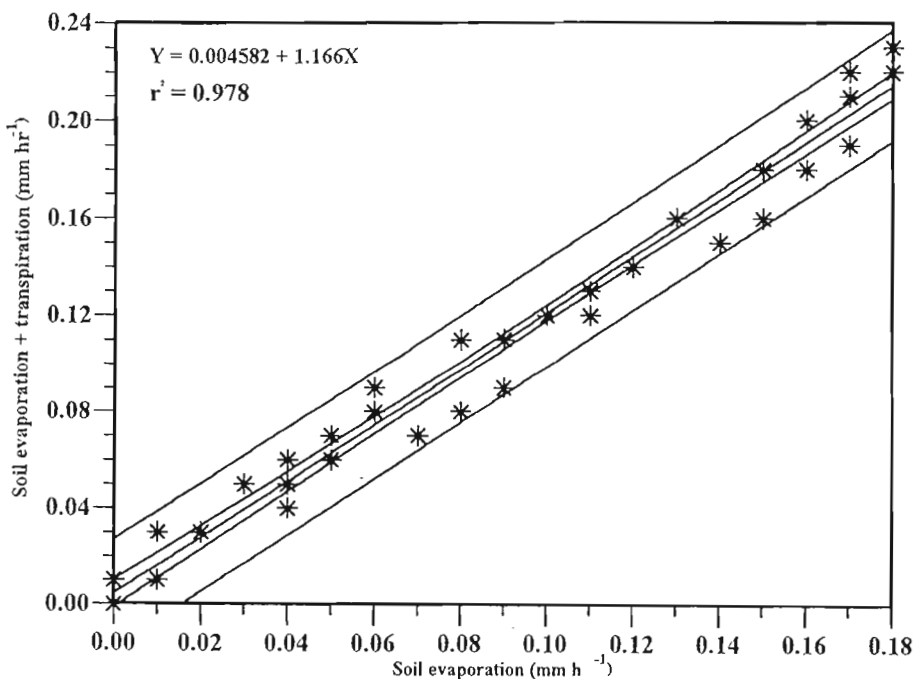


Fig. 6.6 Hourly measurements of soil evaporation and transpiration regressed against soil evaporation for the 2.5 m banana canopy at Inselele for DOY, 240, 2000

The anomaly of results in this study could probably be attributed to the Clothesline effect (Savage, 1998b), whereby in the case of row crops, as the situation in Inselele, usually there is a darker interrow with a lower evaporation rate. The air above the interrow is consequently warmer than the air within the canopy. In the presence of wind, the hotter interrow air is blown over the cooler crop row, hence increasing the crop evaporation rate. Low equipment precision resulting in inaccuracy in weighing of the soil microlysimeters could also be implicated.

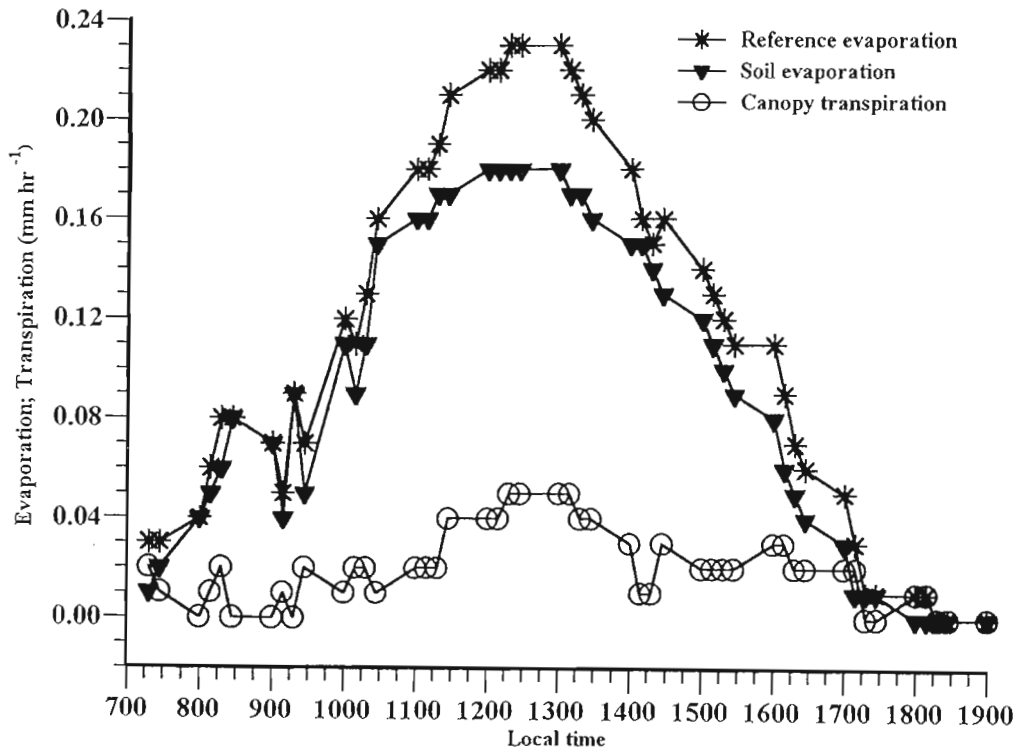


Fig. 6.7 Diurnal variation in reference evaporation, soil evaporation and canopy transpiration trends with local time, on DOY 240

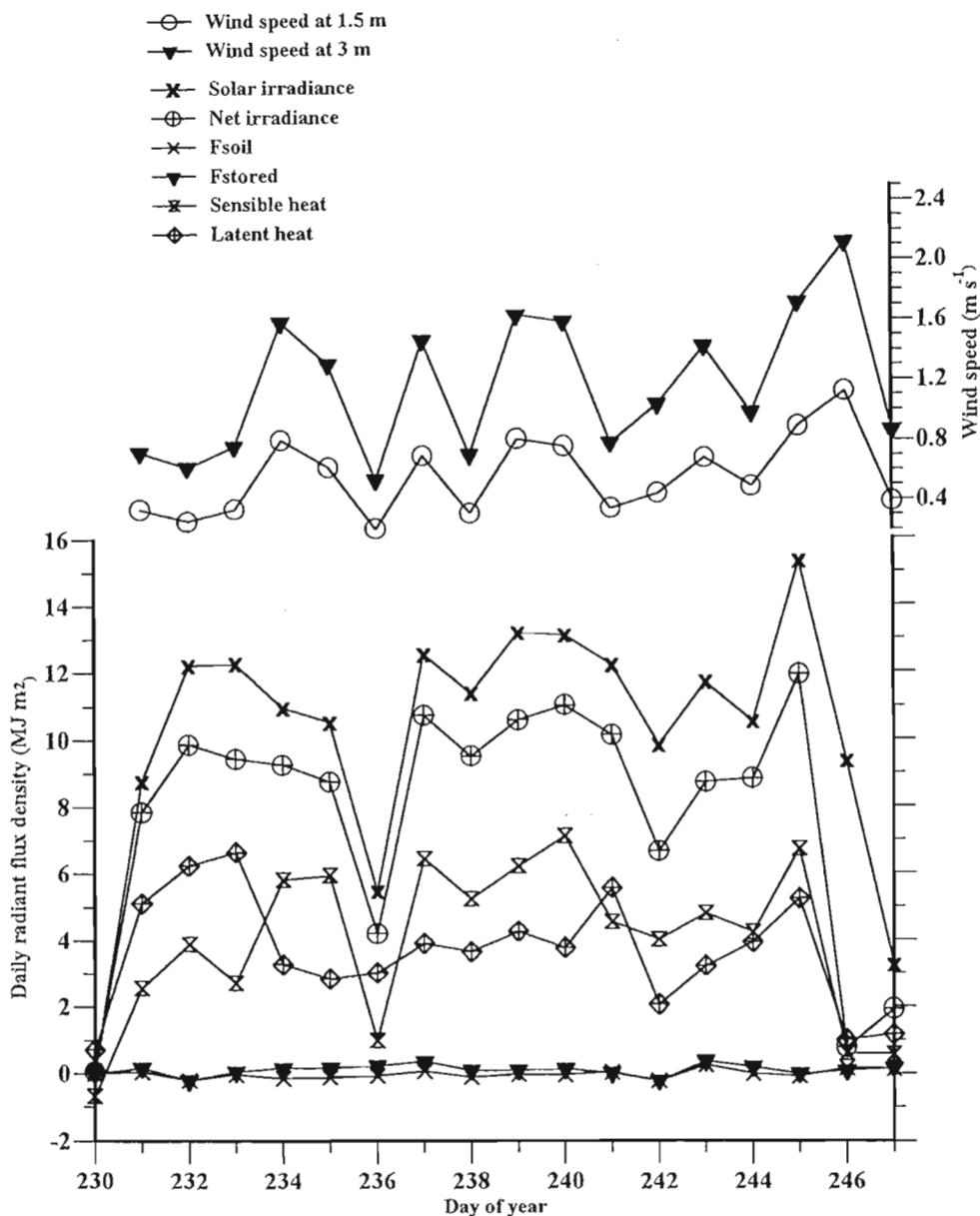


Fig. 6.8 Components of the shortened energy balance (solar and net irradiance, latent heat flux density and sensible heat flux density) (left hand y-axis, MJ m⁻²) as a function of DOY (230 to 247), inclusive, 2000 for Inselele farm for times 0600 hours to 1800 hours. The right-hand y-axis indicates the wind speed (m s⁻¹); (b) the mean daily wind speed profile trends (DOY 230 to 247) with sensors placed at 1.5 meters above ground (within orchard) and 3 m above the ground (0.5 meters above canopy). Both sensors were RM Young 03001 models

Generally, the Bowen ratio, β , was greater than one ($\beta > 1$) except for Doy 230 to 233, 236 and 241. Similar curve trends (Figs 6.8 and 6.9) were observed for both the net irradiance (R_{net}) and sensible heat (H) curves with H consistently lower than R_{net} . A decrease in R_{net} appeared to diminish the λE since this process requires 2.44 MJ of energy for each kg of water vapourised at 25 °C. Hence, a decrease in the R_{net} would necessitate a decline in the λE as well as H (Fig. 6.9).

The magnitude of the boundary layer conductance, is controlled by wind speed and canopy characteristics such as plant height and density which determine canopy roughness (Chay *et al.*, 1998; Roberts *et al.*, 1993). This study did not accommodate investigations into boundary layer conductance but however focussed on the physical environmental changes such as variable plant heights and an increase in canopy gaps. These irregularities result in a very heterogeneous canopy. An effort was however taken to investigate the trends of wind speed variability with profile/height (Fig. 6.8). Wind speed profile measurements showed a consistently lower value for the 1.5 m height compared to the 3 m height. The highest mean wind speed for the 1.5 m height profile was only 0.78 m s⁻¹ as compared to a mean value of 1.52 m s⁻¹ for the 3 m height profile. This probably suggests that there is a higher canopy roughness coupled with pseudostem barriers within the 1.5 m height of the orchard as opposed to the 3 m height profile where there were less bulk leaves and no pseudostem effect.

Trends in H appeared to respond positively to wind speed patterns, Fig. 6.10 and peak values in both variables were achieved at 1100 hours and 1600 hours.

When bunch temperatures, T_{max} and T_{min} were extracted from the data, trends (Fig. 6.11) depicted that the bunches had a lower maximum of about 3 °C and a greater minimum of around 2.6 °C when compared to air temperature variations. However, the trends in both mean bunch temperature and mean air temperature (Fig. 6.11) showed a similar pattern with mean bunch temperature expressing an overall approximate mean lag of 2 °C compared to the mean air temperature. Patterns of wind speed variation related to both bunch and air temperature trends. The overall mean air temperature for an optimum balance between growth (assimilation) and development (leaf emergence) is reported to be about 25 to 27 °C (Robinson, 1996; Stover and

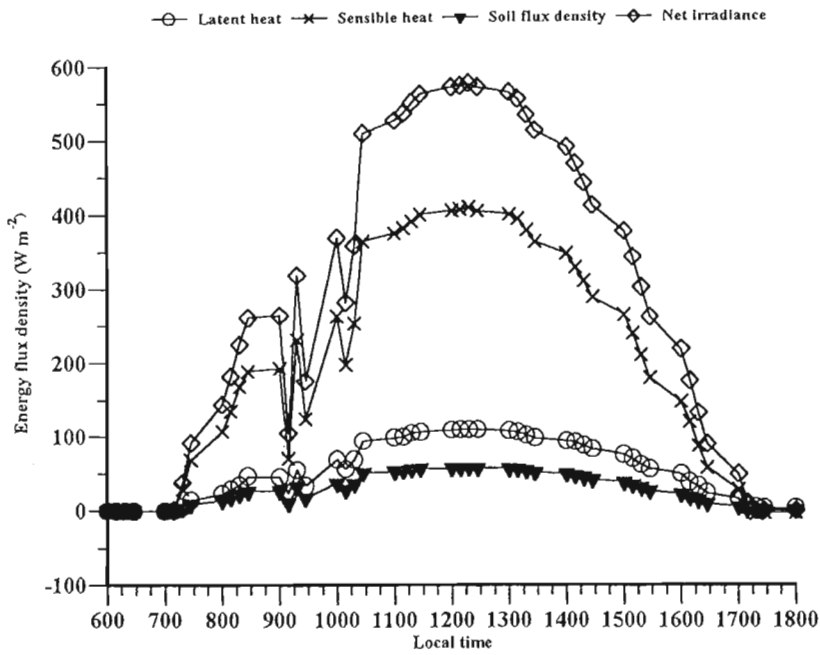


Fig. 6.9 Diurnal variation in some of the components (net irradiance, latent heat flux density and sensible heat flux density) of the shortened energy balance (left hand y-axis, $W m^{-2}$) as a function of local time for DOY 231, 2000 for Inselele farm

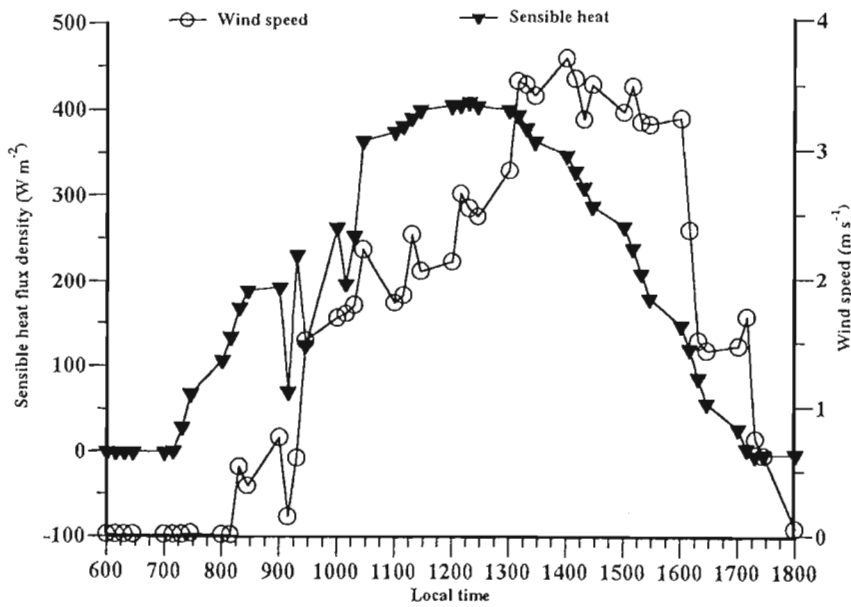


Fig. 6.10 Diurnal variation in sensible heat flux density and wind speed as a function of local time for DOY 231, 2000 for Inselele farm

Simmonds, 1987). However, the mean air temperatures presented in Table 6.1, are below the accepted reported mean temperature range optimal banana productivity (Robinson, 1996).

The canopy and air temperature differentials were often negative at night which seemed fairly reasonable. However, surprisingly, the temperature differentials were sometimes negative during the daytime, especially for the DOY 144, 2000 (not graphically depicted). A negative daytime differential meant that the sensible heat flux was directed toward the canopy and therefore that the latent heat flux exceeded the net irradiance. This suggested that there was advection. Blad and Rosenberg (1974) also stressed that strong advection increased latent heat to a point of using more than the available energy ($R_{\text{net}} - G$).

Contrary to the trends observed in the bunch temperature variation curves, the canopy maximum temperatures (Fig. 6.12) were consistently higher than the maximum air temperatures during this measurement period by 2 °C and had a consistently lower minimum temperature compared to the air temperature.

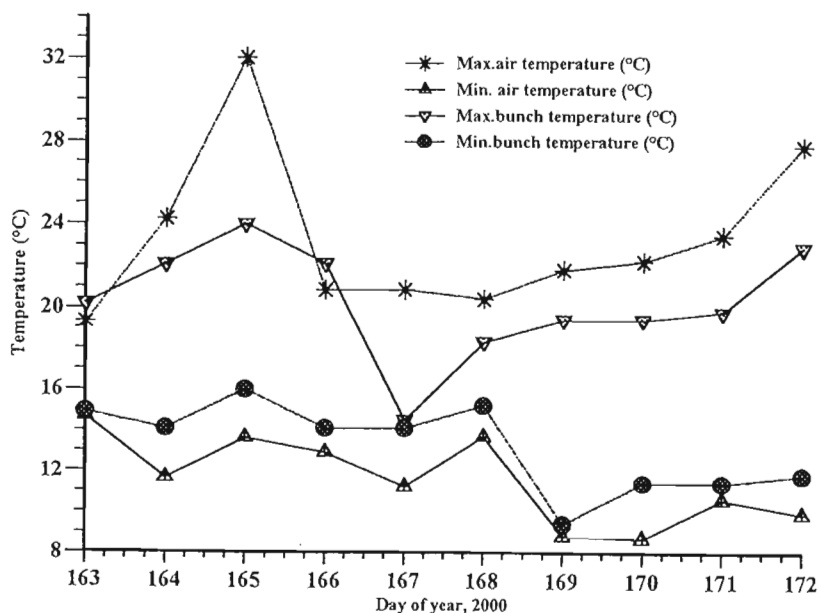


Fig. 6.11 Variation of minimum and maximum air temperatures and bunch temperatures for DOY 162 to 173, 2000, inclusive for Inselele farm

The canopy temperatures had a mean temperature of 3 °C less than the mean air temperature. In cases where higher canopy temperatures were recorded compared to air temperature, this signalled that water stress was setting in, though the magnitude of the difference, barely 1 °C, was not great enough to pose a significant threat.

Trends from Fig. 6.13, indicate that the canopy to air temperature differential (Tdiff) was sensitive to variation in wind speed as this registered the highest value (2.36 m s⁻¹) when wind speed was greatest (2.22 m s⁻¹). However, though wind speed plays a major role in vapour removal, this appears as a rather simplistic argument since wind speed in solitude does not influence water vapour removal from the vegetative surface. It involves a combination of various parameters such as solar irradiance and water vapour pressure deficit among others.

Table 6.1 Monthly summary of the microclimatic variations in the banana orchard, Inselele, 2000

Month	Air temperature (°C)			Solar irradiance (MJ m ⁻²)		Wind speed (m s ⁻¹)		Soil temperature (°C)
	Mean	Max	Min	Mean	Max	Mean	Max	Mean
January	24.3	31.2	19.6	258.7	497.7	1.2	2.9	16.5
February	23.9	30.9	19.2	226.1	512.5	1.3	3	16.2
March	23.9	29.4	18.8	192.8	612.8	1.2	2.9	15.8
April	17.3	27.5	16.6	289.5	597.2	1.4	2.7	15.3
May	16.4	26.5	8.1	400.2	949.1	1.5	3.4	14.4
June	14.7	28.2	7.7	407	890	1.4	2.9	15.4
July	16	28.5	7.4	250.5	480	1.3	2.9	13.9
August	18.3	30.8	10.9	261.8	526.8	1.7	3.4	14.5
September	18.9	30.8	11.8	268.4	587.4	1.6	2.9	14.9
October	19.2	31.1	13.6	312.4	694.6	1.6	3.3	15.5
November	22.8	31.8	15.7	356.7	782.6	1.4	3	16.3
December	24.1	32.6	17.2	367.1	795.3	1.4	2.7	16.5

Analogous to these observations, were the variations depicted in canopy temperature (Fig. 6.14). The mean canopy temperature predominantly remained cooler than the air temperature. This is further evidenced by the negative differential temperature (Tdiff) values. The wind speed pattern

(Fig. 6.14) indicated that wind speed greatly contributed to the nature of Tdiff curve.

However, a plot of the regression relationship between the mean bunch temperature and air temperature (Fig. 6.15) showed a fairly large scatter, possibly due to differences in sensor specifications since two different temperature sensors were utilised. Furthermore, one may expect that the bunch temperature, as measured by a Hobo Temp datalogger in a zip lock bag, would be less than the measured air temperature.

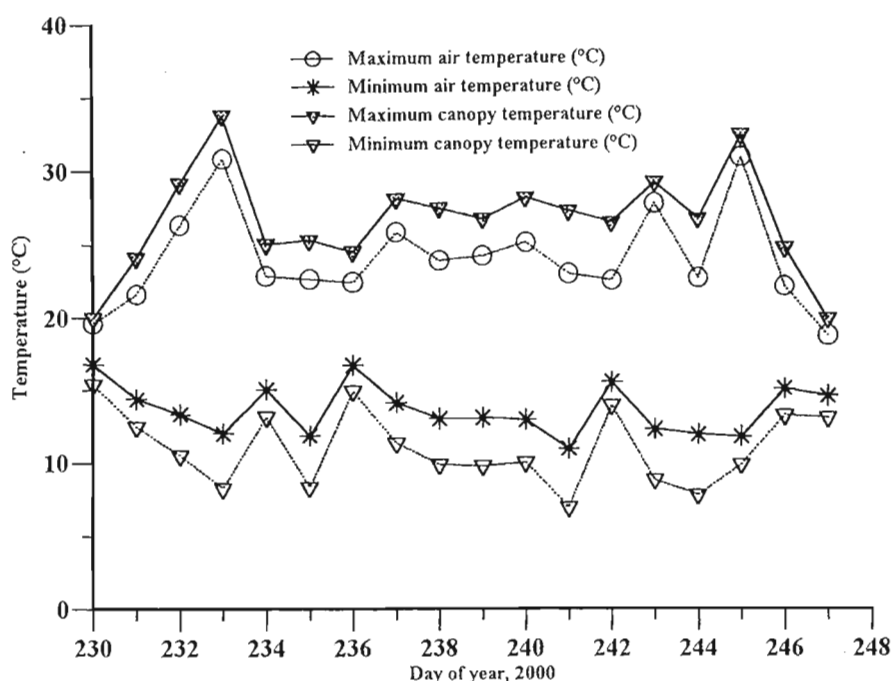


Fig. 6.12 Daily maximum and minimum air and canopy temperatures as well as wind speed for DOY 162 to 173, 2000 inclusive for Inselele farm

The process of vapour removal depends to a large extent on wind and air turbulence which transfers large quantities of air over the evaporating canopy surface. When vaporizing water, the air above the canopy becomes gradually saturated with water vapour (FAO, 2000). If this air is not continuously replaced with drier air, the driving force for water vapour removal, and the vapour pressure deficit (vpd) decreases. This will have a profound effect on the canopy differential

temperature gradients (Allen *et al.*, 1994; FAO, 2000). The combined effect of some micrometeorological factors influencing the canopy to air temperature differential (T_{diff}) is illustrated in Fig. 6.15.

The vpd demand is high in hot (dry) weather due to the dryness of the air and the amount of energy available as direct solar radiation and latent heat. Under these circumstances, much water vapour can be stored in the air while wind may promote the transport of water allowing more water vapour to be taken up. On the other hand, under humid weather conditions, the high humidity of the air and the presence of clouds cause the vpd to be lower. While the energy supply from the sun (net irradiance) and surrounding air (wind speed) (Fig. 6.8) are the main driving forces for the vaporization of water (Fig. 6.16a and b respectively), the difference between the water vapour pressure at the evaporating surface and the surrounding air is the determining factor for the vapour removal (Fig. 6.16c) as depicted in the trends in Fig. 6.16d. A very close pattern was observed in the shape of curves in Figs 6.16c and 6.16d. The canopy to air temperature differential was more sensitive to the vpd and the relative effect of variations in incident irradiance was appreciably less, while the influence of wind speed variations was very low. Similar findings were reported by Daudet *et al.* (1999) in their work on simulation models on tree transpiration processes.

The pertinent features depicted in Figs 6.11, 6.12, 6.13, 6.14, and in particular reference to 6.16 have some common aspects. Savage (1998b) stressed that solar irradiance, air temperature, wind speed and water vapour pressure all interact simultaneously within the plant environment. The plant responses to these factors is synergistic. Hence, no investigation of air temperature can be effected on the plant environment without concurrently specifying the radiant flux density, wind speed and water vapour pressure. Summarily, the microclimate nearby a plant leaf is described by means of these four independent variables. Each of these variables is time dependent as well as varying in space which no doubt signals the complexity of the system.

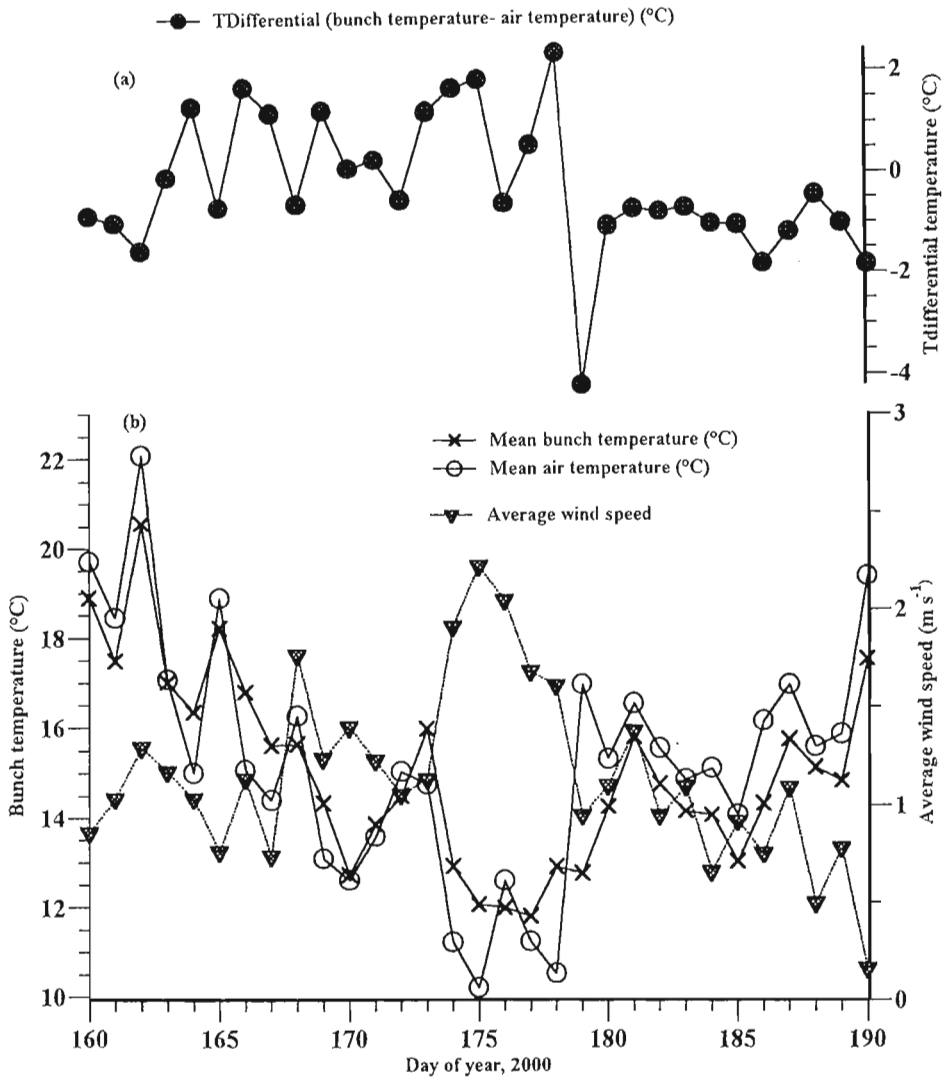


Fig. 6.13 Variation of mean air temperature, canopy temperature, bunch temperature, Tdifferential and wind speed for DOY 160 to 190, 2000 for Inselele farm

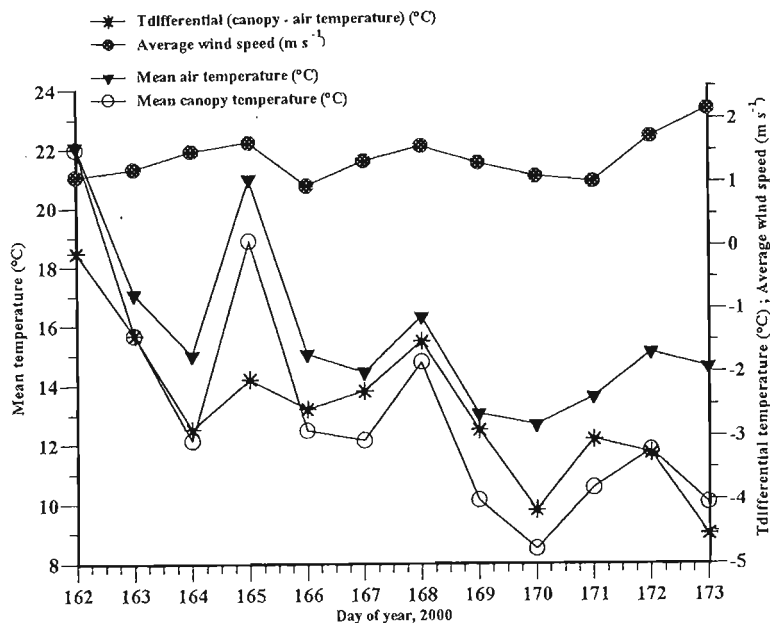


Fig. 6.14 Variation of mean air temperature, canopy temperature, Tdifferential and wind speed for DOY 162 to 173, 2000 for Inselele farm

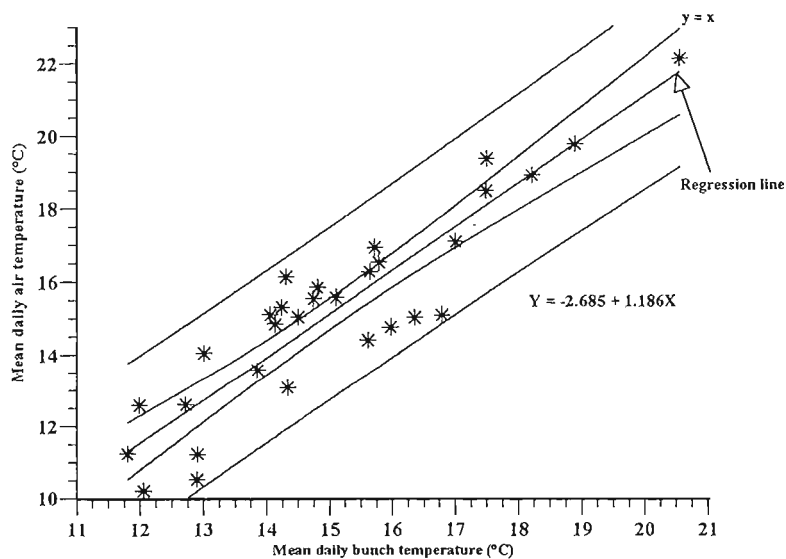


Fig. 6.15 Regression plot of daily mean bunch temperature (°C) as a function of daily mean air temperature (°C). The wide limits are the 95 % confidence limits for an estimated single y value and the narrower limits are the 95 % confidence limits for the population mean. Also shown is the regression line

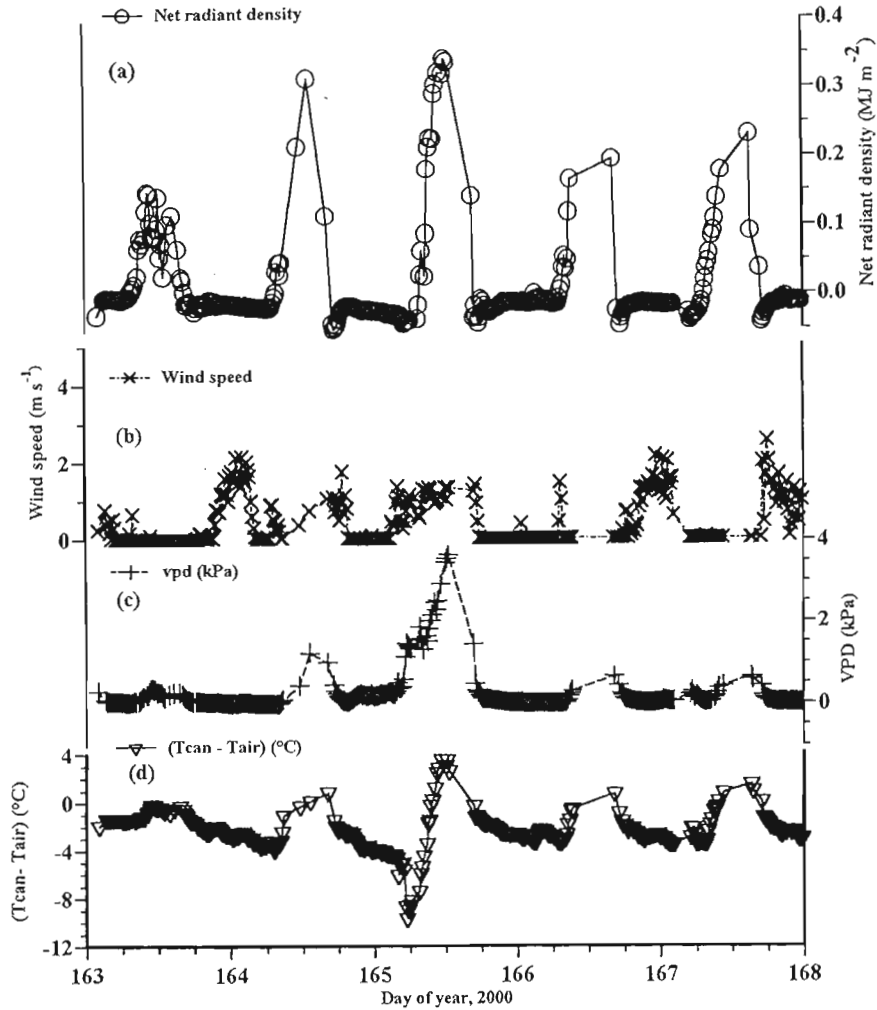


Fig. 6.16 Variation of canopy surface to air temperature differential, wind speed, water vapour pressure and net radiant density for cloudless days, DOY 163 to 168 inclusive

6.7 Light interception and Beer's law

The fraction of radiation lost to scattering and absorption per unit distance in a participating medium, normally given in standard units as a fraction per meter is referred to as the extinction coefficient. The amount of solar radiation received by a given surface can be a source of energy for both physical and biological processes on the earth's surface. The solar irradiance received at the earth's surface consists of two basic components namely: direct solar irradiance and diffuse or sky radiation.

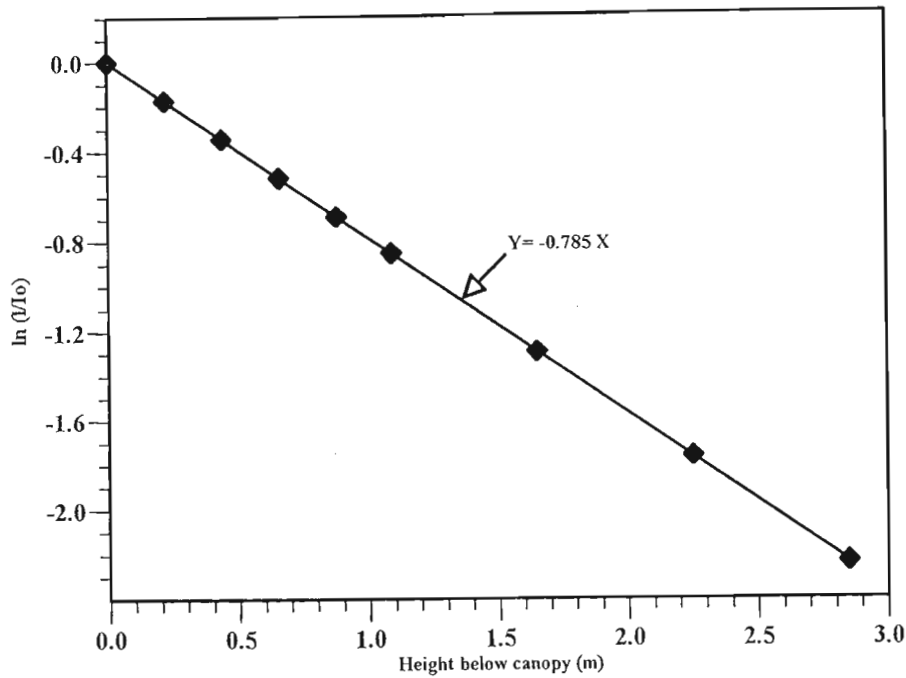


Fig. 6.17 Log of the ratio for incident solar irradiance, $\ln(I/I_0)$, vs height (m), below a banana canopy determined using a Kipp solarimeter on DOY 201

The instruments used to measure solar irradiance are called solarimeters or pyranometers. Investigating the changes in solar radiant flux density at various positions, provides one with a better understanding of energy variations down the crop canopy profile and can be a useful utility in calculating the extinction coefficient of a given crop canopy.

Beer's law describes the transmission of a parallel beam of monochromatic radiation through a homogeneous medium (Savage, 1998a). If a beam of monochromatic light passes through a very small distance, dl , of an absorbing medium, a certain fraction of the light will be absorbed. The fraction is independent of the light's intensity, but is proportional to density, ρ , of the absorbing medium and to the distance, dl . At a depth of, x (m) in a plant canopy, the incident radiant flux density or irradiance is equal to the product of the height, x , and to the amount of incoming radiation, I . Beer's law (Eq. 6.7) assumes that the loss of or lowering of active flux density in a crop canopy layer, dx is proportional to the thickness of the layer and to the amount of incoming radiation.

dI is proportional to I

dI is proportional to dx

Therefore $dI = -k I dx$ where k is the proportionality constant (also called the extinction coefficient)

Integrating $\int_{I_0}^I \frac{dI}{I} = - \int_0^x k dx$

$\ln I - \ln I_0 = -kx$

Therefore $(\ln I)^I = -k(x)^x$

$$\ln I - \ln I_0 = -kx - (-k \cdot 0)$$

Hence $\ln I/I = -kx$

Hence, $I = I_0 \exp(-kx)$ (Beer's Law)

6.7

A plot of $\ln(I/I_0)$ against banana height below canopy (Fig. 6.17, Table 6.2) resulted in a negative linear response with a slope of -0.785 which represents the crop's extinction (attenuation) coefficient.

Table 6.2 Logarithmic function for variation in the ratio of incident solar irradiance with decrease in plant height

$\ln(I/I_0)$	Height below canopy (m)
0	0
-0.17	0.22
-0.35	0.44
-0.52	0.66
-0.69	0.88
-0.86	1.09
-1.3	1.65
-1.77	2.25
-2.24	2.85

Savage (1998a) reported that for a community with more or less horizontal leaves, the k value is between 0.7 and 1.0 m^{-1} . This worker further stated that from theoretical considerations, it would be desirable to reduce the absolute magnitude of k . For if k were to reduce, I would approach I_0 and the solar irradiance down the canopy profile would be more uniform. This would, in effect, reduce the absorptivity of the canopy, resulting in more radiation reaching the lower leaves, this would be desirable in crops which typically produce canopies that result in shading of the lower leaves.

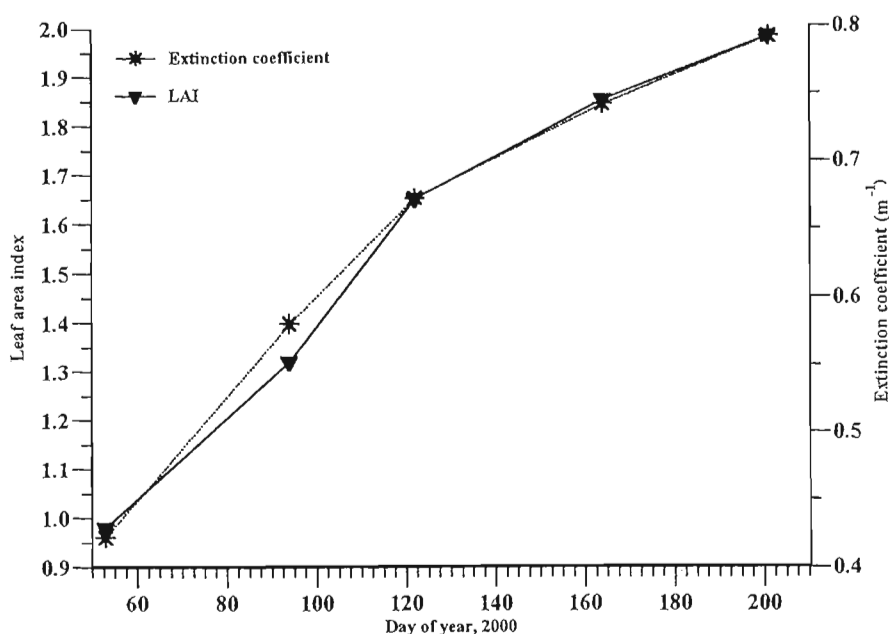


Fig. 6.18 The variation in the LAI and extinction coefficient in a banana orchard over time

This scenario can be applicable in a banana stand because often there is undesirable mutual shading on the suckers, which leads to reduction in incident light to the secondary canopy (Robinson and Nel, 1989). In reference to Table 6.3 and Fig. 6.18 there was a very close relationship of progressive increment in the LAI with the extinction coefficient between DOY 53 and 201. From the applications of Beer's law, certain measurements can be obtained to determine certain cultural methods, for example crop spacing. The effect of radiation becomes quite marked in the interrow of crops and it is necessary to attempt changing the reflection coefficient of the interrow soil. This

may be done using various mulches. It is evident that solarimeters can be used to measure the canopy reflection coefficient which can in turn be used to improve crop management and productivity.

Table 6.3 Variation in banana k with canopy LAI, the former calculated using solarimeter measurements and the later using the LAI 2000. The time slots refer to the measurements done with the solarimeter while the LAI measurements were performed at sunrise

DOY	Time(hours)	I_0 (mV)	I (mV)	I/I_0	LAI	k
53	1130	5.92	3.91	0.965	0.98	0.422
94	1215	6.24	2.89	0.464	1.32	0.581
122	1200	5.84	1.92	0.329	1.65	0.673
164	1145	6.22	1.57	0.253	1.85	0.742
201	1245	5.97	1.24	0.208	1.98	0.792

CHAPTER 7

7 Banana growth, Morphology and Phenology Trends in Response to Shading

7.1 Introduction

The banana is a tropical lowland crop requiring uniformly warm and humid conditions for optimum growth and productivity (Robinson, 1985). Most banana species grow well in the open sun, as long as water is not limiting (Israeli *et al.*, 1995). However, in subtropical climatic conditions, as well as under shaded conditions, the growth cycle is retarded and prolonged considerably. This retardation is principally due to the cold winter air temperatures which reduce the leaf emergence rates (LER) (Robinson, 1985; Stover and Simmonds, 1987). Furthermore, there is considerable reduction in the incident solar irradiance and a very variable radiation load in the understorey canopy of the orchard (Daamen *et al.*, 1999).

Suckers also get some shading resulting from the upper storey canopy. This phenomenon leads to a decrease in the photosynthetically active radiation band (PAR), in the wavelength region of 400 to 700 nm (Ross and Sulev, 2000). Ross and Sulev (2000) further considered penetrated global radiation, and found that quantum efficiency decreased rapidly with canopy depth, being 8 to 9 times lower at the bottom of a fairly dense canopy than above it. Analogous to this phenomena, Stover (1984) observed that when the density of a commercial banana plantation is high and light transmitted to the understorey is reduced to 10 % of the above-canopy irradiance, both growth and productivity of the plants were severely affected. This worker further reported that in a tropical climate, the rate of flowering declines significantly some 6 months after a period of low solar irradiance. Robinson and Nel (1988, 1989) also observed a prolonged cycle time and a decrease in bunch mass under increased plantation density in the cultivar 'Williams' growing in a subtropical climate. These researchers proposed that the reduction in incident irradiance to the secondary canopy contributes to these effects.

7.2 Baseline studies on banana suckers

Banana growth, morphology and phenology as influenced by shading was investigated under similar conditions of climate, soil and agronomic field management with particular reference to the cultivar 'Williams'. A baseline study was conducted to investigate variations in sucker¹ height in the plots where the shading treatments were to be imposed. It is imperative to note that all growth references in this study were done on a ratoon² crop during the pre-vegetative, vegetative and reproductive stages, illustrated in Fig. 7.1, and no plant crop investigations were carried out. Plant height was measured from the pseudostem base to the bunch axis arch. The pseudostem circumference was measured at a height of 1 m from the soil level .

Before the treatments were imposed, baseline data indicated that suckers showed a progressive linear increment in mean pseudostem height (Fig. 7.2) with time of sampling within the respective plots with very similar patterns, with no significant differences, $P \geq 0.05$. However, the plots which were going to have the 20 % irradiance treatment had a 1.42 % higher mean sucker height margin compared to the overall mean of other treatments, while the plots which were going to have 70 % irradiance treatment showed the least mean height with 1.89 % less of the overall mean. These observations are clearly depicted in Fig. 7.2. However, results from the ANOVA table (Appendix V) indicate that there were no statistically significant differences, $P \geq 0.05$, in the baseline heights of the suckers. The graphical representations of the mean baseline pseudostem girth and LAI have not been illustrated, however, trends indicated that there were no differences in curve patterns within the treatments with respect to these two variables.

¹Sucker- A vegetative offshoot from a banana corm which is either destroyed or left for the next crop generation

²Ratoons-The successive cropping cycles of a banana plantation following the plant crop

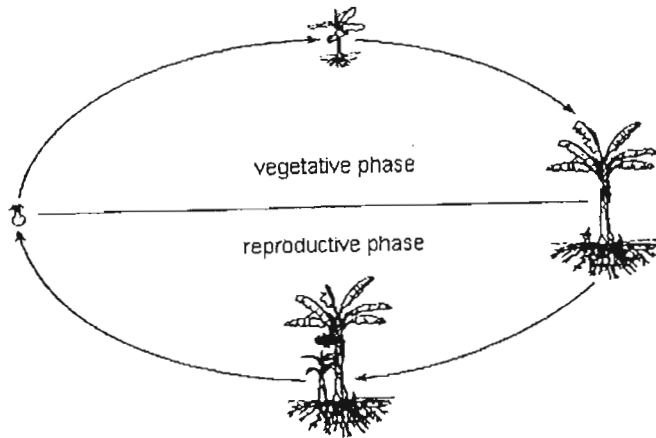


Fig. 7.1 The general growth cycle of banana, *Musa* spp. (source: Rony and Rodomiro, 1997)

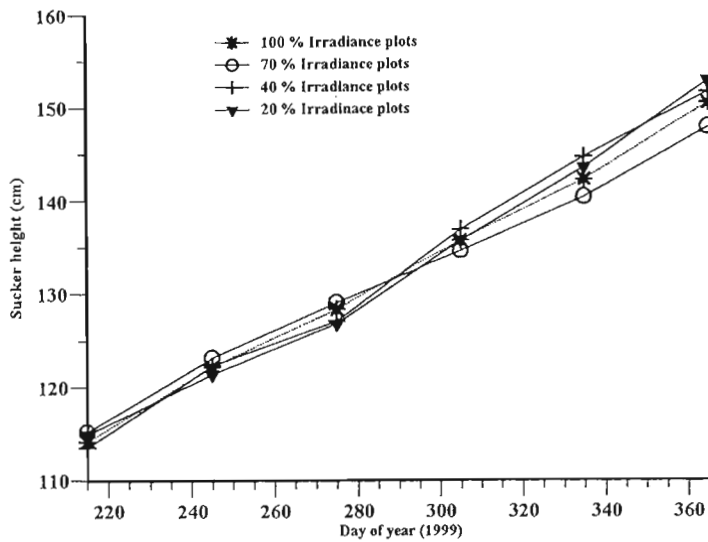


Fig. 7.2 Mean baseline sucker pseudostem height variations with DOY³

³Time of sampling- Monthly measurements (allometrics) done on banana vegetative growth to assess changes in crop morphology. Day 1 corresponds to DOY 215, 1999. Subsequent sampling was then done at 30 days intervals

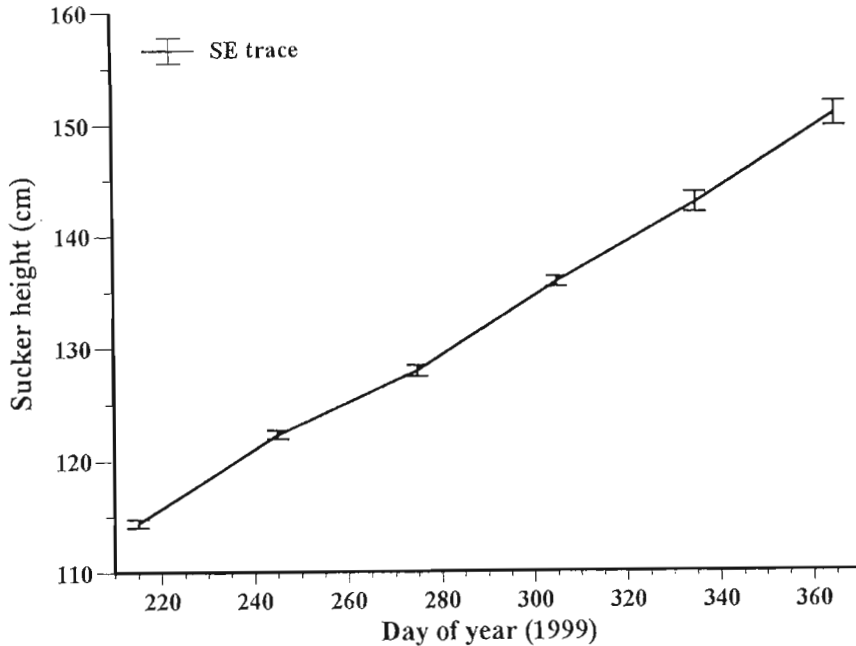


Fig. 7.3 Overall standard error trace for the mean baseline sucker height variation with time

The trace in Fig. 7.3 depicted a progressive and steady increment in the baseline sucker heights with time. Morse and Robinson (1996) found a strong correlation between plant height and leaf length, indicating that as plant height increases (Figs 7.2 and 7.3), the LAI increases for a given plantation density, provided the leaf number is constant.

7.3 Vegetative phase

Plant height and pseudostem circumference were negatively affected by reducing the incident irradiance to 70 % and 40 % of the unshaded control and further diminished, when incident irradiance was further reduced to 20 % of the unshaded control (Fig. 7.4 c and b respectively). Mean pseudostem height was reduced by 17.8 % under the most dense shade as compared to the unshaded control. Pseudostem height increased linearly in all the treatments, with the 100 % irradiance treatment superceding the 70 % irradiance treatment by 6.35 %. The variations observed in mean pseudostem girth followed a similar pattern to the pseudostem height trends.

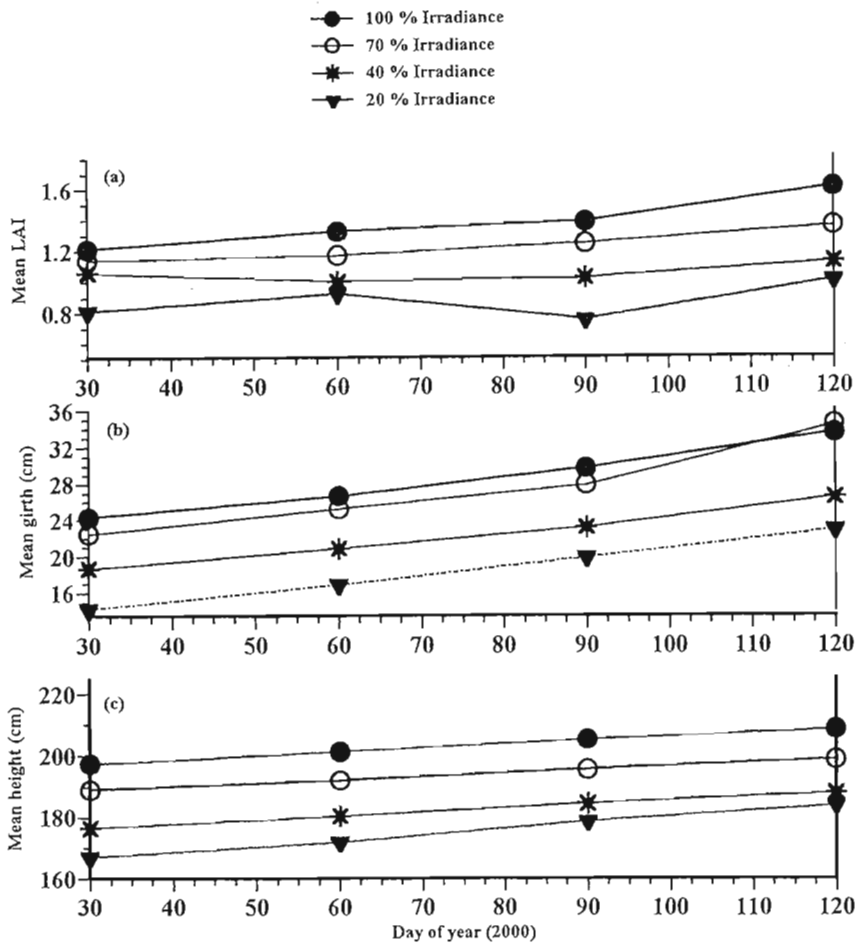


Fig. 7.4 (a) Variation of mean plant LAI with time measured using an LAI 2000 plant canopy analyser at sunset, 1830 hours; Progressive variation in mean pseudostem girth and mean banana height with days of sampling (b and c respectively) during the vegetative phase

However, there was no statistically significant difference, $P \geq 0.05$, between the 100% irradiance treatment and the 70% irradiance treatment though the 70% showed a slightly higher mean girth value by 1.5%. Fig. 7.4 (a) depicted a higher LAI under full irradiance conditions. On the contrary, there was a decline in LAI on some days of year (Fig. 7.4c). The leaf numbers per plant at flower emergence were not significantly different, ($P \geq 0.05$), between the treatments. However, the total number of functional leaves per plant had reduced on some days of sampling which resulted in a decrease in the LAI. A pronounced decrease in LAI was noted on DOY 90 for the 20% irradiance treatment with a decline from 0.9 on DOY 60 to 0.6 on DOY 90.

Leaf senescence could be implicated under such circumstances. Similar findings were reported by Galyuon (1994) working with cocoa.

7.4 Flower emergence to harvest interval

The flowering period of a given crop is a stage at which the crop is at maximum performance in preparation for fruiting. It harnesses all the nutrients and utilises resources such as water and available food reserves to optimum level (Bower, personal comm, 2000). Rony and Rodomiro (1997) reiterated that the mother plant and the ratoon are in competition for resources during the vegetative phase (Fig. 7.1) and most of the resources are directed to the growing mother plant. After flowering, food resources are still directed to the mother plant for fruit development and this therefore represents a very crucial stage in the physiology of the crop. During flowering, ratoon development increases and after harvest, resources are directed to the ratoon (Rony and Rodomiro, 1997).

Trends observed in the LAI (Fig. 7.5 a) were similar to those reported during the vegetative phase. Banana height and pseudostem girth were further assessed from the initiation of flower emergence to the time of harvest. Pseudostem girth and plant height attained their maximum values of 57 cm (Fig. 7.5b) and 290 cm respectively. Maximum plant height trends have not been graphically illustrated but were recorded from the 100 % irradiance control treatment. During the EH interval, no statistically significant differences, $P \geq 0.05$, were observed in the banana pseudostem girth trends within the treatments. The mean girth curves depicted that there were no observable differences between the 40 % and 20 % irradiance treatment curves (Fig. 7.5 b) though distinct curve trends were realised between the 100 % and 70 % irradiance treatments as well as between the 40 % and 70 % irradiance treatments. Pseudostem height variations (Fig. 7.5 c) however, showed a marked trend of differences, with the 100 % control treatment, superceding the rest. The 70 %, 40 % and 20 % treatments were 2.28 %, 3.94 % and 4.56 % less than the control height respectively.

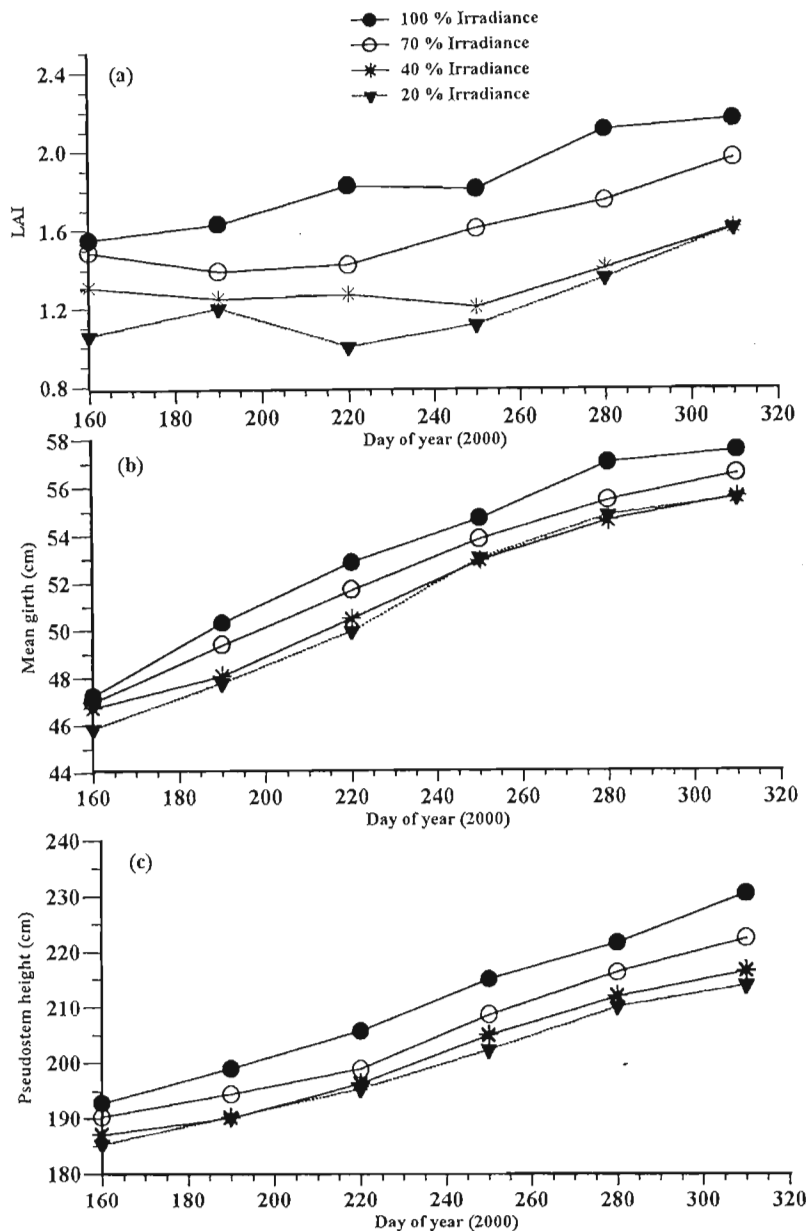


Fig. 7.5 Variation of banana pseudostem height, girth and LAI during the EH interval

A further effort was undertaken to investigate the relationship between levels of incident solar irradiance on LER and EH (Fig. 7.6; Table 7.1). The 100 % control had the highest LER of 3.8 leaves per month and a much shorter EH interval corresponding to 109 days compared to the other treatments. The 20 % irradiance treatment had a LER of 2.4, a statistically significant difference, $P \geq 0.05$, of 1.4 leaves.

Trends observed (Table 7.1) depicted significant differences, $P \geq 0.05$, for both LER and EH interval. This is also evident in reference to the standard error plot (Fig. 7.6 a and b). Generally, increased solar irradiance resulted in a higher LER and shorter EH interval while diminished irradiance resulted in a low LER and high EH interval.

Work performed by Robinson and Nel (1988) also indicated a significant decline in leaf emergence rate and an increase in cycle duration when the plantation density was increased from 1000 plants ha^{-1} to 2222 plants ha^{-1} and the incident irradiance available to the secondary canopy was reduced to 14 % of the full irradiance conditions. A slower rate of leaf emergence and increased cycle duration was also indicated in this study (Figs 7.6, 7.8 and 7.9). In these findings, it is worth noting that in the subtropical region in general and Inselele farm in particular, the dates of flowering were very variable and highly indicative with regard to the rate of growth and crop development in reference to a particular season.

The increase in the flower emergence to harvest interval under shade conditions noted in this research work (Fig. 7.6), also reported by Murray (1961), could also be attributed to a poor supply of photosynthates to the developing fruit as a result of suppressed incident irradiance. The duration from flower emergence to fruit harvest depends on air temperature, cultivar, soil water content levels, and cultural practices (Robinson, 1996) and this ranges from 80 to 180 days in subtropical Florida conditions (Jonathan and Carlos, 2000) while in South Africa the EH interval ranges from 204 days for April flowering to 108 days for November flowering (Robinson and Nel, 1988; Robinson, 1996). The seasonal differences in the LER and EH intervals were pronounced and significant at $P \geq 0.05$, (Table 7.1). The results presented in Fig. 7.6 were from a different data base to those presented in Table 7.1.

Leaf measurements were made at harvest on all leaves of three randomly selected plants from each treatment in the ratoon plantation at Inselele and the results are summarised in Fig. 7.7. A progressive increment in LAI was observed among the treatments in the order 100 %, 70 %, 40 % and 20%. Hence, mean LAI differences within irradiance treatments ranged from 4.6 (100 %); 4.0 (70 %); 3.6 (40 %) and 3.0 (20 %). It should be noted that, at flowering, an autumn flowering

could have die back of all leaves 8 months later, just before harvest. The plantation at a stage close to harvest, is considered to have reached its maximum LAI capacity since no new leaves are generated and thereafter leaf senescence sets in (Robinson, 1996).

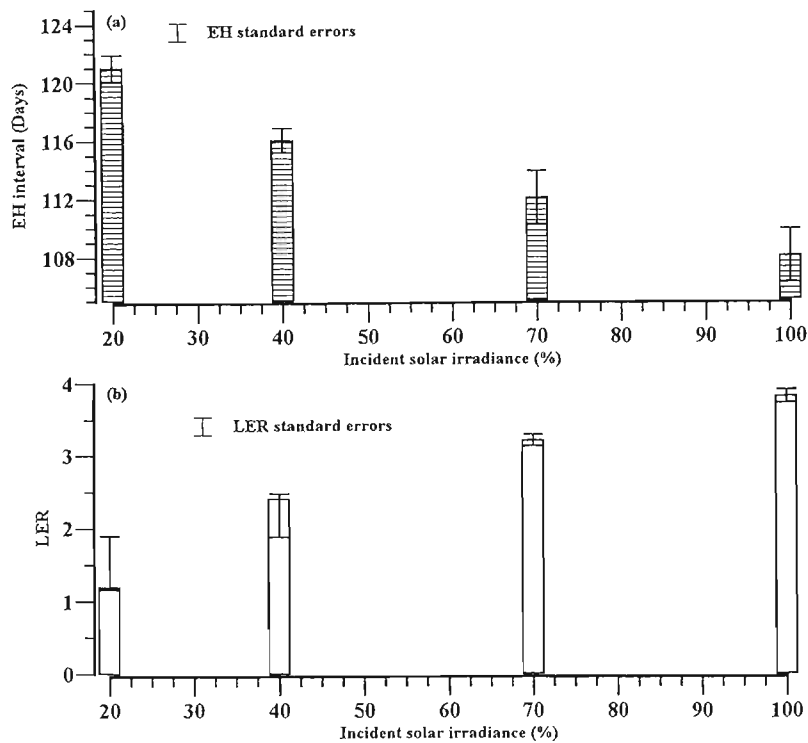


Fig. 7.6 Variation of EH interval (a) and LER (b) with incident solar irradiance levels (Feb-Jul)

Table 7.1. Effect of reduced solar irradiance on LER and EH at Inselele farm

	(% of incident solar irradiance)				cv ⁴
	100	70	40	20	(%)
LER	5.5 ^d	4.2 ^c	3.6 ^b	2.8 ^a	9.072
EH	108 ^a	112 ^{ab}	116 ^{bc}	121 ^d	2.501

Sampling was performed during the months of August to November. Mean separation by Duncan's new multiple range test, $P \geq 0.05$. Different letters in a row indicate statistically significant differences.

⁴cv represents the coefficient of variation

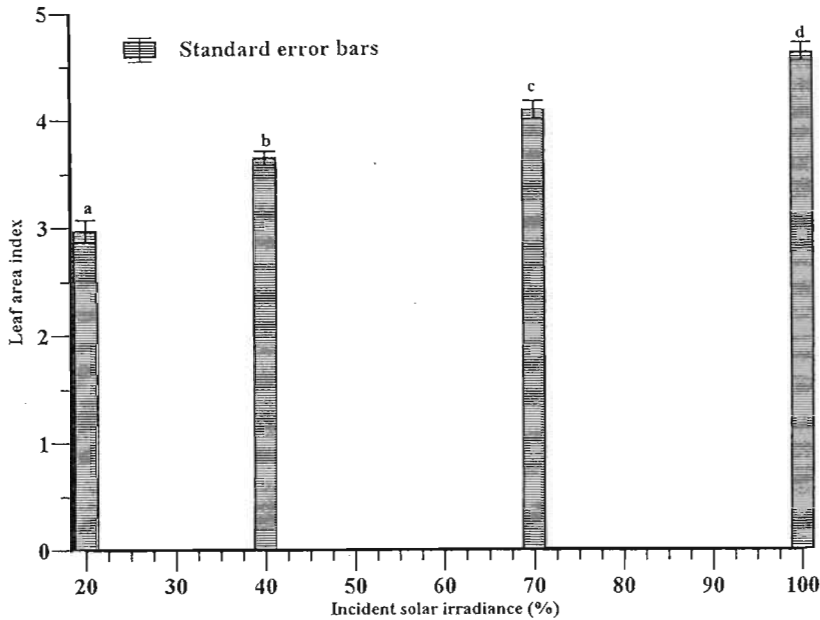


Fig. 7.7 Variation of maximum leaf area index ($L \times W \times 0.83 \times \text{number of functional leaves at flowering} \div \text{ground area}$) of 'Williams' cultivar with varying irradiance levels at Inselele ratoon plantation. Different letters represent statistically significant differences at $P \geq 0.05$

Stover (1984), Robinson and Nel (1988) illustrated the importance of planting at a density that reflects optimum LAI, in order to obtain maximum production per hectare. Robinson and Nel (1989) achieved maximum productivity with a LAI of about 6 but recommended a LAI of 5 if optimum production and maximum gross margin was to be achieved and maintained. Effects of reduced incident irradiance due to increased plantation density could be comparable to the introduction of artificial shade conditions in a plantation. Reduction of incident irradiance to 20 % in this study resulted in a LAI of 3.0. However, Turner (1982) maintained that a transmitted radiation through the leaf canopy of 10 %, resulted in a LAI of 4.0 and contended that 4.5 was optimum. Differences in these two findings could be attributed to variations in agroclimatic zones, cultivar variations, differences in irradiance levels and management conditions. Furthermore, the former study is referring to canopy level irradiance while the latter refers to below canopy irradiance measurements.

Seasonal influences on crop phenology were observed and recorded (Fig. 7.8). These parameters included the leaf emergence rates as well as flowering emergence to harvest intervals. The mean annual LER trends decreased from January which had the highest value of 3.8 with the least value of 1.2 registered in July. The EH interval showed a bell shaped curve relationship with the highest EH registered in the months of March to July and the lowest values in the months of October to February. The reverse was true for the LER variations as depicted in Fig. 7.8.

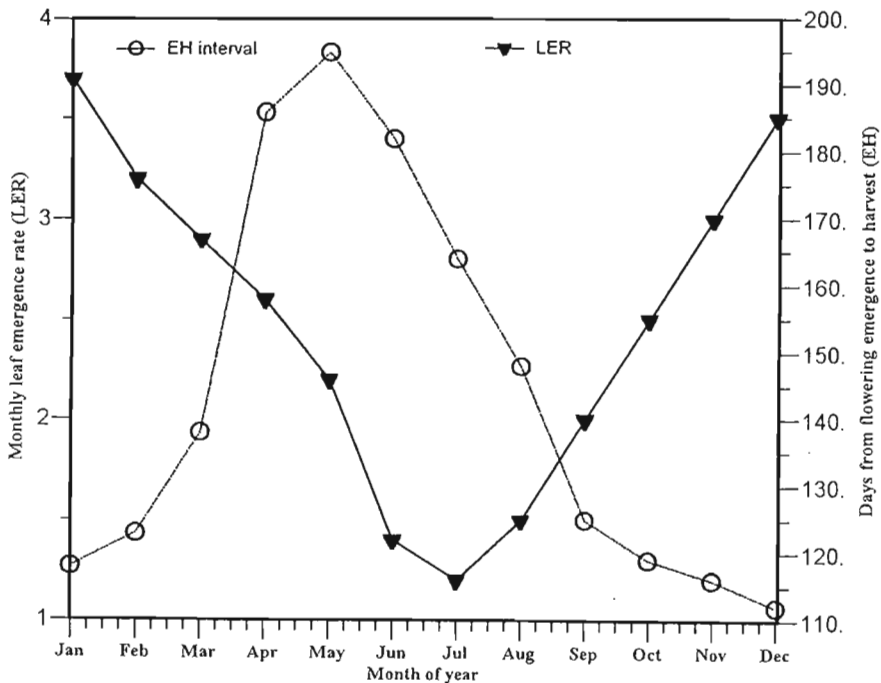


Fig. 7.8 Monthly leaf emergence rates (LER)(\blacktriangledown , left hand y axis) and the emergence to harvest interval (EH) (O, right y axis) of banana in 2000

As reported earlier, the LER decreased from approximately 3.8 leaves per month in January to around 1.2 leaves per month in July which was the lowest value registered (Fig. 7.8). There was a progressive increment in the LER from August with a mean value of 1.5 leaves per plant through to December registering a LER of 3.5. These trends are associated with the mean monthly air temperature patterns as illustrated in Fig. 7.9. The strong seasonal influence on phenological responses is further confirmed by the EH trends (Fig. 7.8). Analogous to this, Robinson (1981)

observed that the flowering to harvest time of 'Williams' varied from 118 days in summer to 213 days in winter.

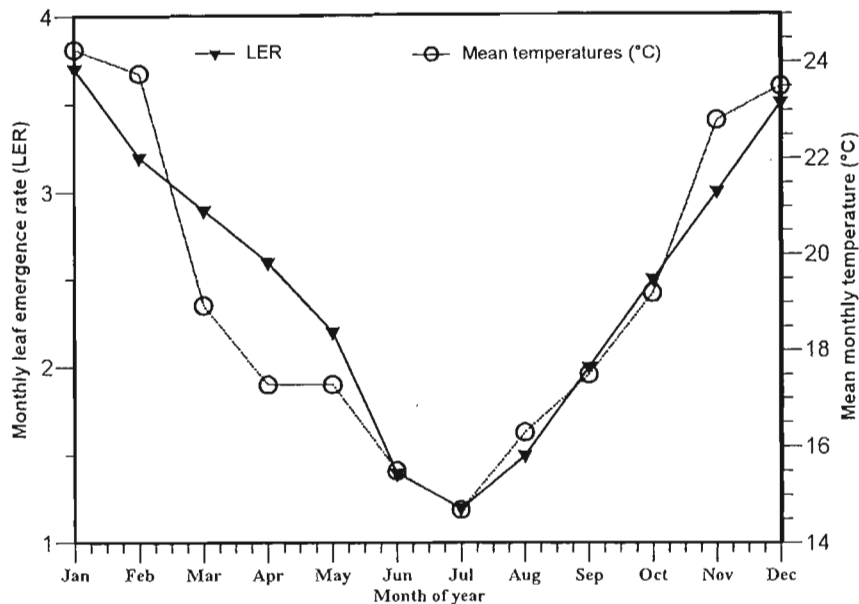


Fig. 7.9 Comparison of monthly LER with mean monthly air temperature trends (°C)

The similar pattern between the LER and mean monthly air temperatures is of interest. Comparison of LER and mean air temperature trends (Fig. 7.9; Table 6.1) showed similar curve patterns and depicted a high positive correlation of 90.4%. Variation in the curve trends (Fig. 7.9) were minimal and the high correlation coefficient reported indicated a good consistency between crop phenology responses and seasonal changes. The drastic changes observed in the EH duration (Fig. 7.8) from 138 days in March to 186 days in April further confirm this.

The highest LER of 3.8 was recorded in the month of January which had the highest mean monthly air temperature of 24.3 °C while the lowest LER of 1.2 was registered in July which had the lowest mean air temperature, 14.7 °C. In Israel, Israeli *et al.*, 1995 also reported similar seasonal trends between LER and EH.

Robinson, (1996) highlighted that the optimum air temperature range (°C) for LER is in the lower 30's which implies that Inselele farm is exposed to sub-optimal conditions. However, Turner and Lahav, (1983), noted that the optimum air temperature range (°C) for dry matter productivity is in the lower 20's. Panozzo *et al.* (1999) also reported air temperature as a major influence on wheat growth especially during the grain filling stage due to variation in the spike temperatures. Analogous to this, variation in temperature of vegetative growth points in banana were performed by Eckstein (1994) who recorded a maximum internal pseudostem temperature difference of 4.2 °C when comparing plants growing in full sun and those growing in the shade of windbreaks. Optimum temperature had enhanced the development potential of the plants with greater exposure to sunlight.

Various measurements have been made on the rates of leaf emergence in bananas in a range of environments and useful correlations with air temperature have been established (Turner and Lahav, 1983; Robinson *et al.*, 1989). The results of this study agree with the trends observed by the above mentioned scientists under field conditions. The response derived curves of LER in relation to air temperature (Fig. 7.9) are critical in studying the progress of crop phenology, especially under different temperature environments (Stover and Simmonds, 1987). This aspect would help in management of the crop and ensure that inputs such as water supply and fertilisers are also optimal during the summer period. However, banana phenological responses have been known to be of little significance in the tropics (Robinson, 1996) due to the consistent fruiting pattern resulting from a fairly stable climate. Knowledge of the growth pattern in the subtropics allows appropriate management modification for slow growth in winter through production timing via planting time modification and crop forecasting. Important aspects to focus on during crop forecasting include crop harvest dates from known flowering dates and bunch size manipulation. These are dependent on the time of initiation because bunches initiated in autumn and winter are smaller than bunches initiated in summer (Israeli *et al.*, 1995; Gevers, 1987). As indicated earlier, the major phenology parameters of importance include the planting to harvest period, leaf emergence rates and primary root growth. Knowledge of these aspects will allow for adjustments on management intensity during the cooler conditions, which would no doubt be beneficial for Inselele farm since it is characterised by sub-optimal conditions.

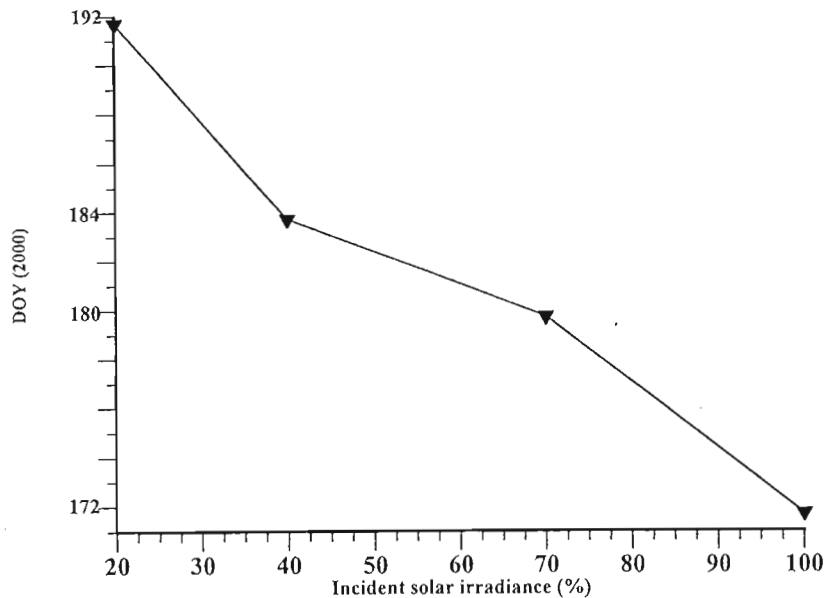


Fig. 7.10 Variation of flowering date with different levels of irradiance

A comparison of the flowering date trends with the levels of incident irradiance (Fig. 7.10) showed an inverse relationship, and had a very high negative correlation of 98.4 % (Genstat, 1983). The lower the level of incident irradiance resulted in a delay of flowering dates as depicted in the Fig. 7.10. Furthermore, the afore mentioned seasonal influences on the flowering dates also contributed to the observed trends. Flowering dates were delayed by 8 days, 13 days and 21 days with incident irradiances of 70 %, 40 % and 20 % of the unshaded control (100 % irradiance), respectively (Fig. 7.10). The delay in flowering dates observed was analogous to the increased cycle interval under higher cropping densities observed by Robinson and Nel (1988). The phenological responses in this study appear to be a result of an interaction of both seasonal responses and shading treatments (Figs 7.6, 7.8, 7.9 and 7.10). This is further evidenced by the high levels of correlation reported.

7.5 Heat Units

An appraisal of heat units allows one to have a better cumulative comparison of the air temperature variations in the respective months of the year and how this affects banana

productivity. Variations shown in Table 7.2 are illustrated in Fig. 7.11. These were derived from the mean of the monthly sum of the daily maximum and minimum temperatures with a base of 14 °C times the number of days per month: Heat Units =

$$\{((\text{daily maximum} + \text{daily minimum}) \div 2) - 14 \text{ } ^\circ\text{C}\} \times \text{number of days per month} \quad 7.1$$

Table 7.2 Annual variation of monthly cumulative heat units for Inselele farm

Month	Jan	Feb	Mar	Apr	May	Jun	Jul	Aug	Sep	Oct	Nov	Dec
Heat Units	273	247	236	209	93	91	55	122	141	175	222	269

The above equation, Eq. 7.1, is in excess of 14 °C, which is regarded as the minimum threshold temperature level for banana growth and productivity (Robinson, 1996). The shape of the heat units curve (Fig. 7.11) is hardly any different from that of the mean monthly air temperature response curve (Fig. 7.9) since the former is actually derived from the latter. Similar explanation in the trends reported in Fig. 7.9 apply to this curve, Fig. 7.10, due to the afore mentioned reasons.

Banana growth is primarily controlled by air temperature and water availability (Robinson, 1996; Table 2.1). Certain critical threshold values have been used for estimation of the production potential of the crop and one of these is the monthly heat unit accumulation (Fig. 7.11; Table 7.2). Assuming an EH interval of 120 days for May to August, Table 7.2 yields a heat unit accumulation of 361 while the same duration from January to April yields a heat unit accumulation of 985, clearly 64 % greater than the May to August duration. Hence, the November to February period is still arguably the most conducive flowering period at Inselele farm, since air temperatures are most conducive in this duration for optimum banana productivity (Fig. 7.9; Table 7.2). A heat unit accumulation of 395, which results from an approximate mean air temperature of 27 °C is considered optimal (Robinson, 1996). Comparing this optimum value with the values reported in Table 7.2, reveals that mean air temperatures in Inselele were below optimum.

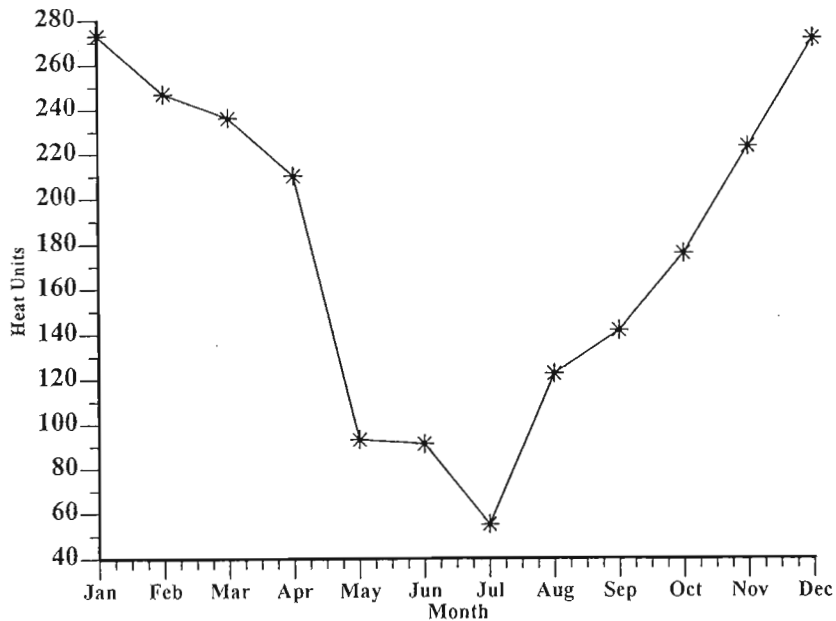


Fig. 7.11 Variation in heat unit accumulation for banana at Inselele, 2000

7.5 Banana yield and productivity dynamics

Reduction in the incident irradiance resulted in a significant decline in some yield indices. Bunch weight was significantly affected, $P \geq 0.05$, in all the treatments and was less than the control by 11.83 %, 27.18 % and 32.57 % in the 70 %, 40 % and 20 % irradiance treatments respectively. On the contrary, results obtained (Table 7.3) from the fresh finger weights did not depict this magnitude of difference. However, fresh finger weight was also significantly affected, $P \geq 0.05$, in all the treatments and was less than the control treatment (100 % irradiance) by 3.5 %, 11.76 % and 13.17 % in the 70 %, 40 % and 20 % irradiance treatments respectively.

Plant density did not appear to decline in any of the plots but would probably be affected in the second production cycle due to poor sucker initiation and slow sucker growth in the dense shade plots. The hands obtained per bunch and finger length did not show significant differences, $P \geq 0.05$, between the 70 %, 40 % and 20 % treatments. However, a level of interaction was observed in the 70 % and 40 % irradiance plots in relation to the 100 % irradiance which showed significant differences, $P \geq 0.05$. Finger lengths observed in the most dense shade with the 20 %

Table 7.3 Influence of reduced irradiance on banana yield indices

Treatment (%) of incident irradiance	Yield parameter	Ranked Mean \pm Standard error	cv (%)
100	Bunch fresh weight (kg)	33.65 ^d \pm 0.7333	7.814
70		29.67 ^c \pm 0.4995	
40		24.53 ^b \pm 0.5219	
20		22.69 ^a \pm 0.7029	
100	Bunch length (cm)	112.57 ^c \pm 1.7509	5.56
70		104.88 ^d \pm 2.4416	
40		94.82 ^a \pm 1.0821	
20		94.42 ^a \pm 0.6744	
100	Hands per bunch	8.42 ^a \pm 0.3361	10.46
70		8.58 ^{ab} \pm 0.1929	
40		9.17 ^{ab} \pm 0.2973	
20		9.25 ^b \pm 0.2175	
100	Finger length ⁵ (cm)	19.78 ^b \pm 0.4896	6.65
70		18.69 ^{ab} \pm 0.1888	
40		18.73 ^{ab} \pm 0.3939	
20		18.19 ^a \pm 0.3061	
100	Fingers per hand	22.08 ^b \pm 1.8152	25.15
70		21.25 ^b \pm 0.7500	
40		19.58 ^{ab} \pm 1.4010	
20		16.58 ^a \pm 1.5833	
100	Finger fresh weight (gm)	126.82 ^d \pm 0.6492	2.63
70		122.31 ^c \pm 0.6298	
40		116.033 ^b \pm 1.0069	
20		110.113 ^a \pm 1.1909	

Ranked means within a given yield parameter with different letters indicate statistically significant differences, $P \geq 0.05$.

⁵Values of finger length, fingers per hand and finger fresh weight were taken from the third hand.

irradiance were shorter than the other treatments suggesting a level of stuntedness. There were significant differences, $P \geq 0.05$, observed in the number of fingers per hand. The 100 % irradiance treatment had the highest recorded fingers per hand and the 20 % irradiance was less by 24 % compared to this control treatment. Bunch length results conformed to the afore mentioned trends, however, no significant differences, $P \geq 0.05$, were observed between the 40 % and 20 % irradiance treatments.

The findings in this study are in agreement with Jonathan and Carlos, (2000) who reported an analogous situation in subtropical Florida, USA. Banana plants were found to be moderately shade tolerant up to 50 %. However, shading delayed plant growth and fruit development. Excessively shaded plants were stunted and produced small fruit. In a subtropical perspective, it is recommended that full incident irradiance would be most appropriate for best production. However, compromises in relation to this aspect make it hard to have a clear cut guideline as to whether to implement shading or not. This hesitation is due to the fact that commercial shade cloth materials are sometimes utilised in agricultural production as a management technique to protect plants from direct sunlight, wind effects, hail and birds. Shading can further reduce the incidence of frost damage, decrease water consumption or delay fruit maturation (Samarakoon *et al.*, 1990; Healey and Rickert, 1998).

The number of hands⁶ per bunch (Table 7.3) in relation to the influence of irradiance patterns was not statistically significant, $P \geq 0.05$. In fact the most dense shade had more hands per bunch compared to the other treatments. One could postulate that this is a predetermined aspect which actually takes place during the crop ontogeny and would not therefore be influenced by environmental factors. On the contrary, however, this study reveals that the size would be affected. Heavier bunches (Table 7.3) were derived from March to April flowering which coincided with fairly warm air temperatures, 18 to 22 °C (Fig. 7.9) at both flower initiation and emergence.

⁶Hand- A cluster of banana fingers attached to the bunch stalk by a collar

CHAPTER 8

Conclusion and Recommendations for Future Research

8.1 Conclusion

The site soil characteristics reflected a sandy loam soil with a dark brown to black colour and loose crumb structure. This aspect coupled with an air filled porosity of 10 % presented a good soil conducive to root penetration for a shallow rooting crop such as banana. Furthermore, the soil had a soil bulk density (ρ_b) of 1400 kg m^{-3} . This relatively low ρ_b and a porosity of 52 %, implied that it had minimal compaction and was poorly graded. It had a fairly high water holding capacity at saturation which meets the high consumptive water demands of banana. Mean soil temperatures measured with averaging thermocouples was $15 \text{ }^\circ\text{C}$. Robinson (1996) reported a pH range of 5.8 to 6.5 as optimum for banana productivity. However, a pH of 5.48 to 5.96 (Table 5.1) recorded in this study is certainly not out of range.

Aerodynamic resistance plotted against wind speed (Fig. 6.2) depicted a hyperbolic relationship. Similar patterns were observed in the energy flux trends (Fig. 6.3 b), net and solar irradiance (R_{net} and I_s respectively). The effect of high wind speed on soil evaporation was further illustrated by the slope of the curve in Fig. 6.3 a. The more windy the atmospheric conditions were, the larger was the effect on the evaporation curve Fig. 6.3 b. These findings are in agreement with Chay *et al.* (1998) and Monteith and Unsworth (1990). These workers reported that evaporation from vegetation was governed by a combination of incident radiant energy supply and atmospheric turbulence conditions. Undoubtedly wind speed is the major component of the latter.

Microlysimeter measurements (Fig. 6.6) of soil evaporation compared against the reference ET (combination of soil evaporation and canopy transpiration) depicted a lower mean difference of 18 %. The trend observed is justified since one would expect soil evaporation to be less than a combination of both canopy transpiration and soil evaporation.

Wind speed profile trends (Fig. 6.7) illustrated a consistently lower value for the 1.5 m height compared to the 3 m height. This observation might have been primarily due to canopy roughness coupled with pseudostem barriers within the 1.5 m height range of the orchard.

Canopy and air temperature differentials in this study were often negative at night. However, these temperature differentials were sometimes negative during day time conditions, implying that sensible heat was directed toward the canopy. It is a compelling argument to suggest that the latent heat was in excess of the net irradiance hence signifying advection influences. Blad and Rosenberg (1974), working on sub-irrigated alfalfa and pastures in the East central great plains of the USA reported similar trends.

The pertinent features depicted in Figs 6.10 (Sensible heat and wind speed for DOY 231), 6.11 (air and bunch temperatures for DOY 163 to 172), 6.12 (air and canopy temperature for DOY 230 to 248), 6.13 (air and bunch temperature and wind speed for DOY 160 to 190) and 6.16 (canopy and air temperature differences, vpd, wind speed and net radiant density for DOY 163 to 168) had a consistent analogy and the trends reported were as expected. Savage (1998b) further stressed that solar irradiance, air temperature, wind speed and water vapour pressure all interact simultaneously within the plant environment. The plant responses to these factors are synergistic. Admittedly, no investigation of air temperature can be effected on the plant environment without concurrently specifying the radiant flux density, wind speed and water vapour pressure. In summary, the microclimate close to a plant is characterised by means of these four independent variables, each of which is time dependent as well as varying in space, and this undeniably signals the complexity of the system.

The 100 % irradiance treatment plots were superior to the other treatments in relation to plant morphology features and productivity. This work indicated the positive affinity of banana plants for solar radiation. However it should be stressed that the threshold value and magnitude of the influence of reduced irradiance could vary according to a given location, depending on the prevailing environmental conditions at the time, agro-climatic zone and cultural plantation management techniques.

Furthermore, the vital role of air temperature dynamics in banana growth and development was clearly illustrated herein (Figs 7.8 depicting the variation in monthly leaf emergence rates (LER) and emergence to harvest interval with time; and 7.9 depicting a comparison between monthly LER with mean monthly air temperature trends). This study indicated that air temperature is yet another environmental factor that plays a very significant role in banana productivity. In both tropical and subtropical conditions, incident irradiance and air temperature could be the most crucial limiting factors when others such as water and nutrient supply are near optimal levels (Israeli *et al.*, 1995).

A pronounced effect of reduced irradiance on banana morphology, phenology, growth and fruit production was realised in this study. Responses to shading have also been reported for bananas grown under the canopy of arecanut palms (Balasimha, 1989) and these responses no doubt also become crucial where banana cultivation is practised under agroforestry conditions (Bonaparte, 1967). There was a decline in leaf area, pseudostem height and girth (Figs 7.4 and 7.5) and a delay in flowering dates (Fig. 7.10) in particular under the most dense shade (20 % irradiance). The 100 % irradiance treatments were distinctly superior to the other shade treatments. These responses observed in all the shade levels signal a level of stuntedness due to reduction in incident solar irradiance. Reduced growth rate, shorter internodes, decreased stem diameter and diminished total dry matter have also been reported for sweet potato in Trinidad (Laura *et al.*, 1986) and cocoa (Galyuon *et al.*, 1994) grown under artificial shade. The findings in this study are in accordance with those of Israeli (1995) who observed a suppression in sucker growth in the understory of a commercial plantation of very high density. Furthermore, Stover and Simmonds (1987) also reported a marked effect of incident solar irradiance on the flowering pattern of banana. A suppression in bunch mass and fresh finger weight, depicted in Table 7.3, was also reported by Robinson and Nel (1989). A response to shading resulting in a decline in banana yield was further reiterated by Israeli *et al.*, (1995), Robinson *et al.*, (1989), indicating the sensitivity of this parameter to reduced levels of incident irradiance. Buisson and Lee (1993) also reported reduced growth and diminished stem diameters in papaya under diminished irradiance conditions.

Seasonality is a vital characteristic of banana growth and production in subtropical conditions (Bower, 1999; Gevers, 1987 and Robinson and Nel, 1985). The summer period is a duration of rapid growth and development, whereas there appears to be a serious drawback on vegetative growth in winter (Fig. 7.5). This work depicted a much slower growth rate and no complete cessation of growth (Table 7.1; Fig 7.6). This contrasts with results highlighted by Israeli *et al.* (1995) who reported a complete cessation of vegetative growth during winter. Overall, shading decreased the rate of leaf emergence, plant height and pseudostem circumference and also delayed the flowering as a result of reduced incidence irradiance levels.

Seasonality has also been found to be a crucial characteristic of banana growth and productivity at Inselele since it lies in the subtropical climatic region. The summer period indicated rapid growth and development while a near cessation of vegetative growth was realised in the winter period. It is recommended that optimal management such as irrigation and fertiliser application should take place during the summer months when crop performance is optimal.

It is crucial to note that there are interactions between variable solar irradiance levels and the seasonal changes that influence banana phenological trends and no single parameter can easily be examined in isolation. The results presented in this study assume that other interactions, such as the impact of pests and diseases, which can occur, are not influencing factors on the trends or responses under consideration.

Such an implication could be regarded as rather unrealistic and simplistic since it does not represent the actual situation under field conditions since there are many factors having various interactions and influences on crop growth and productivity. Meaningful research on multi-component parameters involving interactions and mass transport systems in bananas would be a critical and useful breakthrough in banana knowledge, however, it is not easy to achieve this ideal situation. Furthermore, the resources and time constraints experienced by the author of this study could not permit this cherished desire to come true though a considerable input has been given with rigorous attention to detail to present the findings highlighted herein.

Conclusively, this research revealed that reduction in solar radiation to levels below 40 % of the incident amount will negatively affect crop growth, the crop will not achieve its potential production capacity hence resulting in yield decline. It is anticipated that this study on effects of varying irradiance levels, as well as microclimatic variations in a banana plantation will be beneficial in the assessment of crop performance. This would further lead to a better understanding of radiation dynamics in banana plantations in a bid to maximise growth and productivity.

8.3 Recommendations for future research

Further research on reduction of incident solar irradiance to levels not so dense as to introduce stuntedness or photo-inhibition, such as reduction of irradiance to only 20 % incident irradiance highlighted herein should be conducted. This would be beneficial to farmers practising agroforestry, dense intercropping stands in tropical countries like Uganda, plantations with cropping densities or in regions exposed to prolonged periods of cloudiness. This would then permit one to reap benefits such as reduction of soil evaporation hence conserving scarce soil water, protection plants from direct sunlight, wind effects, hail and birds under appropriate levels of tolerable reduced irradiance.

Changing of the radiation environment may affect biomass accumulation via its effects on radiation use efficiency (RUE). This alteration may also affect the partitioning of assimilates. Therefore future studies done on reducing levels of incident irradiance would need to concurrently have detailed studies on RUE and the responses of leaf carbon dioxide assimilation rates in different radiation regimes.

Crop modelling to ascertain shade tolerance levels coupled with measurements of RUE could help resolve whether intercepted radiation is being used by the crop at its potential efficiency, or whether other factors such as water availability or air temperature could be limiting crop growth and productivity.

There is need to ascertain the results of this study over longer crop cycles. It would be beneficial to compare results of this study with those performed on a different site with the same cultivar. This would yield more representative results and possibly derive crop models needed to better quantify and test relationships (highlighted in this study) of banana shade tolerance levels in a greater range of radiation environments.

Measurement of radiation interception in banana using tube solarimeters under various shade levels should be conducted. This coupled with photosynthetic studies and assessment of dry matter accumulation would appreciably quantify the influence of shading on plant productivity and ascertain banana RUE.

The need for more time involving investigations on banana morphology, phenology and productivity is paramount if reproducible results are to be achieved. This would also help to ascertain energy balance dynamics in a banana orchard using equipment such as the Kipp and Zonen net radiometer. This accurately takes into account the far red infrared radiation as well as the reflected incident solar irradiance.

Conducting further research on evapotranspiration by measuring of air temperature and atmospheric water vapour pressure at the two level approach using both Bowen ratio and Eddy correlation methods would be critical and useful. These can then be compared with either micro-lysimeter results or the single level values derived by calculation in the Penman-Monteith (PM) equation. Utilisation of the PM equation would have the advantage of using meteorological data which are commonly available. This will present more realistic, reliable and representative results.

Canopy evapotranspiration appeared to be controlled primarily by the vapour pressure deficit followed by net irradiance and wind speed patterns. A vital question in this study is whether these results are specific to the conditions under which this study was performed, or if they are valid for a wide range of environments. The results of this study should thus be considered with caution, as the data correspond to a specific area, Inselele farm on the KwaZulu-Natal South

coast. For this reason, further experiments might be very interesting, particularly a comparison between growth and productivity results with those obtained under different weather and site index conditions.

In future research, more attention needs to be given to accurate sensor height placement especially with reference to the infrared and net radiometer sensors.

REFERENCES

- Allen, R. G., Smith, M., Perrier, A., and Pereira, L. S. (1994). An update for the definition of reference evapotranspiration. *ICID bulletin*, **43** (2), 4-34.
- Allen, S. J. (1990). Measurement and estimation of evaporation from soil under sparse barley crops in northern Syria. *Agric. For. Meteorol.* **49**, 291-309.
- Ashktorab, H., Pruitt, W. O., Paw, U. K. T., and George, W. V. (1989). Energy balance determinations close to the soil surface using a micro-Bowen system. *Agric. For. Meteorol.* **46**, 259-274.
- Aston, A. R. (1984). Evaporation from *Eucalyptus* growing in weighing lysimeters: A test of the combination equations *Agric. For. Meteorol.* **31**, 241-249.
- Balasimha, D. (1989). Light penetration patterns through arecanut canopy and leaf physiological characteristics of intercrops. *J. Plant crops*, **16**, 61-67.
- Baldocchi, D., Hutchinson, B., Matt, D., and McMillen, R. (1986). Seasonal variation in the statistics of photosynthetically active radiation penetration in an oak-hickory forest. *Agric. For. Meteorol.* **36**, 343-361.
- Batchelor, C. H. (1984). The accuracy of evapotranspiration functions estimated with the FAO modified Penman equation. *Irrig. Sci.* **5**(4), 223-234.
- Blad, B. L., and Rosenberg, N. J. (1974). Evapotranspiration in sub-irrigated alfalfa and pasture in the east central great plains. *Agron. J.* **66**, 248-252.
- Blake, G. R. and Hartge, K. H. (1986). Bulk density. In Campbell, G. S., Jackson, R. D., Mortland, M.M., Nielsen, D. R., and Klute, A. (Eds), *Methods of soil analysis. Part 1; Physical and mineralogical methods.* Agronomy No. 9, 2nd ed., 363-376. Am. Soc. Agron. Inc., Madison, Wis.
- Boast, C. W., and Robertson, T. M. (1982). A 'microlysimeter' method for determining evaporation from bare soil: Description and laboratory evaluation. *Soil Sci. Soc. Am. J.* **46**, 689-696.
- Bonaparte, E. E. N. A. (1967). Interspecific competition in cocoa shade and fertilizer experiment. *Trop. Agric. (Trinidad)*. **44**, 13-19.

- Bower, J. P., Wolstenholme, B. N., and DeJager, J. M. (1978). Incoming solar radiation and internal water status as stress factors in avocado, *Persea americana* (Mill) cv. Edranol. *Crop Prod. (S.A.)* 7, 129-133.
- Bower, J. P. (1999). Unpublished Horticultural Science 340 course notes. 'Tropical and Subtropical Crops Management'. University of Natal, Pietermaritzburg.
- Bower, J. P. (2000). Personal communication.
- Buisson, D., and Lee, D. W. (1993). The development responses of papaya leaves to simulated canopy shade. *Am. J. Bot.* 80, 947-952.
- Campbell, G. S. (undated). On-line measurement of potential evapotranspiration with the Campbell Scientific automated weather station. *Application note by Campbell Scientific Inc.*, Department of Crop and Soil sciences, Washington state University.
- Campbell, G. S., and Norman, J. M. (1990). Estimation of plant water status from canopy temperature: An analysis of the inverse problem. In Steve M.D and Clark, J.A (Eds), *Application of Remote Sensing in Agriculture*, p 255-271. London.
- Campbell, G. S., and Stockle, C. O. (1993). Prediction and simulation of water use in agricultural systems. In international Crop Science I. *Crop Sci. Soc. Am.* 677. S. Segoe Rd., Madison, WI 53711, USA.
- Chay, A., Paul, G. J., and Paul, V. G. (1998). Evaporation of intercepted precipitation based on an energy balance in unlogged and logged forest areas of central Kalimantan, Indonesia. *Agric. For. Meteorol.* 92, 173-180.
- Daamen, C. C., Dugas, W. A., Prendergast, P. T., Judd, M. J., and McNaughton, K. G. (1999). Energy flux measurements in a sheltered lemon orchard. *Agric. For. Meteorol.* 93, 171-183.
- Daudet, F. A., Le Roux, X., Sinoquet, H., and Adam. B. (1999). Wind speed and leaf boundary layer conductance variation within tree crown. Consequences on leaf-to-atmosphere coupling and tree functions. *Agric. For. Meteorol.* 97, 171-185.
- Davies, W. J., and Zhang, J. (1991). Root signals and the regulation of growth and development of plants in drying soil. *Ann. Rev. Plant Physiol. Plant Mol. Biol.* 42, 55-76.
- Delta-T Device. (1995). ThetaProbe soil moisture sensor. Cambridge, England.

- Eckstein, K. (1994). Physiological responses of banana (*Musa* AAA; Cavendish sub-group) in the subtropics. PhD thesis, Institut für Obstbau and Gemusebau, Universität Bonn, Germany, 203 pp.
- Eckstein, K., and Robinson, J. C. (1996). Physiological responses of banana (*Musa* AAA; Cavendish subgroup) in the tropics. 6. Seasonal responses of leaf gas exchange to short term water stress. *J. Hort. Sci.* **71**, 679-692.
- FAO. (2000). Crop evapotranspiration. Guidelines for computing crop water requirements. FAO irrigation and drainage paper 56, Chapter 3. Meteorological data.
<http://www.fao.org/docrep/X0490E/x0490e07.htm>
- Farina, M. P. W., Channon, P., and Thibaud, G. R. (2000). A comparison of strategies for ameliorating subsoil acidity: I. Long-term growth effects. *Soil Sci. Soc. Am. J.* **64**(2), 646-651.
- Francisco, R. L., Tomás, L. C., Javier, M. M., and Antonio, D. C. B. (2000). LAI estimation of natural pine forest using a non-standard sampling technique. *Agric. For. Meteorol.* **101**, 95-111.
- Gallagher, J. N., and Biscoe, P. V. (1978). Radiation absorption, growth and yield of cereals. *J. Agric. Sci. Cambridge.* **91**, 47-60.
- Gallo, K. P., and Daughtry, C. S. T. (1986). Techniques for measuring intercepted and absorbed photosynthetically active radiation in corn canopies. *Agron. J.* **78**, 752-756.
- Gallo, K. P., Daughtry, C. S. T., and Wiegand, C. L. (1993). Errors in measuring absorbed radiation and computing crop radiation use efficiency. *Agron. J.* **85**, 1222-1228.
- Galyuon, I. K., McDavid, C. R., Lopez, F. B., and Spence, J. A. (1994). The effect of irradiance level on cocoa (*Theobroma cacao* L.): 1. Growth and leaf adaptations. *Trop. Agric. (Trinidad).* **73**, 23-28.
- Gee, G. W., and Bauder, J. W. (1986). Particle size analysis. In Campbell G. S., Jackson R. D., Mortland, M. M., Nielsen, D. R., and Klute, A. (eds). Methods of soil analysis. Part 1. Physical and mineralogical methods. *Agron. monog. no.9* 2nd ed., 383-409 Madison, Wis., USA.
- Genstat Manual. (1983). GENSTAT a general statistical program. Release 4.04. Oxford. Numerical algorithms Group. UK.

- Gevers, E. H. (1987). A situational Survey of Management Limitations to Banana (*Musa* spp) Production on the Natal South Coast. *MSc Thesis (Department of Horticulture)* University of Natal, Pietermaritzburg.
- Ghavani, M. (1974). Irrigation of valery bananas in Honduras. *Trop. Agric.* **51**, 443-446.
- Ham, J. M., Heilman, J. L., and Lascano, R. L. (1991). Soil and canopy energy balances of a row crop at partial cover. *Agron. J.* **83**, 744-753.
- Hamlyn, G. J. (1999). Use of infrared thermometry for estimation of stomatal conductance as a possible aid to irrigation scheduling. *Agric. For. Meteorol.* **95**, 139-149.
- Hatfield, J. L. (1983). Evapotranspiration obtained from remote sensing methods. *Adv. Irrig.* **2**, 395-415.
- Hatfield, J. L. (1984). Evaluation of canopy temperature evapotranspiration models over various crops. *Agric. For. Meteorol.* **32**, 41-53.
- Healey, K. D., and Rickert, K. G. (1998). Shading material changes the proportion of diffuse radiation in transmitted radiation. *Aust. J. Exp. Agric.* **38**, 95-100.
- Hill, T. R., Bissell, R. J., and Burt, J. R. (1992). Yield, plant characteristics and relative tolerance to bunch loss of four banana varieties. (Musa AAA Group, Cavendish sub-group) in semi-arid subtropics of western Australia. *Aust. J. Exp. Agric.* **32**, 237-240.
- Hillel, D. (1982). *Introduction to Soil Physics*. Academic press, Orlando, Florida.
- Hillel, D. (1998). *Soil and Water. Phy. Prin. and Proc.* **58**, 10-13
- Idso, S. B., Jackson, R. D., Pinter, P. J., Reginato, R. J., and Hatfield, J. L. (1981). Normalising the stress-degree parameter for environmental variability. *Agric. Meteorol.* **24**, 45-55.
- Internet, (2000). <http://www.apogee-inst.com/irtspecs.htm>
- Internet, (2000). <http://www.industryzone.com/fostoria/PhIRprop.htm>
- Israeli, Y., Plaut, Z., and Schwartz, A. (1995). Effect of shade on banana morphology, growth and production. *Scie. Hort.* **62**, 45-56.
- Jackson, N. A., and Wallace, J. S. (1999). Soil evaporation measurements in an agroforestry system in Kenya. *Agric. For. Meteorol.* **94**, 203-215.
- Jacobson, O. H., and Schjonning, P. (1993a). A laboratory calibration of time domain reflectometry for soil water measurement including effects of bulk density and texture. *J. Hydrol.* **151**, 147-157.

- Jacobson, O. H., and Schjonning, P. (1993b). Field evaluation of time domain reflectometry for soil water measurements. *J. Hydrol.* **151**, 159-172.
- Jensen, M. E., Burman, R. D., and Allen, R. G. (ed). 1990. "Evapotranspiration and irrigation water requirements", ASCE Manuals and reports on Engineering practices. *Am. Soc. Civil Engrs*, NY. **70**, 360.
- Johnston, M. A. (2000). Methods of analysis of Soil Physical Properties. Unpublished Soil Science 351 and 352 course notes. University of Natal, Pietermaritzburg.
- Jonathan, H. C., and Carlos, F. B. (2000). The banana in Florida. Internet:
http://edis.ifas.ufl.edu/BODY_MG040
- Judd, M. J., Raupach, M. R., and Finnigan, J. J. (1996). A wind tunnel study of the turbulent flow around single and multiple windbreaks, part 1: velocity fields. *Boundary Layer Meteorol.* **80**, 127-165.
- Kiniry, J. R., Jones, C. A., O'Toole, J. C., Blanchet, R., Cabelguenne, M., and Spanel, D. A. (1989). Radiation-use efficiency and biomass accumulation prior to grain-filling for five grain-crop species. *Field Crops Res.* **20**, 51-64.
- Kramer, P. J. (1988). Changing concepts regarding plant water relations. *Plant, cell envt.* **11**, 565-568.
- Kuhne, F. A., Kruger, J. J., and Green, G. C. (1973). Phenological studies of the banana plant. *Cit. and subtrop. fru. J.* **472**, 12-16.
- Laura, B. R. N., Lawrence, A. W., and Theodore, U.F. (1986). Responses of four sweet potato cultivars to levels of shade: 1. Dry matter production, shoot morphology and leaf anatomy. *Trop. Agric. (Trinidad)*, **63**, 258-264.
- LI-COR, Inc., (1991). LAI-2000 plant canopy analyser manual.
- Luvall, J. C., and Holbo, H. R. (1986). Using the thermal infrared multispectral scanner (TIMS) to estimate surface thermal responses. International conference on measurement of soil and plant water status. **2**, 115-120. Logan, Utah.
- Malcom, J. M., and Doug, W. S. (1995). Radiation-use efficiency in summer rape. *Agron. J.* **87**, 1139-1142.
- Mariscal, M. J., Orgaz, F., and Villalobos, F. J. (2000). Modelling and measurement of radiation interception by olive canopies. *Agric. For. Meteorol.* **100**, 183-197.

- McAnaney, K. J., Prendergast, P. T., Judd, M. J., and Green, A. E. (1992). Observations of equilibrium evaporation from a wind break-sheltered kiwifruit orchard. *Agric. For. Meteorol.* **57**, 253-264.
- McNaughton, K. G. (1988). Effects of wind breaks on turbulent transport and microclimate. *Agric. Ecosyst. Environ.* **22/23**, 17-39.
- Monteith, J. L. (1977). Climate and the efficiency of crop production in Britain. *Philos. Trans. R. Soc. London B.* **281**, 277-294.
- Monteith, J. L., and Unsworth, M. H. (1990). Principles of Environmental Physics, 2nd edn. Chapman & Hall, New York, 291 pp.
- Monteith, J. L. (1994). Discussion: Validity of the correlation between intercepted radiation and biomass. *Agric. For. Meteorol.* **68**, 213-220.
- Morse, R. L., and Robinson, J. C. (1996). Cultivar and planting density interaction with banana (*Musa* AAA; Cavendish sub-group) in a warm subtropical climate.1. Vegetative morphology, phenology and fruit development. *J. S. Afr. Soc. Hort. Sci.* **65**, 121-127.
- Muchow, R.C., and Sinclair, T.R. (1994). Nitrogen response of leaf photosynthesis and canopy radiation use efficiency in field-grown maize and sorghum. *Crop Sci.* **34**, 721-727.
- Muchow, R.C., Spillman, M. F., Wood, A. W., and Thomas, M. R. (1994). Radiation interception and biomass accumulation in a sugarcane crop grown under irrigated tropical conditions. *Aust. J. Agric. Res.* **45**, 37- 49.
- Murray, D. B. (1961). Shade and fertiliser relations in banana. *Trop. Agric.* **38**, 123-132.
- Murray, D. B., and Nichols, R. (1965). Light, Shade and Growth in some Tropical trees, in : Light as an Ecological Factor (ed. Bainbridge, R., Evans, G. C., and Rakham, O.) **18**, 249-263.
- Nam, N. H., Subbarao, G. V., Chauhan, Y. S., and Johansen, C. (1998). Importance of canopy attributes in determining dry matter accumulation of pigeon pea under contrasting moisture regimes. *Crop Sci. J.* **38**, 955-961.
- New Africa. (2000). Cote d'Ivoire. Cocoa production.
<http://www.newafrica.com/agriculture/cotedeivoire/cocoa.htm>

- Norman, M. J. T., Pearson, C. S., and Searle, P. G. E. (1984). Bananas (*Musa* spp.) 271-285. In Norman *et al.*, (ed). The Ecology of Tropical Food Crops. Cambridge Univ. Press, Cambridge.
- Panozzo, J. F., Eagles, H. A., Cawood, R. J., and Wootton. M. (1999). Wheat spike temperatures in relation to varying environmental conditions. *Aus. J. Agric. Res.* **50**, 997-1005.
- Penman, H.L. (1948). "Natural evaporation from open water, bare soil and grass." *Proc. R. Soc. London Ser. A***193**, 120-146.
- PlotITW.V3.2. (1999). Scientific Programming Enterprises (SPE).
- Ritchie, J. T. (1972). Model for predicting evaporation from a row crop with incomplete cover. *Water Resour. Res.* **8**, 1204-1213.
- Roberts, J., Cabral, O. M. R., Fisch, G., Molion, L. C. B., Moore, C. J., and Shuttleworth, W. J. (1993). Transpiration from an Amazonian rainforest calculated from stomatal conductance measurements. *Agric. For. Meteorol.* **65**, 175-196.
- Robinson, J. C. (1981). Studies on the phenology and production potential of Williams banana in a subtropical climate. *Subtropica.* **2**, 12-16.
- Robinson, J. C. (1983). Banana cultivar comparison between 'Williams' and two local cavendish selections. *Subtropica*, **4(2)**, 15-16.
- Robinson, J. C. (1993). Phenology of the banana in the subtropics. In: Robinson, J. C. (Ed), Handbook of Banana growing in South Africa. ITSC, Nelspruit, pp. 18-23.
- Robinson, J. C. (1995). Determination of optimal plant populations and spatial arrangements for bananas. ITSC Banana research summaries. 9-12.
- Robinson, J. C. (1996). Bananas and Plantains. Crop Production Science in Horticulture series. CAB International, Wallingford. U. K.
- Robinson, J. C., and Alberts, A. J. (1989). Seasonal variations in the crop water use coefficient of banana (cultivar 'Williams') in the subtropics. *Scie. Hort.* **40**, 215-225.
- Robinson, J. C., and Bower, J. P. (1987). Transpiration characteristics of banana leaves (cultivar 'Williams') in response to progressive depletion of available soil moisture. *Scie. Hort.* **30**, 289-300.
- Robinson, J. C., and Bower, J. P. (1988). Transpiration from banana leaves in the subtropics in response to diurnal and seasonal factors and high evaporative demand. *Scie. Hort.* **37**,

129-143.

- Robinson, J. C., and Nel, D. J. (1985). Comparative morphology, phenology and production potential of banana cultivars 'Dwarf Cavendish' and 'Williams' in the Eastern Transvaal lowveld. *Scie. Hort.* **25**, 149-161.
- Robinson, J. C., and Nel, D. J. (1986). The influence of banana plant density and canopy characteristics on ratoon cycle interval and yield. *Acta Hort.* **175**, 227-232.
- Robinson, J. C., and Nel, D. J. (1988). Plant density studies with banana (cv. Williams) in a subtropical climate. I. Vegetative morphology, phenology and plantation microclimate. *J. Hort. Sci.* **63**, 303-313.
- Robinson, J. C., and Nel, D. J. (1989). Plant density studies with banana (cv. Williams) in a subtropical climate. 2. Components of yield and seasonal distribution. *J. Hort. Sci.* **64**, 211-222.
- Robinson, J. C., Nel, D. J., and Bower, J. P. (1989). Plant density studies with banana (cv. Williams) in a subtropical climate. III The influence of spatial arrangement. *J. Hort. Sci.* **64**, 513-519.
- Rony, S., and Rodomiro, O. (1997). Morphology and growth of plantain and banana. IITA research guide 66. <http://www.isnar.org/iita/publib/>
- Rose, C. W., and Sharma, M. L. (1984). Summary recommendations of the workshop on "Evapotranspiration from plant communities" *Agric. Water manage.* **8**, 325-342.
- Ross, J., and Sulev, M. (2000). Sources of error in measurement of PAR. *Agric. For. Meteorol.* **100**, 103-125.
- Ross, J., Ross, V., and Koppel, A. (2000). Estimation of leaf area and its vertical distribution during growth period. *Agric. For. Meteorol.* **101**, 237-246.
- Russell, G. (1980). Crop evaporation, surface resistance and soil water status. *Agric. Meteorol.* **21**, 213- 226.
- Samarakoon, S. P., Wilson, J. R., and Shelton, H. M. (1990). Growth, morphology and nutritive quality of shaded *Stenotaphrum secundatum*, *Axonopus compressus* and *Pennisetum clandestinum*. *J. Agric. sci. Cambridge.* **114**, 161-169.
- Savage, M. J. (1980). Radiation and some of its important applications in agriculture *Vector* **7**, 12-14.

- Savage, M. J., Everson, C. S., and Meterlerkamp, B. R. (1997). Evaporation measurement above vegetated surfaces using micrometeorological techniques. Water Research Commission Report No. 349/1/97, p248, ISBN No: 1 86845 363 4.
- Savage, M. J. (1998a). Unpublished Agrometeorology 210 course notes. The atmosphere and Earth: Radiation and Radiation laws. *SPAC Res. Unit, School of Applied Environ. sci. Univ. Natal. South Africa.*
- Savage, M. J. (1998b). Unpublished Agrometeorology 210 course notes. Momentum, mass and energy exchange of plant communities. *SPAC Res. Unit, School of Applied Environ. sci. Univ. Natal South Africa.*
- Savage, M. J. (1999). Personal communication.
- Savage, M. J. (1999a). 3D Wind propeller Campbell datalogger (CR10X, 21X and 7X) Program. Agrometeorology. *SPAC Res. Unit, School of Applied Environ. sci. Univ. Natal South Africa.*
- Savage, M. J. (1999b). A spreadsheet for calculating reference evaporation. *SPAC Res. Unit, School of Applied Environ. sci. Univ. Natal South Africa.*
- Savage, M. J. (2001). Personal communication.
- Schmid, H. P. (1994). Source areas for scalars and scalar fluxes. *Boundary layer meteorol.* **67**, 293-318.
- Schulze, E. D., Stuedle, E., Gollan, T., and Schurr, U. (1988). Response to Dr P. J. Kramer's article. Changing concepts regarding plant water relations. *Plant, cell envt.* **11**, 565-568; **1**, 573-576.
- Simmonds, N. W. (1962). The Evolution of Bananas. Longmans, London, 170pp.
- Sinclair, T. R., and Ludlow, M. M. (1985). Who Taught Plants Thermodynamics? The Unfulfilled Potential of Plant Water Potential. *Austral. J. Plant Physiol.* **12**, 213-217.
- Sinclair, T. R., and Muchow, R. C. (1999). Radiation use efficiency. *Adv. Agron. J.* **11**, 215-265.
- Singh, B., and Szeicz, G. (1980). Predicting the canopy resistance of a mixed hardwood forest. *Agric. Meteorol.* **21**, 49-58.
- South African Sugar Association. (1999). Long term climatic data for South Africa.
- Stockle, C. O., and Kiniry, J. R. (1990). Variability of crop radiation-use efficiency associated with vapour pressure deficit. *Field Crops Res.* **25**, 171-81.

- Stone, L. R., and Horton, M. L. (1974). Estimating evaporation using canopy temperature. *Agron. J.* **66**, 450-454.
- Stover, R. H. (1984). Canopy Management in Valery and Grand Nain using Leaf Area Index and Photosynthetically Active Radiation Measurements. *Fruits.* **36**, 89-93.
- Stover, R. H., and Simmonds, N. W. (1987). *Bananas*. 3rd Edition, Longman, London. **8**, 193-211.
- Texaset. (2000). Internet address: <http://texaset.tamu.edu/include/crop/cropcoe.html>.
- Thom, A. S. (1975). Momentum, Mass and Heat Exchange in Plant Communities. In Monteith, J. L. (ed), *Vegetation and the Atmosphere*, Academic Press, London. **1**, 57-105.
- Topp, G. C., Davis, J. L., and Annan, A. P. (1980). Electromagnetic determination of soil water content: Measurements in coaxial transmission lines. *Water Resour. Res.* **16**, 574-582.
- Turner, D. W. (1972). Banana plant growth 2. Dry matter production, leaf area and growth analysis. *Aus. J. Expt. Agric. Ani. Hus.* **12**, 216-224.
- Turner, D. W. (1982). A review of plant physiology in relation to cultural practices in the Australian banana industry. In: *Australian banana industry development workshop*, Lismore, New South Wales pp.34-58.
- Turner, D. W., and Lahav, E. (1983). The growth of banana plants in relation to temperature. *Aus. J. Plant physiol.* **10**, 43-53.
- Turner, D. W., and Thomas, D. S. (1998). Measurements of plant and soil water status and their association with leaf gas exchange in banana (*Musa* spp): a lactiferous plant. *Scie. Hort.* **77**, 177-193.

APPENDIX I Wiring of the Campbell Scientific 21 X datalogger

CR21X INPUT	CONNECTION	COLOUR CODING
1H	SOLAR IRRADIANCE	RED
1L	AIR TEMPERATURE	BLACK
AG	SOLAR IRRADIANCE	BLACK
2H	RELATIVE HUMIDITY	BROWN
2L	WIND SPEED AND	WHITE
	DIRECTION	
AG	WIND SPEED AND	BLUE
	DIRECTION	
3H	WIND SPEED AND	YELLOW
	DIRECTION	
3L	WIND SPEED AND	RED
	DIRECTION	
AG	WIND SPEED AND	GREEN AND BLACK
	DIRECTION	
4H	SOIL HEAT FLUX	BLACK
4L	SOIL HEAT FLUX	BLACK
AG	SOIL HEAT FLUX	WHITE
5H	SOIL TEMPERATURE	BLUE
5L	NET IRRADIANCE	BLACK
AG	NET IRRADIANCE	RED
6H	NET IRRADIANCE	BLACK
6L	SOIL TEMPERATURE	RED

WIRING CODES FOR SENSORS 05 JANUARY 2000:

1. PYRANOMETER PY 9481
 RED (HIGH)
 BLACK (GROUND)
 2. RAIN GAUGE
 RED (PULSE)
 BLACK (GROUND)
 3. VAISALA RH AND TEMPERATURE CS500 (S2030038)
 TEMPERATURE BLACK (HIGH)
 RH BROWN (HIGH)
 GREEN AND CLEAR (GROUND)
 4. 3D PROPELLER WIND SPEED AND DIRECTION SENSOR
 218 U WHITE (HIGH) BLUE (GROUND)
 225 V YELLOW (HIGH) GREEN (GROUND) NORTH
 240 W RED (HIGH) BLACK (GROUND) EAST
 5. SOIL HEAT FLUX PLATES
 BLACK (HIGH) WHITE (GROUND)
 6. SOIL THERMOCOUPLE
 BLUE (HIGH) RED (GROUND)
 7. NET RADIOMETERS Q94330 & 92262
 BLACK (HIGH) RED (GROUND)
 8. APOGEE IRTs (IRTP1144 AND IRTP1147)
 SINGLE ENDED
 SHIELD & RED (GROUND)
 YELLOW (HIGH OR LOW)
 DIFFERENTIAL
 SHIELD (GROUND)
 YELLOW (HIGH)
 RED (LOW)

```
; {21X}
;
*Table 1 Program
  01: 30      Execution Interval (seconds)
```

MEASURE PANEL TEMP, BATTERY VOLTAGE

```
1: Internal Temperature (P17)
  1: 1      Loc [ Tpanel ]

2: Batt Voltage (P10)
  1: 2      Loc [ Vbattery ]
```

SOLAR IRRADIANCE

```
3: Volt (SE) (P1)
  1: 1      Repts
  2: 02     15 mV Slow Range
  3: 1      SE Channel
  4: 3      Loc [ Is_W_m2 ]
  5: 80     Mult?
  6: 0.0    Offset
```

RAINFALL

```
4: Pulse (P3)
  1: 1      Repts
  2: 1      Pulse Input Channel
  3: 02     Switch Closure, All Counts
  4: 4      Loc [ Rainfall ]
  5: 0.5    Mult
  6: 0.0    Offset
```

AIR TEMPERATURE

```
5: Volt (SE) (P1)
  1: 1      Repts
  2: 05     5000 mV Slow Range
  3: 2      SE Channel
  4: 5      Loc [ Tair ]
  5: 0.1    Mult
  6: -40    Offset
```

RELATIVE HUMIDITY AND SVP

```
6: Volt (SE) (P1)
  1: 1      Repts
  2: 5      5000 mV Slow Range
  3: 3      SE Channel
  4: 6      Loc [ RH ]
```

```
5: 0.1      Mult
6: 0.0      Offset

7: Saturation Vapor Pressure (P56)
  1: 5      Temperature Loc [ Tair ]
  2: 7      Loc [ e_kPa ]

8: Z=X*Y (P36)
  1: 7      X Loc [ e_kPa ]
  2: 6      Y Loc [ RH ]
  3: 7      Z Loc [ e_kPa ]

9: Z=X*F (P37)
  1: 7      X Loc [ e_kPa ]
  2: 0.01    F
  3: 7      Z Loc [ e_kPa ]

WIND SPEED
10: Volt (SE) (P1)
  1: 3      Repts
  2: 04     500 mV Slow Range
  3: 4      SE Channel
  4: 8      Loc [ Volt_w1 ]
  5: 1.0    Mult
  6: 0      Offset

11: Beginning of Loop (P87)
  1: 0      Delay
  2: 3      Loop Count

12: Z=X*F (P37)
  1: 8      -- X Loc [ Volt_w1 ]
  2: 0.127   F
  3: 11     -- Z Loc [ Windms1 ]

13: End (P95)

WIND DIRECTION
14: Z=ARCTAN(X/Y) (P66)
  1: 13     X Loc [ Windms1 ]
  2: 12     Y Loc [ Windms1 ]
  3: 23     Z Loc [ Winddir ]

SOIL HEAT FLUX
15: Volt (SE) (P1)
  1: 2      Repts
  2: 02     15 mV Slow Range
  3: 7      SE Channel
  4: 14     Loc [ Fplate ]
  5: 50     Mult
  6: 0.0    Offset

SOIL TEMPERATURE
16: Thermocouple Temp (SE) (P13)
  1: 1      Repts
  2: 01     5 mV Slow Range
  3: 9      SE Channel
  4: 1      Type T (Copper-Constantan)
  5: 1      Ref Temp (Deg. C) Loc [ Tpanel ]
  6: 16     Loc [ Tsoil ]
  7: 1.0    Mult
  8: 0.0    Offset

NET IRRADIANCE
17: Volt (SE) (P1)
  1: 2      Repts
  2: 02     15 mV Slow Range
  3: 10     SE Channel
  4: 17     Loc [ Inet1Wm2 ]
  5: 1.0    Mult
  6: 0.0    Offset

18: If (X<=>F) (P89)
  1: 17     X Loc [ Inet2Wm2 ]
  2: 3      >=
  3: 0      F
  4: 30     Then Do
```

```

9:  Z=X*F (P37)
1:  17      X Loc [ Inet2Wm2 ]
2:  9.43    F
3:  18      Z Loc [ Inet2Wm2 ]

0:  Else (P94)

1:  Z=X*F (P37)
1:  18      X Loc [ Inet2Wm2 ]
2:  11.83   F
3:  18      Z Loc [ Inet2Wm2 ]

2:  End (P95)
3:  If (X<=>F) (P89)
1:  18      X Loc [ Inet2Wm2 ]
2:  3        >=
3:  0        F
4:  30      Then Do

24: Z=X*F (P37)
1:  18      X Loc [ Inet2Wm2 ]
2:  8.69    F
3:  18      Z Loc [ Inet2Wm2 ]

25: Else (P94)

26: Z=X*F (P37)
1:  18      X Loc [ Inet2Wm2 ]
2:  10.69   F
3:  18      Z Loc [ Inet2Wm2 ]

27: End (P95)

MEASURE APOGEE IRT TEMPERATURES
28: Thermocouple Temp (SE) (P13)
1:  4      Reps
2:  1      500 mV Slow Range
3:  11     SE Channel
4:  3      Type K (Chromel-Alumel)
5:  1      Ref Temp (Deg. C)Loc [ Tpanel ]
6:  19     Loc [ IRTT1 ]
7:  1.0    Mult
8:  0.0    Offset

29: If time is (P92)
1:  0      Minutes into a
2:  15     Minute Interval
3:  10     Set Output Flag High

30: Real Time (P77)
1:  1220   Year,Day,Hour/Minute (midnight =
2400)

31: Average (P71)
1:  2      Reps
2:  2      Loc [ Vbattery ]

32: Totalize (P72)
1:  1      Reps
2:  4      Loc [ Rainfall ]

33: Average (P71)
1:  1      Reps
2:  5      Loc [ Tair ]

34: Average (P71)
1:  4      Reps
2:  7      Loc [ e_kPa ]

35: Average (P71)
1:  9      Reps
2:  14     Loc [ Fplate ]
    
```

```

36: Histogram (P75)
1:  1      Reps
2:  15     No. of Bins
3:  1      Closed Form
4:  23     Bin Select Value Loc [ Winddir ]
5:  0000   WV Loc Option [ _____ ]
6:  0      Low Limit
7:  360    High Limit
    
```

```

*Table 2 Program
02: 10      Execution Interval (seconds)
    
```

```

1: Serial Out (P96)
1: 30      SM192/SM716/CSM1
    
```

```

*Table 3 Subroutines
End Program
    
```

-Input Locations-

1	Tpanel	1	2	1
2	Vbattery	1	1	1
3	Is_W_m2	1	1	1
4	Rainfall	1	1	1
5	Tair	1	2	1
6	RH	1	1	1
7	e_kPa	1	4	3
8	Volt_w1	5	2	1
9	Volt_2	9	1	1
10	Volt_3	9	1	1
11	Windms1	9	1	2
12	_____	9	1	1
13	_____	9	0	1
14	Fplate	14	1	2
15	Fplate_2	15	1	2
16	Tsoil	16	1	2
17	Inet1Wm2	17	1	2
18	Inet2Wm2	18	4	2
19	IRTT1_1	5	1	1
20	IRTT1_2	9	1	1
21	IRTT1_3	9	1	1
22	IRTT1_4	9	1	1
23	Winddir	9	2	2
24	_____	9	0	1
25	_____	9	0	1
26	_____	9	0	1
27	_____	9	0	1
28	_____	9	0	1
29	_____	9	0	1
30	_____	9	0	1
31	_____	9	0	1
32	_____	9	0	1
33	_____	9	0	1
34	_____	9	0	1
35	_____	9	0	1
36	_____	9	0	1
37	_____	9	0	1
38	_____	9	0	1
39	_____	9	0	1
40	_____	17	0	1

```

-Program Security-
0000
0000
0000
    
```

Final Storage Label File for: 0501TRIA.CSI
Date: 1/5/2000
Time: 20:25:47

124 Output_Table 15.00 Min
1 124 L
2 Year_RTM L

Day_RTM L
 Hour_Minute_RTM L
 Vbattery_AVG L
 Is_W_m2_AVG L
 Rainfall_TOT L
 Tair_AVG L
 Pe_kPa_AVG L
 .0 Volt_w1_AVG L
 .1 Volt_2_AVG L
 .2 Volt_3_AVG L
 i3 Fplate_AVG L
 i4 Fplate_2_AVG L
 i5 Tsoil_AVG L
 i6 Inet1Wm2_AVG L
 i7 Inet2Wm2_AVG L
 i8 IRTT1_AVG L
 i9 IRTT1_2_AVG L
 i20 IRTT1_3_AVG L
 i21 IRTT1_4_AVG L
 i22 Winddir_BIN01 L
 i23 Winddir_BIN02 L

24 Winddir_BIN03 L
 25 Winddir_BIN04 L
 26 Winddir_BIN05 L
 27 Winddir_BIN06 L
 28 Winddir_BIN07 L
 29 Winddir_BIN08 L
 30 Winddir_BIN09 L
 31 Winddir_BIN10 L
 32 Winddir_BIN11 L
 33 Winddir_BIN12 L
 34 Winddir_BIN13 L
 35 Winddir_BIN14 L
 36 Winddir_BIN15 L

Estimated Total Final Storage Locations used
 per day 3456.0

Program Trace Information File for: 0501TRIA.CSI
 Date: 1/5/2000
 Time: 20:25:47

T = Program Table Number
 N = Sequential Program Instruction Location Number
 Instruction = Instruction Number and Name

Inst ExTm = Individual Instruction Execution Time
 Block ExTm = Cumulative Execution Time for program block,
 i.e., subroutine
 Prog ExTm = Cumulative Total Program Execution Time

T N Instruction	Inst ExTm (msec)	Block ExTm (msec)	Prog ExTm (msec)	Output Flag High		
				Inst ExTm (msec)	Block ExTm (msec)	Prog ExTm (msec)
1 1 17 Internal Temperature	14.0	14.0	14.0	14.0	14.0	14.0
1 2 10 Batt Voltage	7.6	21.6	21.6	7.6	21.6	21.6
1 3 1 Volt (SE)	57.2	78.8	78.8	57.2	78.8	78.8
1 4 3 Pulse	1.4	80.2	80.2	1.4	80.2	80.2
1 5 1 Volt (SE)	12.1	92.3	92.3	12.1	92.3	92.3
1 6 1 Volt (SE)	12.1	104.4	104.4	12.1	104.4	104.4
1 7 56 Saturation Vapor Pressure	4.2	108.6	108.6	4.2	108.6	108.6
1 8 36 Z=X*Y	1.2	109.8	109.8	1.2	109.8	109.8
1 9 37 Z=X*F	0.9	110.7	110.7	0.9	110.7	110.7
1 10 1 Volt (SE)	95.6	206.3	206.3	95.6	206.3	206.3
1 11 87 Beginning of Loop	0.2	206.5	206.5	0.2	206.5	206.5
Execution times in the loop are calculated for one pass only.						
1 12 37 Z=X*F	0.9	207.4	207.4	0.9	207.4	207.4
1 13 95 End	0.2	207.6	207.6	0.2	207.6	207.6
1 14 66 Z=ARCTAN(X/Y)	6.7	214.3	214.3	6.7	214.3	214.3
1 15 1 Volt (SE)	76.4	290.7	290.7	76.4	290.7	290.7
1 16 13 Thermocouple Temp (SE)	64.0	354.7	354.7	64.0	354.7	354.7
1 17 1 Volt (SE)	57.2	411.9	411.9	57.2	411.9	411.9
1 18 89 If (X<=>F)	0.4	412.3	412.3	0.4	412.3	412.3
1 19 37 Z=X*F	0.9	413.2	413.2	0.9	413.2	413.2
1 20 94 Else	0.2	413.4	413.4	0.2	413.4	413.4
1 21 37 Z=X*F	0.9	414.3	414.3	0.9	414.3	414.3
1 22 95 End	0.2	414.5	414.5	0.2	414.5	414.5
1 23 13 Thermocouple Temp (SE)	133.6	548.1	548.1	133.6	548.1	548.1
1 24 92 If time is	0.3	548.4	548.4	0.3	548.4	548.4
Output Flag Set @ 124 for Array 124						
1 25 77 Real Time	0.1	548.5	548.5	1.0	549.4	549.4
Output Data 3 Values						
1 26 71 Average	1.9	550.4	550.4	8.1	557.5	557.5
Output Data 2 Values						
1 27 72 Totalize	1.1	551.5	551.5	2.1	559.6	559.6
Output Data 1 Values						
1 28 71 Average	1.4	552.9	552.9	5.1	564.7	564.7

Output Data 1 Values							
. 29 71 Average	2.9	555.8	555.8	14.1	578.8	578.8	
Output Data 4 Values							
. 30 71 Average	5.4	561.2	561.2	29.1	607.9	607.9	
Output Data 9 Values							
. 31 75 Histogram	3.5	564.7	564.7	46.2	654.1	654.1	
Output Data 15 Values							

Program Table 1 Execution Interval 10.000 Seconds

Table 1 Estimated Total Program Execution Time in msec 564.7 w/Output 654.1

Table 1 Estimated Total Final Storage Locations used per day 3456.0

----- Table 2 -----

2 1 96 Serial Out	2.0	2.0	2.0	2.0	2.0	2.0	
-------------------	-----	-----	-----	-----	-----	-----	--

Program Table 2 Execution Interval 10.000 Seconds

Table 2 Estimated Total Program Execution Time in msec 2.0 w/Output 2.0

Table 2 Estimated Total Final Storage Locations used per day 0.0

Estimated Total Final Storage Locations used per day 3456.0

**APPENDIX III Calculation procedure used for estimating the particle size distribution
(Gee and Bauder, 1986)**

$\% \text{ coSi} + \text{ fiSi} + \text{ clay} = 265 g_{\text{coSi} + \text{ fiSi} + \text{ clay}} (1 + w)$	1
$\% \text{ fiSi} + \text{ clay} = 265 g_{\text{fiSi} + \text{ clay}} (1 + w)$	2
$\% \text{ clay} = 265 g_{\text{clay}} (1 + w)$	3
$\% \text{ coSi} = 1 + 2$	4
$\% \text{ fiSi} = 2 - 3$	5
$\% \text{ coSa} = 5 g_{\text{coSa}} (1 + w)$	6
$\% \text{ meSa} = 5 g_{\text{meSa}} (1 + w)$	7
$\% \text{ fiSa} = 5 g_{\text{fiSa}} (1 + w)$	8
$\% \text{ VfSa} = 5 g_{\text{VfSa}} (1 + w)$	9

where

coSi: coarse silt

fiSi: fine sand

coSa: coarse sand

meSa: medium sand

fiSa: fine sand

VfSa: very fine sand

APPENDIX IV Density, surface tension and viscosity of water and viscosity of air at various temperatures (source: Johnston, 2000)

Temperature (°C)	Density of water (kg m ⁻³)	Surface tension of water (x 10 ⁻² N m ⁻¹)	Water Viscosity (x 10 ⁻³ Pa s)	Air Viscosity (x 10 ⁻⁵ Pa s)
5	999.9	7.48	1.519	-
10	999.73	7.42	1.307	-
15	999.13	7.34	1.139	1.816
16	-	-	1.115	1.819
17	-	-	1.085	1.823
18	-	-	1.053	1.827
19	-	-	1.023	1.830
20	998.23	7.27	1.002	1.832
21	-	-	0.982	1.837
22	-	-	0.960	1.841
23	-	-	0.937	1.844
24	-	-	0.916	1.848
25	997.08	7.19	0.890	1.852
26	-	-	0.870	1.856
27	-	-	0.852	1.859
28	-	-	0.830	1.862
29	-	-	0.811	1.866
30	995.68	7.11	0.798	1.870
35	994.06	7.03	0.719	1.888
40	992.25	6.95	0.653	1.904

APPENDIX V Baseline sucker height measurements

Day of year (1999)	Sucker height 100%	Sucker height 70%	Sucker height 40%	Sucker height 20%
215	114.13	115.19	113.49	114.89
245	122.2	123.18	122.3	119.48
275	128.34	129.03	123.18	123.61
305	135.65	134.53	136.8	135.6
335	142.1	140.27	144.5	143.4
365	150.18	147.61	151.4	152.6

Different letters in a row would have represented statistically significant differences at $P = 0.05$, however, no statistically significant differences were observed at $P = 0.05$, hence no letters were shown in the table to avoid monotony.